



NTNU – Trondheim
Norwegian University of
Science and Technology

Emission Reduction Technology and Cost Efficiency for Ships Operating on the Northern Sea Route

A Case Study

Runa A. Skarbø

Marine Technology

Submission date: December 2014

Supervisor: Soren Ehlers, IMT

Co-supervisor: Vilmar Æsøy, Høgskolen i Ålesund

Norwegian University of Science and Technology
Department of Marine Technology

Preface

This thesis is written as the final work of an integrated master in Marine Technology at the Norwegian University of Science and Technology (NTNU), in Trondheim the autumn of 2014.

Working on this thesis has been very challenging but also rewarding. I have never before taken on such a big task. Working with this thesis, I have learnt extremely much during the last 20 weeks, both about the topics but also about myself.

I would not have been able to finish this thesis without the help of so many good people. Firstly, I would like to give a big thank you to my supervisors Sören Ehlers (NTNU) and Vilmar Æsøy (HiÅ) for their guidance, support and encouragement. They have both been nothing but helpful, and have assisted me greatly with understanding the topics at hand. I would also like to thank the ship owner who provided me with input on cost figures. Furthermore, I would like to thank (then) PhD student Bernhard Schartmüller (NTNU), who have also assisted me in discussing the formulation and framework of my model. Also, he has helped me with obtaining data and code that was very helpful for my work. Further, a thank you to my friends and family is in place. A big thanks go out to my awesome friends in office A2.011 at Marinteknisk senter at Tyholt (both the "old" and the "new" girls – you know who you are). You have been ever so helpful in discussing issues at hand. To say you have also contributed quite a bit in the social part of my life would definitely not be an understatement either. I would also like to thank my parents for supporting me throughout my studies and for always believing in me. Also, I would like to thank my boyfriend who has been a tremendous support during this whole process. And last, but not least, I would like to thank the city of Trondheim, the city where I have lived and studied for over five years. You will always have a special place in my heart.



Runa A. Skarbø
Trondheim, 17th December 2014

Summary

The purpose of this thesis is to determine whether the Northern Sea Route (NSR) is a more cost effective alternative than the Suez Canal Route (SCR) between Asia and Europe, given an introduction of an Emission Control Area (ECA) in the Arctic Ocean.

A case study is performed, based on transport of iron ore between Murmansk, Russia and Tianjin, China. The vessel used in the study is a 75 000 DWT Panamax bulk carrier with ice class 1A. The study is performed for a time period of one year. Actual ice data from 2008 and 2009 is used in the study. A MATLAB model is developed to perform the simulations.

The study compares several scenarios for complying with ECA regulations. The alternative approaches to compliance are either fuel switch, retrofitting the vessel with exhaust cleaning technology, converting the main machinery to also run on alternative fuels or a combination of these. The scenarios in the study are defined as follows:

1. Exhaust cleaning only: The vessel burns only Heavy Fuel Oil (HFO). The vessel is retrofitted with a scrubber to clean SOx emissions, and a selective catalytic reduction (SCR) unit to reduce NOx emissions.
2. Combine fuel switch and exhaust cleaning: The vessel burns HFO outside ECAs, and switch to Marine Gas Oil (MGO) upon entering an ECA. MGO has a negligible sulphur content, and therefore no abatement technologies are required to abate SOx emissions. A SCR unit is retrofitted to reduce NOx emissions.
3. Conversion of main machinery to dual fuel (DF) operation combined with exhaust cleaning: The main engine of the vessel is converted to operate on DF. Thus, the vessel can operate on both HFO and liquified natural gas (LNG). In addition, the vessel is retrofitted with an exhaust gas recirculation (EGR) unit, for reduction of NOx emissions.

Scenarios 1-3 sail on the NSR when the ice conditions allow for sailing. For the case vessel, this is found to be for ice thicknesses below 123 cm. When the maximum ice thickness along the NSR grows thicker than 123 cm, the vessels sail on the SCR.

The performances of scenarios 1-3 are evaluated against a base case. The base case is defined as the vessel sailing only on the SCR for the whole simulation time period, with no emission abatement measures installed. The vessel switch to MGO when sailing through the SOx ECA in Northern Europe.

The scenarios are evaluated based on costs, emissions and cost effectiveness. Investment costs (CAPEX), operating costs (OPEX) and equivalent annual costs (EAC) are calculated for each scenario. For CAPEX and OPEX, only differences from the base case scenario are considered. For emissions, the scenarios are evaluated in terms of total reduced emissions and also reduced emissions per tonne cargo transported. Emissions of CO₂, SOx, NOx and particulate matter (PM) are considered. Also cost effectiveness for reduced emissions and per tonne transported cargo is considered.

Resistance, speed and fuel consumption for the vessel along the NSR vary according to the ice conditions. As emissions are related to both fuel consumption and engine load, emissions and specific fuel consumption are modeled accordingly in the model.

The main findings of the study are as follows:

- By utilising the NSR, the vessels can sail one extra roundtrip each year (six roundtrips on the NSR vs five roundtrips on the SCR);
- Scenarios 1-3 have less total emissions per year than the base case scenario. Scenario 3 give the greatest reductions in total emissions;
- Scenarios 1-3 are more environmentally friendly, and emits less per tonne cargo freight for all emission types;
- The base case scenario is the most cost effective in terms of USD/tonne cargo. All scenarios 1-3 come out relatively equal in cost effectiveness.

The study concludes that utilising the NSR with an ECA in the Arctic Ocean will not be cost effective compared to sailing the SCR. The main reasons for this are the limited operation window on the NSR, the high investment costs of retrofitting abatement technology and the increased operating costs in ECAs due to operation on more expensive fuel.

Sammendrag

Hensikten med denne oppgaven er å bestemme om det er kostnadseffektivt å seile via den Nordlige sjørute, heller enn via Suez-kanalen mellom Asia og Europa, dersom Polhavet blir definert som et område hvor det stilles maksimumkrav til eksosutslipp ("Emission Control Area" (ECA)).

Det er gjennomført studie av transport av jernmalm mellom Murmansk (Russland) og Tianjin (Kina). Skipet som ble brukt i studien er et bulklasteskip på 75 000 dødvekttonn av Panamax størrelse. Tidsperioden for studien er ett år. Isdataene i studien er basert på fra reelle observasjoner fra 2008 og 2009. Modellen som utførte studien ble laget i MATLAB.

Studien sammenligner flere scenarier for å oppfylle kravene som stilles i når man opererer i et ECA. De reelle alternativene er å bytte drivstoff, å ettermontere utstyr som renser eksosgassene eller å konvertere hovedmaskineriet til å kunne gå på alternativt drivstoff. Kombinasjoner av disse tiltakene er også mulig. Scenariene som er betraktet i studien er definert som følger:

1. Bare eksosrensing: Skipet bruker bare tungolje (HFO). En gasskrubber ("scrubber") blir installert for å rense SO_x-utslipp. En "selective catalytic reduction"-enhet (SCR) blir installert for å rense NO_x-utslipp.
2. Kombinasjon av drivstoffbytte og eksosrensing: Skipet bruker tungolje utenfor ECAene, og bytter til gassolje (MGO) når det seiler i ECAer. MGO har svært lavt innhold av svovel, så ingen renseteknologier behøves for SO_x. NO_x-utslipp renses med en etterinstallert SCR.
3. Konvertering av hovedmaskineri til å gå på "dual fuel" (DF) kombinert med eksosrensing: Hovedmaskineriet til skipet blir konvertert til DF-operasjon. Dermed kan skipet operere på både tungolje og metan (LNG). I tillegg installeres en enhet for eksosgassresirkulering (EGR), som reduserer NO_x-utslipp.

Scenario 1-3 seiler via Polhavet når isforholdene tillater det. Skipet kan ikke seile i mer enn 123 cm is. Derfor seiler skipet via Suez-kanalen når isykkelsen langs ruten er tykkere enn dette.

Resultatene for scenario 1-3 blir evaluert mot et sammenligningsscenario. Dette scenarioet seiler bare via Suez Canalen gjennom hele tidsperioden, og har ingen eksosrensemetoder installert. Dette skipet bytter til MGO når det seiler gjennom den Engelske kanal og i Nordsjøen, som er definert som område hvor SO_x-utslipp må begrenses.

Scenario 1-3 er evaluert basert på kostnader, eksosutslipp og kostnadseffektivitet. For hver scenario er investeringskostnader (CAPEX), operasjonskostnader (OPEX) og ekvivalente årlige kostnader (EAC) regnet ut. For CAPEX og OPEX er det bare betraktet kostnader som er forskjellige på de to rutene. For eksosutslipp er scenarioene vurdert ut i fra totale reduserte utslipp og utslipp per tonn last som blir fraktet. Utslipp av CO₂, SO_x, NO_x and partikler (PM) er tatt med i betraktningene. Også kostnadseffektivitet for reduksjon av utslipp og per tonn transportert last er vurdert.

Skipets motstand, hastighet og drivstofforbruk i Polhavet varierer i samsvar med isforholdene. Eksosutslipp er relatert til både drivstofforbruk og motorlast. Dermed er utslipp og spesifikt drivstofforbruk modelert deretter.

Hovedfunnene i studien er som følger:

- Ved å seile via Polarhavet kan skipene seile en ekstra rundtur i løpet av året (seks rundturer via den Nordlige sjørute mot fem rundturer via Suez-kanalen);
- Scenario 1-3 har mindre årlige eksosutslipp enn sammenligningsscenarioet. Scenario 3 har de største reduksjonene for utslipp;
- Scenario 1-3 er mer miljøvennlige enn sammenligningsscenarioet, og eksosutslipp per tonn frakt er betraktelig lavere for alle typer utslipp;
- Sammenligningsscenarioet er det mest kostnadseffektive for kostnad per tonn last som blir fraktet. Scenario 1-3 kommer ut relativt likt på kostnadseffektivitet.

Studien konkluderer med at å seile via den Nordlige sjørute når det er et ECA i Polarhavet vil ikke være kostnadseffektivt sammenlignet med å seile via Suez-kanalen. Hovedgrunnene til dette er det begrensede operasjonsvinduet i Polhavet, de høye investeringskostnadene for å etterinstallere eksosrenseteknologi og de økte operasjonskostnadene i ECAer som følge av operasjon på dyrere drivstoff.

Contents

1	Introduction	1
1.1	Background and motivation	1
1.2	Thesis objectives	2
1.3	Scope and limitations of the study	2
1.4	Structure of thesis	3
1.5	Shipping routes between Asia and Europe	3
1.5.1	The Suez Canal Route (SCR)	3
1.5.2	The Northern Sea Route (NSR)	4
1.5.3	Previous work on comparison of the Northern and Southern routes	5
1.6	Aspects of NSR navigation	5
1.6.1	Navigation in ice	5
1.6.2	Ice conditions	6
1.6.3	Navigational season	6
1.6.4	Traveling times on the NSR	8
1.6.5	Requirements for operation	8
1.6.6	Challenges related to NSR operation	9
1.6.7	Added costs for operation on the NSR	10
1.7	The NSR's potential as a trade route	12
1.7.1	Ports on the NSR	12
1.7.2	Potential for container shipping	12
1.7.3	Potential for LNG shipping	12
1.7.4	Potential for bulk shipping	13
1.8	Air emissions from shipping	14
1.8.1	The combustion process in marine diesel engines	14
1.8.2	Marine fuels	15
1.8.3	Emissions impacts on health and environment	16
1.9	International legislation regulating emissions from shipping	16
1.9.1	Emission Control Areas (ECAs)	16
1.9.2	Energy Efficiency Measures	19
1.9.3	Discussion on emission controls	22
1.9.4	Regulatory consequences for shipping operations	23
1.10	Measures for emission abatement	23
1.10.1	CO ₂ reduction measures	24
1.10.2	SO _x reduction measures	24
1.10.3	NO _x reduction measures	26
1.10.4	Previous work on emission control and ECA compliance	31
2	Modeling of simulations	33
2.1	Vessel model	33
2.1.1	Resistance in open water and ice	35
2.1.2	Available thrust for overcoming ice resistance	43

2.1.3	Attainable speed in ice	44
2.1.4	Attained EEDI for the case vessel	44
2.2	Route modelling	44
2.2.1	Modeling the Suez Canal Route (SCR)	45
2.2.2	Modeling the Northern Sea Route (NSR)	45
2.3	Simulation time period	49
2.4	Operation profile	49
2.5	Definition of scenarios in study	50
2.5.1	Selection of abatement technologies	50
2.5.2	The base case scenario	50
2.5.3	Scenario 1: Exhaust cleaning only	51
2.5.4	Scenario 2: Combine exhaust cleaning and fuel switch	51
2.5.5	Scenario 3: LNG conversion and exhaust cleaning	51
2.6	Modeling machinery and abatement technologies	52
2.7	Modeling of emissions	53
2.7.1	Formation of pollutant emissions in marine diesel engines	53
2.7.2	Modeling of emissions in study	55
2.7.3	Emission reductions from abatement technology	57
2.8	Costs used in study	57
2.8.1	Direct add to costs from abatement technologies	57
2.8.2	Fuel prices	59
2.8.3	Route tariffs	59
2.9	Methods for comparing different scenarios	60
2.9.1	Equivalent annual costs (EAC)	60
2.9.2	Cost effectiveness ratio (CER)	60
2.10	Description of MATLAB model	61
2.10.1	General description	61
2.10.2	Descriptions of main files in model	63
3	Results from simulations	81
3.1	Note on presented results	81
3.2	Results from scenario simulations	81
3.2.1	Results for the base case scenario	81
3.2.2	Results for scenario 1 (exhaust cleaning only)	82
3.2.3	Results for scenario 2 (exhaust cleaning and fuel switch combined)	83
3.2.4	Results for scenario 3 (LNG conversion and exhaust cleaning)	84
3.3	Route and voyage results	85
3.3.1	Voyage duration and freight potential	86
3.3.2	Ice conditions and speed for the voyages	86
3.4	Performance comparison	88
3.4.1	Emissions performance	88
3.4.2	Costs performance	94
3.4.3	Cost effectiveness performance	96
4	Discussion	101
4.1	Emissions performance	101
4.2	Cost performance	101
4.3	Assessment of the framework for the study	102
4.3.1	Modeling of the route and ice conditions	102
4.3.2	Time period of simulations	102
4.3.3	Scenario configuration	102
4.3.4	Cost comparison criteria	102
4.4	Evaluation of MATLAB model	102

4.4.1	Known errors in model	103
4.4.2	Impact of errors on results	103
4.4.3	Simplifications in model	103
5	Conclusion	105
5.1	Future work	105
	Bibliography	107
A	General arrangement of Panamax bulk carrier	113
B	Method for calculation of attained EEDI for a specific ship	115
C	Calculation of attained EEDI calculations for the case vessel	117
D	Diagram to find C_R for slenderness ratio = 5.0	119
E	Diagram to find k for estimating the wet surface S	121
F	Method of determining brash ice resistance	123
G	MATLAB model	125

Nomenclature

α	Waterline entrance angle
CO_2	Carbon Dioxide
Δ	Weight displacement
η_s	Transmission efficiency coefficient
∇	Volume displacement
ν	Kinematic viscosity
ϕ_2	Stem angle between the waterline and the vertical at $B/4$
ρ_{sw}	Density of salt water, 1,025 g/m ³
A_{wf}	Waterline area of the foreship
C_B	Block coefficient
C_M	Midship area coefficient
C_P	Prismatic coefficient
C_{BT}	Correctional coefficient for breadth/draught (B/T) relationship
C_{bulb}	Correctional coefficient for bulbous bow
C_{frame}	Correctional coefficient for frame shape
C_{scale}	Correctional coefficient for scale effects and coarseness
D_p	Propeller diameter
H_F	Thickness of the brash ice layer that is displaced by the bow and is moved to the side along the parallel midbody
H_M	Brash ice thickness
K_e	Quality constant of the bollard pull
L	Characteristic length
L_{par}	Length of the parallel midbody at the waterline
L_{wl}	Length in waterline
P_s	Total propulsion power
R_F	Frictional resistance

R_F	Residual resistance
R_I	Resistance in ice
R_{ow}	Open water resistance
T_{net}	Net thrust
T_{pull}	Bollard pull
V_m	Max speed
V_s	Service speed
per	Pollutant emission ratio
spe	Specific pollutant emissions
AECA	Arctic Emission Control Area
B	Breadth
BC	Black Carbon
CAPEX	Capital Expenditure
CER	Cost effectiveness ratio
CER	Cost effectiveness ratio
DF	Dual Fuel
DWI	Direct Water Injection
DWT	Dead weight
EAC	Equivalent annual costs
ECA	Emission Control Area
EEDI	Energy Efficiency Design Index
EEOI	Energy Efficiency Operational Indicator
EGR	Exhaust Gas Recirculation
EPA	(United States) Environmental Protection Agency
F_n	Froude number
FP	Fixed pitch
FS	Finnish-Swedish (ice class rules)
GA	General arrangement
GHG	Greenhouse Gas
GT	Gross Tonnage
HAM	Humid Air Motor
HC	Hydrocarbons

HFO	Heavy Fuel Oil
IEM	Internal Engine Modification
IEM	Internal Engine Modification
IFO	Intermediate Fuel Oil
IMO	International Maritime Organization
ISO	International Organization for Standardization
LCB	Longitudinal centre of buoyancy
LFO	Light Fuel Oil
LNG	Liquified Natural Gas
LOA	Length over all
LPG	Liquified Petroleum Gas
LPP	Length between perpendiculars
MCR	Maximum continuous rating
MDO	Marine Diesel Oil
MEPC	Marine Environment Protection Committee (IMO)
MGO	Marine Gas Oil
NECA	NO _x Emission Control Area
NO _x	Nitrous Oxides
NPV	Net present value
NSR	Northern Sea Route
NT	Net tonnage
OPEX	Operational expenditure
PM	Particulate Matter
Re	Reynold's number
rpm	Revolutions per minute
SC	Suez Canal
SCR	Selective Catalytic Reduction
SCR	Suez Canal Route
SECA	Sulphur Emission Control Area
SEEMP	Ship Energy Efficiency Management Plan
SFC	Specific fuel consumption
SO _x	Sulphur Oxides

SWS	Sea Water Scrubber
T	Draught
TEU	Twenty-foot equivalent unit
UHC	Unburnt hydrocarbons
VOC	Volatile Organic Compound
WLS	Lightweight

Chapter 1

Introduction

1.1 Background and motivation

There is an extensive shipping activity between Europe and Asia. The most used shipping route today is via the Suez Canal, known as the Suez Canal Route (SCR) or the Southern route. An alternative route, almost half the length of the SCR, is emerging in the Arctic Seas due to the decline in sea ice extent in recent years. This route is known as the Northern Sea Route (NSR). The two routes are shown in Figure 1.1. As the polar ice cap diminishes, the operational window on the NSR increases. The utilisation of the route by merchant vessels has been increasing for each year since the route was first used for commercial purposes in 2009. Both time used and fuel usage may be reduced significantly if the NSR can be utilised, hence sailing the NSR can introduce great savings for the ship owners.



Figure 1.1: The Northern Sea Route is significantly shorter than the Suez Canal Route. Source: ‘Polar bearings’ (2014)

However, some express concerns about the effect of emissions from increased shipping traffic in the Arctic. The region’s has a vulnerable climate and ecosystem, and is believed to have a great significance for the global climate. Due to the substantial air emissions from shipping, the International Maritime Organization (IMO) have introduced measures to limit the emissions. Through the Annex VI in the

MARPOL convention, IMO introduced limits on the main air pollutants in ship exhaust emissions; sulphur oxides (SO_x), nitrous oxides (NO_x) and particulate matter (PM). Some especially vulnerable geographic areas have even stricter regulations, called Emission Control Areas (ECAs). There are several ways of complying with the ECA regulations, both operational and technical. These measures all represent substantial costs, either as investments or as operational costs or both. Hence, the cost of complying with the ECA regulations may be substantial, and ship owners must evaluate the economic situation for operating in ECAs. Existing ECAs under Annex VI are the North Sea and English Channel, the Baltic Sea and the North American coast lines (IMO, 2014f). More areas are expected to achieve ECA status in the future. The Mediterranean Sea, the Melacca Strait and the Japanese coastal waters have all been proposed as potential candidates (Meech, 2010). Some have also proposed the Arctic Ocean as a future candidate for ECA status (Meech, 2010). However, no actual plans of this currently exist.

1.2 Thesis objectives

The topic of comparing sailing on the NSR vs the SCR has been extensively studied in recent years, as a consequence of the declining sea ice extent and the forecasted further decrease. Also compliance strategies for ECA regulations and the cost effectiveness of the alternatives have been studied. However, the combination of these scenarios has not yet been studied in any published works. Therefore, the main research question of the study was formulated as follows:

- Will combining operation on the Northern Sea Route (NSR) and the Suez Canal Route (SCR) be more cost effective than only sailing on the SCR, given an introduction of a new emission control area (ECA) in the Arctic Ocean?

Furthermore, supporting research questions were formulated:

- What are the additional costs of sailing the NSR, compared to sailing the SCR?
- What are the additional costs that will apply for ship owners operating on the NSR if an ECA is introduced in the Arctic Ocean?
- Which alternatives do the ship owners have for complying with ECA requirements?
- What method of ECA compliance is the most cost effective for an existing vessel?
- How does sailing in different ice concentrations and thicknesses affect the emission rates from the vessel?

A study was performed in order to answer the research questions. The scope of work for the study is given in section 1.3.

1.3 Scope and limitations of the study

The framework of the study shall be determined. A model shall be developed to evaluate the framework. The model should be able to simulate a time period of operation for a specific case vessel, and give output on costs, emissions and operation profile. Thus, analysing the results of the model shall give answers to the research questions.

A base case, sailing only on the SCR shall be defined as the foundation for comparison for scenarios sailing which utilise the NSR. Several approaches to comply with the constructed Arctic ECA compliance shall be defined in the study. The model shall be able to analyse the different scenarios, and give the required output for each scenario. Ice conditions along the NSR for the whole simulation period shall be included in the model. Thus, the model shall consider the operating conditions on the routes, and

select routes accordingly throughout the time period. Based on the operating conditions on the NSR, an operational profile shall be developed. Further, the performance of the vessel along the NSR shall reflect the ice conditions. The emissions from the vessel should be modeled to consider the varying operating conditions. A framework for evaluating the costs of the scenarios shall also be developed.

The study is limited to a one year time series study only, based on historical ice data. No future predictions are to be made regarding ice extent in the Arctic. Further, the study shall only consider the differences in cost between the base case and the scenarios utilising the NSR. Only mature and tested technologies shall be evaluated in the scenarios, in order to get realistic cost figures.

1.4 Structure of thesis

This thesis is composed by five main chapters. The contents of the thesis are described below.

The remaining part of chapter 1 gives a general introduction of the relevant topics for the thesis. The framework for the simulation study is presented in chapter 2. The chapter explains the methods which are used in the calculations. Also, the MATLAB model who was developed is presented and explained in detail. Findings and results are presented in chapter 3. Lastly, the results are discussed in chapter 4. Concluding remarks and advice for further work are finally given in chapter 5. Additional information can be found in the appendices. The text will refer to appendices where relevant.

1.5 Shipping routes between Asia and Europe

As mentioned in section 1.1, the main shipping route between Asia and Europe has traditionally been the Suez Canal Route (SCR). This section describes the conventional Suez Canal Route and also the alternative sailing route via the Northern Sea Route.

1.5.1 The Suez Canal Route (SCR)

The SCR is a well established shipping route between Asia and Europe, with thousands of vessels passing each year. From Far East Asia, the route passes through the South China Sea, the Malacca Strait, past the southern tip of India, enters the Gulf of Aden, through the Suez Canal (SC), across the Mediterranean Sea, through the Gibraltar Strait and around the west side of Europe to reach the north European ports.

There are restrictions on vessel dimensions when sailing the SCR due to restrictions in the SC. The maximum allowed vessel dimensions for the SC are shown in Table 1.1. However, the Egyptian government has recently announced that they will expand the canal (Holmes and Kalin, 2014). The project is to be completed within five years. In consequence, limitations on vessel dimensions may be insignificant in the future.

Table 1.1: Restrictions on maximum vessel dimensions in the Suez Canal. Sources: SCA (2007); SCA (2010)

Dimension	Max
Length	No restrictions
Beam	77.5 m
Air Draught	68 m
Draught, ballast	12.1 m
Draught, loaded	20.1 m ^a

^aFor vessels with a beam of 50 m or narrower. For wider vessels, the draught restriction increase.

Currently, there is only one ECA along the SCR, the SO_x ECA (SECA) in the English Channel and the North Sea. Although no concrete plans exist at the current time, the Mediterranean Sea is expected as

a strong candidate to be classified as an ECA in the years to come (Halvorsen, 2010; Meech, 2010). Also the Malacca strait has been brought up as a possible candidate for future ECA status (Meech, 2010).

The Gulf of Aden has in the later years had issues with pirate activity. The piracy threat increase the insurance costs, and also poses a hazard for the crew. The number of attacks has decreased significantly in recent years, due to the extensive military and private security presence in the region, the hardening of vessels and the stabilizing influence of the Somali government. Even so, piracy is still considered a significant threat in the region (Schuler, 2014).

In addition to the sailing costs, canal tolls for the SC incur for vessels sailing on the SCR. Suez Canal fees are easily calculated based on the tonnage of the vessel.

1.5.2 The Northern Sea Route (NSR)

The Northern Sea Route is the Russian name of the sea lanes running north of Siberia – sea lanes which connect the northern parts of the Atlantic and Pacific Oceans (Ragner, 2000). The route connects the Barents Sea in the west with the Bering Sea in the east. In between, the route passes through the Kara, Laptev, East Siberian and Chuckchi seas, before reaching the Bering Strait. The route is illustrated in Figure 1.2. By sailing via the NSR, the total route distance between Asia and Europe can be up to 50 % shorter compared to the SCR.



Figure 1.2: Map of the Northern Sea Route. Source: Ragner (2000)

The NSR has been utilized for many years by Russia and the Soviet Union to supply the local Siberian communities and export natural resources. Russia is now taking steps to make the NSR a viable and attractive option for foreign ship operators. Since 2009, the number of vessels that have used the route has increased strongly every year. Although the traffic on the NSR has increased significantly over the later years, the route is still not in direct competition with the SCR. 71 vessels sailed on the NSR in 2013, while over 17,000 vessels traversed the Suez Canal (Kendrick, 2014).

Even though the amount of ice is declining, the route is still not ice free. Although some merchant ships have passed the route without escort of icebreakers in summer, most ships require icebreaker escort. Actually, the demand for icebreakers on the NSR is growing so large that, Atomflot, the company that operates Russia's icebreakers, will no longer escort tourist expeditions to the North Pole after 2015, in order to be able to cover the demand from commercial shipping (Staalesen, 2014). However, Russia's icebreaker fleet is aging, and despite lifetime extension efforts, several of the icebreakers will inevitably be decommissioned in the coming years (Ragner, 2008). This can result in more inaccessible icebreaker

services in the future. Regardless, Atomflot has recently ordered three new icebreakers, to be delivered in 2019 and 2020 (Pettersen, 2014), which will hopefully relieve the situation. The icebreakers are also larger than the current ones in operation, making it possible for wider ships to navigate in icebreaker channels in the future.

Section 1.6 aims to further explore the viability of the NSR as an alternative trade route to the SCR.

1.5.3 Previous work on comparison of the Northern and Southern routes

Comparisons of the Suez Canal (sometimes referred to as the “Royal Route”) and Arctic routes has been widely explored in recent years, due to the receding polar ice cap.

After making the route open for foreign vessels in 1991, the Russians wanted to attract large-scale shipping on the NSR. This led to the Russian-Norwegian-Japanese International Northern Sea Route Programme (INSROP) from 1993 to 1999. The six year research programme aimed to create an extensive knowledge base of the NSR. The conclusions from the programme was that the NSR had “considerable commercial potential” (Ragner, 2000), though this depended on Russia’s ability to accommodate the needs and requirements from the international shipping industry.

As a part of the INSROP, Shinagawa (2000) were not positively impressed, due to the lack of possibilities to transport the cargo safely, on schedule, speedily and cheaply. Shinagawa (2000) concluded that the NSR had most potential for transporting cargo from Russian NSR areas and for transporting special cargo that may meet with difficulties passing through coastal areas of other countries.

Sørstrand (2012) found that the ice classed vessels were marginally more profitable using the NSR during summer and the SCR in winter, than a similar vessel without ice class sailing the SCR all year. The profitability of the NSR route was found to be highly dependent on ice conditions.

Verny and Grigentin (2009) compared container shipping between Shanghai and Hamburg, and found the cost of transporting one container (TEU) along the NSR was about twice as high as along the SCR.

1.6 Aspects of NSR navigation

This section discuss aspects of navigation on the NSR.

1.6.1 Navigation in ice

Navigation in ice provide huge challenges to the structure and operation of ships. The first ice rules were given in 1890, and are still continually updated (Riska, 2013).

All classification societies, except the Russian Register, have adopted the International Association Of Classification Societies’ (IACS) ice classes (Riska, 2013). The Finnish-Swedish (FS) ice class rules are aimed at Baltic operations, but are also used as a reference for classing ships operating in other areas with ice condions. The Russian Register’s ice class ‘Arc4’ are equivalent to the FS ice class notation 1A.

According to Riska (2013), all ice rules contain some of the following components:

- Requirements for hull scantlings, in order not to damage the hull by the ice action;
- Requirements for the shaft line, so the propeller and the propeller shaft line and it’s components are not damaged, and
- Requirements for ship power, so the ship performance in ice is adequate for the trade in the sea area.

Due to the extra steel weight of ice strengthening, the vessel’s lightship weight will increase as a consequence of ice classification. Figure 1.3 shows the additional steel required for three different polar classes as a function of container vessels size. Also the brake power for the ship will increase, as the extra resistance from the ice must be overcome in addition to the open water resistance.

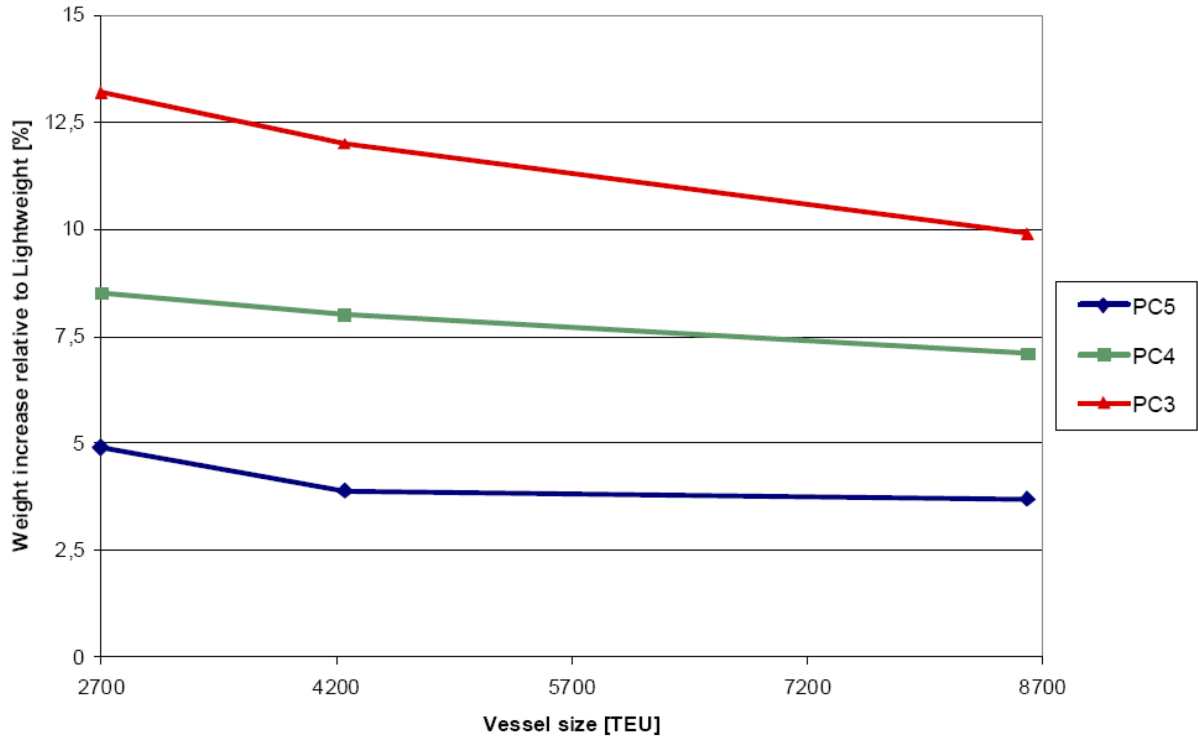


Figure 1.3: Additional steel for ice strengthening for container vessel. Source: DNV ('DNV ARCON-project')

1.6.2 Ice conditions

Arctic temperatures has risen considerably the recent years, and the sea ice concentrations has seen a steady decline Østreng et al., 2013. This can easily be observed in Figure 1.4. Even though the ice extent is declining, most vessels still need icebreaker support throughout the year. However, this may change in the future if the decline continues as predicted.

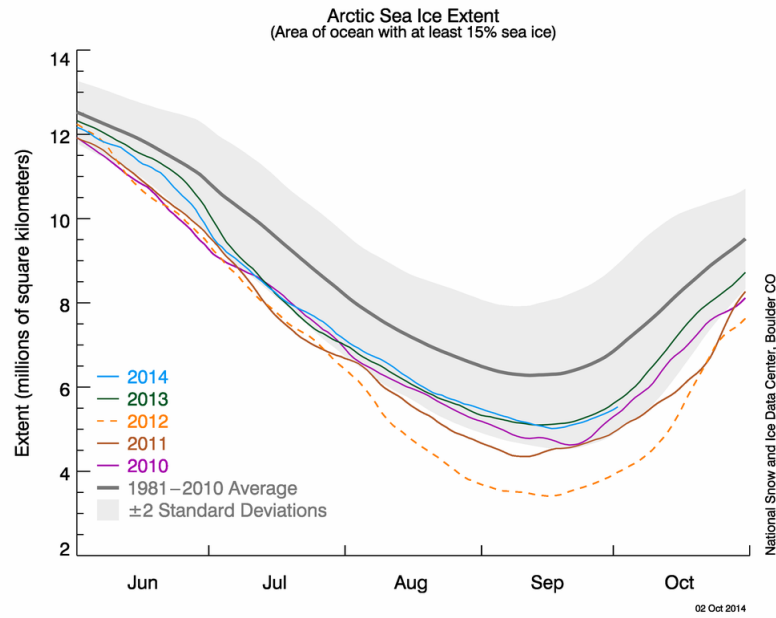
All NSR seaways are located in areas with first year ice, seen from Figure 1.5. First year ice grows up to 1.6 metres in Arctic conditions (NSRIO, 2014).

1.6.3 Navigational season

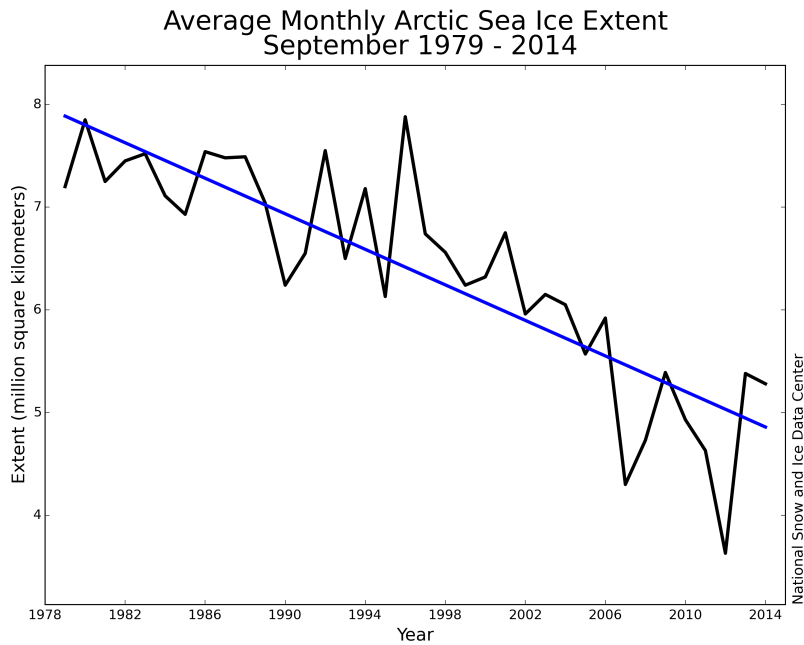
Due to the ice extent, the NSR can only be navigated during parts of the year. According to NSRIO (2014), the navigation season for transit passages on the NSR starts approximately at the beginning of July and lasts through to the second half of November. In September and October, the route may be completely ice free, and vessels may navigate with open water speeds. There are no specific dates for commencement and completion of navigation, it all depends on the current ice conditions.

In 2011, the navigational season lasted for 141 days. Russia's biggest shipping company, Sovcomflot, reported in 2013 that they were able to offer trans-shipment along the NSR for up to six months of the year (Staalesen, 2013b).

Due to varying ice conditions, keeping a fixed schedule on the NSR may prove difficult. This uncertainty is a drawback for the route, especially with regards to shipping which requires predictability.



(a) Arctic sea ice extent as of 2014-10-02. Daily ice extent data for four previous years are also shown.



(b) Monthly September ice extent for 1979 to 2014

Figure 1.4: Sea ice extent. Source: NSIDC (2014)

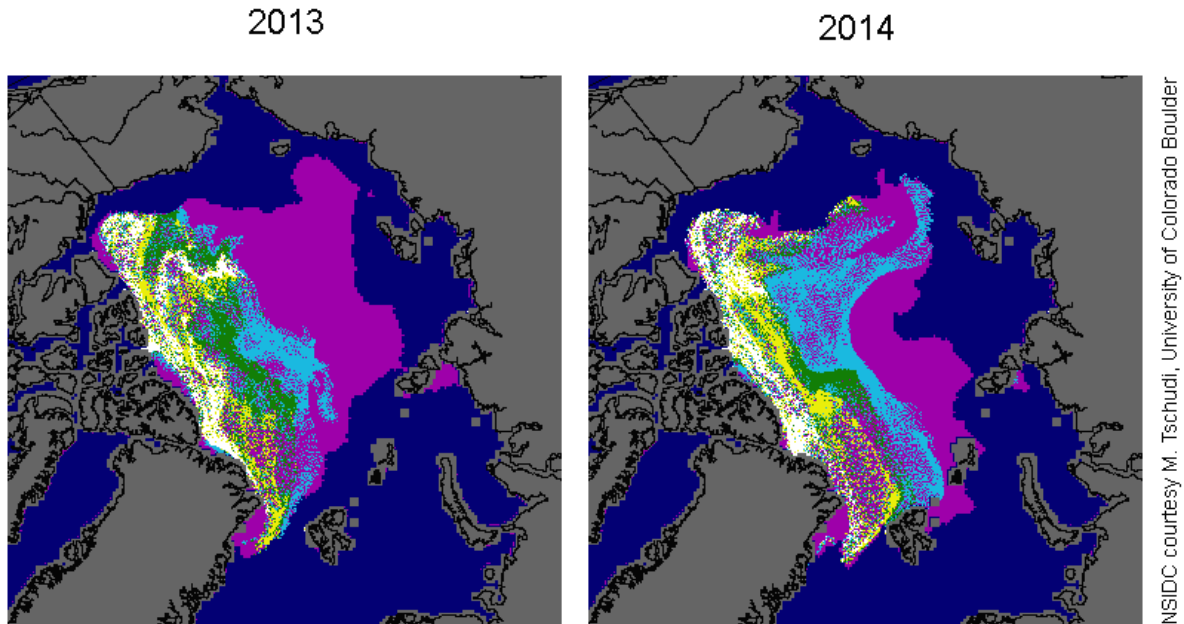


Figure 1.5: Ages of the ice in the Arctic in September 2013 and 2014. Purple colour represent first year ice. Source: NSIDC (2014)

1.6.4 Traveling times on the NSR

The traveling time on the NSR highly depend on the ice conditions. Therefore, the traveling time can be difficult to estimate. Also waiting time for icebreaker support can be unpredictable, and add to the total travel time on the NSR.

Reimer and Duong (2013) developed a model that predicted traveling time and emissions on the NSR within the years 2000 and 2007 with various ice conditions. In the study, they found a significant decrease of traveling time for 2007 compared to 2000 due to the decrease of ice extent. Additionally, they found that the shorter distance on the NSR compared to the SCR lead to a decrease in total consumed amount of fuel.

Erceg et al. (2013) performed a study assessing the performance along the route from Rotterdam to Yamal for the period between 2013 until 2050, using ice forecasting trends. They found an increasing trend in number of roundtrips, from five in 2013 to eight in 2050.

1.6.5 Requirements for operation

The Russian government via the NSR Administration sets criteria for navigation on the NSR. The *Rules for navigation in the Northern Sea Route water area* define the admittance criteria for navigation on the different seas along the NSR according the vessel's ice class. The admittance criteria is defined both for independent navigation and also for icebreaker support. The criteria are define whether navigation is allowed or not in light, moderate and severe ice conditions, according to the definition by the Rosgidromet official information.

Vessels without ice reinforcement are only allowed to independently navigate in the Northern Sea Route water area in open water (NSRIO, 2014), and can sail on the NSR with icebreaker support in light ice conditions. Vessels with lower ice classes than 1A are only allowed to navigate on the NSR in the period July to 15th of November. Vessels with ice class 1A and higher can navigate on the NSR throughout the whole year (NSRIO, 2014). For ice class 1A, independent navigation requires light ice conditions.



Figure 1.6: A convoy of ships in ice. Source: Riska (2013)

Both icebreaker support and ice pilotage is available. Due to icebreaker channel width, ships navigating the NSR assisted by icebreakers should have a maximum breadth of no more than 30 m (Ragner, 2008). The new icebreakers will have a width of 33 m, so the restrictions on breadth will be less in the future. Alternatively, two icebreakers can be utilised and the beam restriction will then be doubled to 60 m. This will increase cost significantly. Maximum draught should be 17 m, due to depth restrictions. Vessel dimension restrictions are listed in Table 1.2.

Table 1.2: Restrictions on vessel dimensions for ships navigating the NSR. Source: Ragner (2008)

Dimension	Max
Breadth	30 m ^a
Draught	17 m

^a60 m if two icebreakers are utilised.

1.6.6 Challenges related to NSR operation

There are several issues related to navigating in Arctic waters, both due to the climate, the lack of infrastructure and also to the geographical location.

Depth mapping is currently lacking along the route. This is a critical issue, as parts of the NSR passes through straits with a depth of less than ten meters. Large ships mostly follow a route north of the New Siberian Islands, which is at least 18 meters deep. According to the Department of State Policy for Maritime and River Transport of Russia, they have expanded their hydrographic work, and have commissioned work to cover the white spots on maps that lack depth data in 2015 and 2016 (Kendrick, 2014). Mapping and charting will also be addressed in the IMO's Polar Code.

Search and rescue is also a critical issue, as the Northern Russia is largely uninhabited and lacks infrastructure. As of today, icebreaker escort is the first instance in search and rescue operations. However, Russia is planning to have ten search and rescue centers along the route by next year (Kendrick, 2014).

The cold temperatures during the winter half of the year poses a challenge for operation. Winterization should be performed, meaning to design the ship's system so they can withstand the cold environment. This could i.e. be heating of ballast tanks and sea chest and additional corrosion protection due to ice abrasion. The stability should also be sufficient taking into account the probability of icing (HELCOM, 2004).



Figure 1.7: Icing on the manifold on deck of a tanker. Source: Riska (2013)

Also, the route's far north location provide additional challenges. Weak satellite signals and consequently poor communication can result in unsafe navigation. In addition, winter darkness can pose as a threat, and sets additional demands to light and radar equipment on board. In the summer, the route is light all day round, which ensures more safe navigation. This may be a challenge to crew that is not used to the midnight sun. The all day lightness can result in sleeping problems for the crew, resulting in tired crew on duty with less awareness.

According to Gold (2000), operation in close proximity of icebreakers require highly trained crew. This could require special training for the crew and/or use of Russian ice-pilot while navigating the NSR.

1.6.7 Added costs for operation on the NSR

The costs of using the NSR can increase compared to using the southern route due to a number of reasons. Costs that could be included when analysing the NSR are costs of icebreakers, ice-pilots, possible delays, cargo damage due to temperature variations, possible ice-damage, higher hull and machinery and liability insurance costs (Gold, 2000). The following sections explore some of these costs, and give estimates as to their influence on the total costs.

Investment costs

The initial investment costs will increase for ice classed vessels, due to several factors. Increased construction cost due to ice strengthening. According to Erikstad and Ehlers (2012), this is in the order of 6 % to 12 % for FS ice classes 1C to 1AS respectively. Another reason for increased investment costs for an ice classed ship is the increased size of the propulsion plant. Winterization, such as deck heating, deck machinery coverings, etc, also adds up.

Operating costs

The higher resistance in both ice and open water for an ice classed hull will contribute to increase the operational costs for the vessel. The higher resistance in open water stems from the increased weight and the altered bow shape (Erikstad and Ehlers, 2012). According to Erikstad and Ehlers (2012), the increased costs can be assumed to be in the range of 5 % to 15 % for a vessel sailing at about 21 knots.

Voyage cost

The voyage costs are influenced mostly as savings, due to the reduced fuel consumption. As the NSR route can be more than 50 % shorter, fuel savings can be significant. The fuel consumption is of course dependent on speed. Slow steaming on the NSR will increase the savings additionally.

The Russian government charges fees for icebreaker assistance. The administration of the NSR is very bureaucratic and has little transparency. Applications to traverse the route must be filed months in advance (Østreng et al., 2013). The route fees are hard to compare, as Russia does not have set tariffs for passing the NSR. Regardless, an “icebreaker support fee” must be paid, even if no icebreaker support is required.

The size of the fee is difficult to determine. According to Østreng et al. (2013), it is dependent on a number of factors, such as:

- Type of ship/cargo,
- Size of ship,
- Ice class of ship,
- Ice conditions,
- Competences of captain and crew and
- The actual route.

The fees can also be negotiated. Østreng et al. (2013) lists average icebreaking fees for major cargo types from 2003. The fee varies significantly in USD/ton, on average 23 USD/ton. However, according to Erikstad and Ehlers (2012) it can be as low as 5 USD/ton, which is similar to the Suez Canal fee. The general director of Atomflot has expressed that the cost of using the NSR should not be particularly higher than the Suez Canal fees (Pettersen, 2010).

Also increased insurance costs need to be considered. Erikstad and Ehlers (2012) claim that a medium sized vessel can be expected to pay an insurance fee of 40,000 USD per transit on the NSR. According to Levander (2009), the annual insurance costs can be estimated as 0.8 % of the ship price, which amounts to approximately 340,000 USD for a typical Panamax bulk carrier. Thus, the additional insurance fee for the NSR is a significant cost, especially for a vessel that makes several trips on the NSR each year. However, the fee is comparable in size to the additional insurance fee for piracy threats near the Gulf of Aden on the SCR (Erikstad and Ehlers, 2012). Therefore, the number of trips will be the determining factor for the total difference in insurance costs.

Regardless, the number of pirate attacks has been declining the recent years. Thus, the additional “pirate insurance fee” can be expected to be reduced or disappear in the future. But there is no reason to assume that the increased insurance cost on the NSR will decrease in near future. Most likely, better infrastructure, hydrographic mapping and search and rescue availability must be in place on the NSR before this insurance fee is reduced significantly.

Lost opportunity costs

For weight constrained vessels, the additional steel weight of the ice classed hull can lead to reduced cargo carrying capacity. The lost opportunity costs corresponds to the reduced freight income. The case vessel is a bulk carrier, which is weight constrained for heavy cargoes such as iron ore. As discussed in section 2.1, the vessel’s increase in lightweight due to ice class was assumed to 4 %, which corresponds to approximately 575 tonnes. The case vessel has a maximum cargo capacity of 75,600 tonnes, so the increase in lightweight corresponds to a reduction in cargo carrying capacity of only about 0.75 %. Thus, the reduced freight income is small for a ship of this size, and will not be included in the study.

1.7 The NSR's potential as a trade route

This section will look at the potential for utilising the NSR for the following trades:

- Container shipping,
- LNG transport and
- Bulk shipping.

1.7.1 Ports on the NSR

The port of Murmansk is one of the largest transportation hubs in Russia (Østreng et al., 2013). The port is ice free, and operate on a year-round basis. Large amounts of oil, coal, minerals and other type of cargo is shipped from here each year. The main limiting factor is that its port is currently unable to accommodate vessels larger than 45,000 DWT. However, with more traffic on the NSR and larger icebreakers that can support larger vessels, the port is expected to expand it's facilities in coming years (Østreng et al., 2013). There are several other ports on the NSR. However, most ports and terminals are small and support only domestic shipping. The operational status throughout the year is also uncertain.

1.7.2 Potential for container shipping

Container shipping between Asia and Europe is extensive. The first container vessel sailed on the NSR last year, the 19,000 DWT chinese vessel "Yong Sheng" (Staalesen, 2013a). It reported to save two weeks of sailing time between China and Rotterdam.

A liner trade may be difficult to sustain on the NSR. The uncertainty related to ice conditions and availability of icebreaker support makes scheduling and reliability an issue. Although great time savings are possible, shippers and cargo owners in container shipping are heavily dependent on a reliable schedule. Additionally, a liner trade such as container shipping often stops in multiple ports underway, as the containers' origins and destinations differ widely. On the NSR there are only small ports and local communities, which would likely not be of interest for transshipment. This would mean that cargo containers would have to have largely the same origin and destination, which makes cargo extent more limited. In addition, the economy of scale effect is great in container shipping. Cheap transport is already available, made possible by gigantic new vessels. One example is the Maersk Group's new Triple E-class container vessels of 165,000 DWT and a beam of 59 m (Maersk Group, 2014). Vessels operating on the NSR would have to be less than half the size of these vessels, which would make competing hard.

1.7.3 Potential for LNG shipping

The discovery of large amounts of natural gas in the Barents Sea has lead to liquified natural gas (LNG) production in Arctic areas in Norway and Russia. The LNG terminal Snøhvit in Hammerfest produces over 5 billion Sm³ tons of LNG annually (NPD, 2013). A great part of the production is exported through pipelines, but a substantial amount is also exported by ship. At peak production, a LNG tanker leaves Hammerfest every five or six days with 150,000 m³ LNG (Nilsen, 2010).

The original plan for the Hammerfest plant was to export the production to the US markets, but since the discovery of domestic shale gas, the US import of foreign gas stalled. On the other hand, in the wake of the 2011 Fukushima nuclear plant disaster, Japan was in desperate need of alternative energy sources to replace the lost power production. As a consequence they turned to importing fossil fuels, especially gas. Hence, the first transport of LNG along the NSR took place in 2012, when the ice-classed tanker "Ob River" transported 66,500 tons (approx. 135,000 m³) LNG from Hammerfest to Japan (Tobata). The distance to Japan from Hammerfest via the NSR is almost half compared to the SCR, with estimated time savings of up to 20 days (Nilsen, 2012).



Figure 1.8: Icebreakers escorting the “Ob River” in 2012. Source: McGrath (2012)

On the Russian side, as a part of the Yamal LNG development in the Russian Arctic, preparations are also being made to export gas. Last year, Yamal LNG signed a tender with Daewoo to build Arc7 ice class LNG tankers (DownstreamToday, 2013; SCF Group, 2013). The 170,000 m³ tankers are being designed for year-round transport, capable of operating down to temperatures of -50°C and breaking ice up to 2.1 m thick. They will be fitted with a diesel-electric propulsion system with three Azipods, each with an output of 15 MW. Delivery will take place in 2016.

LNG tankers are expensive vessels. However, their cargo is so valuable that the profit margins are huge. Also, it is conventional that newbuilt tankers run on LNG machinery. The convention is that boil off from the cargo may be used by the ship operator, which leads to a heavy favourisation of LNG machinery in LNG tankers. This machinery type eliminates some of the emission concerns, as previously mentioned. Additionally, exhaust cleaning equipment would make up only a small fraction of the total investment cost for such a vessel. This makes the comparison not that interesting to look at, compared to other trades.

1.7.4 Potential for bulk shipping

There are substantial exports of iron ore from Northern Europe, both from Norway and Russia. The bulk trade is dominated by tramp shipping.

Bulk ships are generally cheap vessels, and the profit margins are small. The majority of costs related to the shipping is fuel costs. To install exhaust gas cleaning equipment would be a considerable investment on such a vessel. The uncertainty in sailing schedule is not a big concern in tramp shipping. Cargo owners are usually more flexible with regards to delivery times, and the hurry is not so great as with for instance container shipping. The uncertainty can also be accounted for in the charter party, with flexible pick up and delivery times. In addition, one cargo may utilise the whole ship's capacity, especially with small ships that can operate on the NSR, so the problem with multiple stops, such as in container shipping, can be eliminated.

Bulk ships that operate on the NSR in summer may for instance operate in the Baltic Sea or sail on

the SCR during the winter season.

1.8 Air emissions from shipping

Emissions from the maritime transport sector are a significant source of air pollution (Miola et al., 2010). IMO's MARPOL convention from 1973 was established to prevent and minimize pollution from ships, and has been revised and annexed a number of times since. MARPOL Annex VI, first adopted in 1997, limits the main air pollutants from ship exhaust gas.

1.8.1 The combustion process in marine diesel engines

The primary energy transformation in conventional machinery systems is by combustion of fuel and air:

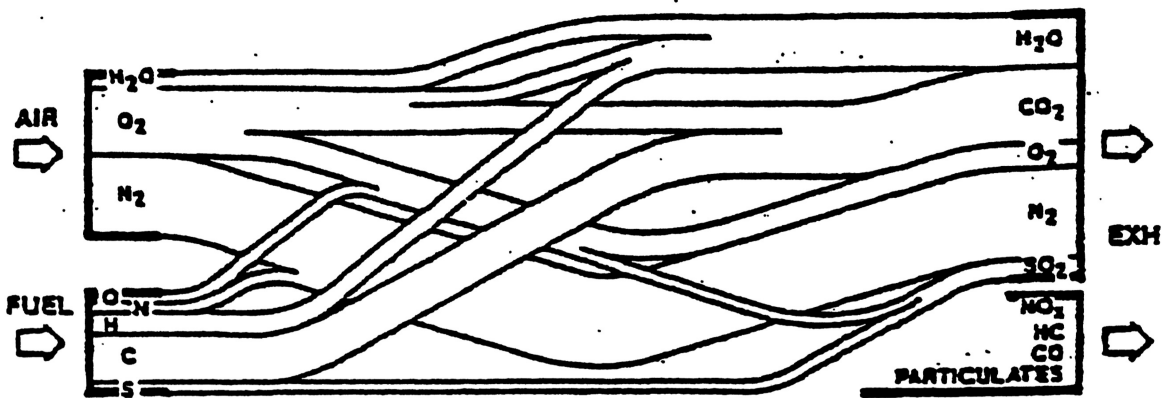
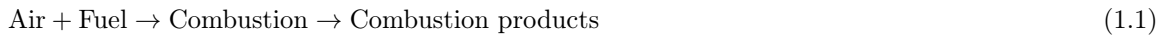


Figure 1.9: Transformation of fuel and air constituents to combustion products in a diesel engine combustion process. H_2O , CO_2 , O_2 , N_2 and SO_x are determined by the air and fuel composition, while NO_x , HC , CO and particulate matter formations are determined by the combustion process. Source: Valland (2008)

During the combustion process, the chemicals in the fuel and air are transformed to combustion products. Figure 1.9 illustrates the transformation of the air and fuel constituents into combustion products during the combustion process, and also the other substances that are formed as a function of the combustion process. The composition of the combustion products depend on both the composition of the air and the fuel, and also the mass relationship between fuel and air. Given that there are sufficient amounts of oxygen present, the carbon content in the fuel will form carbon dioxide (CO_2). The hydrogen in the fuel will form water vapor (H_2O), and the sulphur form sulphur dioxide (SO_2). The nitrogen in the air reacts only to a small extent with the other substances, and will exist as nitrogen (N_2) in the combustion products. Accordingly, the fuel's content of carbon, hydrogen and sulphur determines the emissions of CO_2 , H_2O and SO_2 .

However, the combustion process is rapid and happens under such circumstances that complete combustion is not possible. Other substances are also formed during combustion, such as noxious gases and particulate matter. The formation of these substances depend on the physical factors of the combustion process, such as the mixing of fuel and air, flow velocity, turbulence intensity, pressure and temperature. Furthermore, chemical reaction speeds and combustion time are also important factors. These substances are formed in much smaller quantities than the combustion products. For a marine diesel engine, the total

amount of such substances is typically in the range of 0.25 % of the total amount of combustion products (Valland, 2008).

Table 1.3 lists which composition products are determined by the fuel and air composition and mass ratios, and which are determined by the combustion process.

Table 1.3: Determining factors for diesel engine combustion products. Source: Valland (2008)

Determined by fuel and air	Decided by the combustion process
H ₂ O	CO
CO ₂	HC
O ₂	NO _x
N ₂	PM
SO _x	

1.8.2 Marine fuels

There are several grades of marine fuels in use today. Generally, they can be divided in distillate and residual fuels. Distillate marine fuels are comparable to other distillate hydrocarbon liquids. Residual marine fuels, also called Intermediate Fuel Oils (IFO) or Heavy Fuel Oils (HFO), are composed of heavy, residuum hydrocarbons which is a by-product from the petroleum refining process. The fuels may contain contaminants such as heavy metals, water and high sulphur levels, which may harm engines and fuel distribution lines. For this reason, residual fuels are cleaned and treated before combustion. Both fuel types are required to meet international fuel specification as established by the International Organization for Standardization (ISO) (US EPA, 2009).

Marine distillate fuel is divided into four fuel types: DMX, DMA, DMB, and DMC. DMX is a very low sulphur fuel, and is usually quite expensive compared to the others. DMA and DMB are often called Marine Gas Oil (MGO) and Marine Diesel Oil (MDO) respectively. These comprise the majority of marine fuel oils that are sold today. DMC is a higher sulphur fuel.

Marine residual fuel is categorized based on the viscosity of the fuel at a set reference temperature. These fuels have such high viscosities that they are almost solid at room temperature, and require constant heating to effectively pump and combust it in diesel engines. According to US EPA (2009), the most commonly used fuel in the marine transportation industry is Intermediate Fuel Oil (IFO) 180 and 380.

Natural gas (LNG) as a marine fuel is a technology which is maturing rapidly. It has received increasing attention as bunker fuel prices has risen over the last years and there are increasing focus on reducing emissions.

LNG is largely made from methane (CH₄), and have a different chemical composition than the conventional marine fuels. By using LNG, SO_x emissions are negligible and only small amounts of NO_x and PM are emitted. Additionally, it reduces CO₂ emissions (Nikopoulou et al., 2013).

LNG prices vary with geographical locations. Availability has also been an issue. Only a few ports provide LNG bunkering facilities at the present moment. However, many ports are planning to develop such facilities in the future (Acciaro, 2014).

LNG is capital intensive, and ship owners are reluctant to choose LNG machinery due to the uncertainty of the future supply for bunkering. Also, natural gas suppliers are hesitant to invest in bunkering terminals without longterm supply contracts from ship owners (Graykowski, 2013). However, LNG terminals are observed “popping up” in existing ECAs. Thus, more ECAs may push the shipping industry towards more LNG operation.

1.8.3 Emissions impacts on health and environment

Main air emissions from ships include sulphur dioxide (SO₂), nitrogen oxides (NO_x), volatile organic compounds (VOCs), particulate matter (PM) and carbon dioxide (CO₂) and other greenhouse gases (GHGs). The effects of these pollutants are well documented, as they affect air quality and contribute to climate change and human health issues. Impact on local (or regional) air quality are mainly linked to pollutants such as PM, NO_x and sulphur, while the GHGs have a global impact on climate.

PM and NO_x have negative effects on local air quality and human health. Nitrogen oxide emissions can cause acid rain and nutrient overload in water bodies, which can lead to eutrophication¹. Health problems include premature mortality and asthma attacks. In addition, particles and NO₂ can have impacts on visibility by reducing the visual range.

SO₂ emissions are also detrimental to public health. Sulphur particles can induce asthma, bronchitis and heart failure. Sulphur emissions over open seas are spread out and the effects are moderated. However, in certain areas the emissions create environmental problems, especially on routes with narrow passages and heavy traffic such as the English Channel, the South China Sea or the Strait of Malacca (IMO, 2014a).

Both sulphur and nitrogen compounds can also cause acid depositions that can be detrimental to the natural environment. Emissions of these components can affect vegetation and land-based objects thousands of kilometers away.

An additional contribution from shipping to climate change is from black carbon (BC). BC amounts to approximately 10 % of the total PM emitted from shipping activities (Miola et al., 2010). By absorbing the energy from the incoming sunlight, BC reduces the albedo effect² of the surface it covers (Dalsøren et al., 2013). This leads to a hotter climate, hence more melting of snow and ice. As more melting occur, surfaces uncovered have less albedo, and so even less heat is reflected, which in turn results in more melting. Hence, emissions of BC contributes to an acceleration of the snow and ice melting process and thus the global warming process.

1.9 International legislation regulating emissions from shipping

This section presents which emissions from shipping that are regulated by legislation. It also presents the controls of regulation. Table 1.4 give a summary of which emissions are currently regulated.

Table 1.4: Air pollutants and regulatory measures

Emissions	Legislated through IMO	How
SO _x	Yes	Cap on fuel sulphur content
NO _x	Yes	Emission limits in designated areas
CO ₂	Indirectly	Minimum efficiency level per capacity-mile
CO	No	
PM	No	

1.9.1 Emission Control Areas (ECAs)

IMO has introduced emission control areas (ECAs) to reduce emissions of SO_x, NO_x and/or PM in designated sea areas (IMO, 2014d). Existing ECAs under Annex VI are the North Sea and English Channel, the Baltic Sea and the North American coast lines (IMO, 2014f). Other areas are expected to follow in the future, such as the Mediterranean and Arctic Ocean (Meech, 2010; Ågren, 2011).

¹Excessive richness of nutrients in a lake or other body of water, which causes a dense growth of plant life and death of animal life from lack of oxygen.

²A materials ability to reflect radiation.

Limits on SO_x and particulate matter emissions (PM)

In order to reduce emissions of SO_x and PM, MARPOL Annex VI, Regulation 14, introduces limits on sulphur contents of fuel oil. The controls divide between those applicable inside ECAs established to limit emission of SO_x and PM (SECAs), and the global limits. The limits are introduced in a series of step changes, as given in Table 1.5 and Table 1.6.

Table 1.5: Global fuel oil sulphur content limits. Limits are expressed in terms of % m/m (by weight). Source: IMO (2014h)

Date	Sulphur content limit
Before 2012-01-01	4.5 %
From 2012-01-01	3.5 %
From 2020-01-01 ^a	0.5 %

^aSubject to a feasibility review to be completed by 2018. Could be deferred to 2025-01-01.

Table 1.6: SECA fuel oil sulphur content limits. Limits are expressed in terms of % m/m (by weight). Source: IMO (2014h)

Date	Sulphur content limit
Before 2010-07-01	1.5 %
From 2010-07-01	1.0 %
From 2015-01-01	0.1 %

Most ships that operate both inside and outside of SECAs will operate on different fuel oils in order to comply with the SECA regulations. Fuel switch-over must be completed before entering a SECA, and must not be initiated before leaving the area.

The control of SO_x and PM emissions are primarily achieved through limiting the maximum sulphur contents of loaded fuel oils. The actual sulphur content must be stated by the fuel oil supplier on the bunker delivery note. Low sulphur fuel oil shall not be loaded in tanks partly filled and hence mixed with higher sulphur content fuel oils.

However, IMO allows utilization of other means to achieve the equivalent levels of emission control for SO_x and PM. IMO (2014h) divides these means in primary and secondary methods. Primary methods implies that the formation pollutants is avoided, through e.g. onboard blending of fuel oils or dual fuel (gas/liquid) use. As of October 2010 there are no guidelines in terms of primary methods (IMO, 2014h). Secondary methods are defined as means where the pollutants are formed, but subsequently removed to some degree before discharging the exhaust gas to the atmosphere. The MEPC has developed guidelines for exhaust gas cleaning systems.³ In using such arrangements there would be no constraint on the sulphur content of the fuel oil. Methods for emission reductions are discussed in detail in section 1.10.

Regulations on emissions of PM other than in SECAs are currently not in existence. The lack of standardized methods for measuring PM and BC emissions makes the development of such regulations difficult (Libra, 2013). However, these concerns are not absent in the regulatory bodies. The Marine Environment Protection Committee (MEPC) under IMO has delegated the issue of drafting such regulations to the Sub-Committee on Pollution Prevention and Response (PPR)⁴. The Sub-Committee aims to develop a technical definition as a basis for future measurement methods and investigate appropriate control measures (Lundy, 2013). In 2013, a group of environmental non-governmental organizations submitted a request to IMO for preliminary inclusion of BC in the Polar Code. However, the request was denied from

³See MEPC.184(59).

⁴The former Sub-Committee on Bulk Liquids and Gases (BLG).

the MEPC, as they determined to await the conclusions of the Sub-Committee’s work. The work of the Sub-Committee is still ongoing.

Limits on NOx emissions

NOx emissions are regulated through MARPOL Annex VI, Regulation 13. The control is achieved through survey and certification requirements on marine diesel engines (IMO, 2014c). Levels (tiers) of control apply based on the construction date of the ship, and the limit value is determined from the engine’s rated speed. Emission limits are shown in Table 1.7.

Table 1.7: NOx emission limits. Source: IMO (2014c)

Tier	Ship construction date (on or after)	Total weighted cycle emission limit (g/kWh)		
		$n < 130$	$n = 130 - 1999$	$n \geq 2000$
I	2000-01-01	17.0	$45 \cdot n^{-0.2}$	9.8
II	2011-01-01	14.4	$44 \cdot n^{-0.23}$	7.7
III	2021-01-01 ^a	3.4	$9 \cdot n^{-0.2}$	2.0

^a2016-01-01 for the North American and U.S. Caribbean Sea NECAs

The Tier III controls apply only to ships operating in ECAs established to limit NOx emissions (NECAs). Outside such areas the Tier II controls apply. Tier I limits apply for older vessels.

NECAs already introduced are in North America and the United States Caribbean Sea (IMO, 2014f). These areas have both SECA and NECA status. The countries surrounding the Baltic Sea and North Sea have recently been preparing to submit a proposal to IMO also to achieve NECA status for the areas already classified as SECAs. However, Russia has been blocking the Baltic Sea countries’ NECA proposal, and so far the prospect of having a Baltic Sea NECA in the near future is slim (Ågren, 2014).

The 2013 MEPC revision of the 2008 Regulation 13 leads to a delay of the implementation date of the Tier III limits, from 2016-01-01 to 2021-01-01 (IMO, 2014b). However, this delay does not apply to the North American and U.S. Caribbean Sea NECA, which had already been approved and adopted before the revision. As a result of the delay, only ships built after the adaptation of a NECA would have to comply with Tier III standards. For instance if a new NECA enters into force in 2020, the Tier III standards would not apply to the ships built in the years 2016 to 2019.

The emission value for a diesel engine is determined by the *NOx Technical Code 2008*⁵ in case of the Tier II and Tier III limits. Most Tier I engines have been certified to the earlier version of the NOx Technical code (1997), and this certification is valid over the service life of such engines (IMO, 2014c).

The prospect of an Arctic ECA

The IMO Sub-Committee on Ship Design and Construction (SDC) is currently developing a mandatory International Code of safety for ships operating in polar waters, known as the Polar Code. The Polar Code will cover the full range of design, construction, equipment, operational, training, search and rescue and environmental protection matters relevant to ships operating in the waters around the poles (IMO, 2014e). Part II-a of the draft Polar Code includes mandatory measures for pollution prevention. It will be made mandatory through appending it to MARPOL as a new chapter of MARPOL (IMO, 2014g). However, prevention of air pollution is not included in the latest version of the draft, which focuses on the prevention of oil pollution, pollution from noxious liquid substances, sewage and discharge of garbage. The MEPC will further consider the environmental chapter at its next session in October (MEPC 67).

Although the Arctic Sea has not yet been proposed for special emission status, it may be introduced through the Polar Code or directly through MARPOL.

⁵See (IMO, 2008)

1.9.2 Energy Efficiency Measures

IMO has introduced different technical and operational measures in order to improve energy efficiency and reduce GHG emissions from international shipping. The measures include an Energy Efficiency Design Index (EEDI), a Ship Energy Efficiency Management Plan (SEEMP) and an Energy Efficiency Operational Indicator (EEOI). A new Chapter 4 in MARPOL Annex VI introduces the EEDI and SEEMP, and the regulations entered into force on 2013-01-01. The regulations apply to all ships over 400 GT. The EEDI is mandatory for all new ships and ships which have undergone major conversions. The SEEMP is mandatory for all ships (IMO, 2014i). The use of EEOI is not mandatory.

The aforementioned regulations apply to cargo transport ships only. Ship categories currently under regulations are bulk carriers, gas carriers, tankers, container ships, general cargo ships, refrigerated cargo carriers and combination carriers (IMO, 2011). The regulations were recently extended also to include LNG carriers, ro-ro cargo ships, ro-ro passenger ships and cruise passenger ships with non-conventional propulsion. Ships not propelled by mechanical means and independently operating cargo ships with ice-breaking capability will be exempt from the regulation in the amendments. The extended regulations are expected to enter into force on 2015-09-01 (IMO, 2014b).

The Energy Efficiency Design Index (EEDI)

According to IMO (2012c), the purpose of the Energy Efficiency Design Index (EEDI) is to *"provide a fair basis for comparison, to stimulate the development of more efficient ships in general and to establish the minimum efficiency of new ships depending on ship type and size."*

The EEDI requires a minimum energy efficiency level per capacity-mile for a ship. The index is expressed for an individual ship design as grams of CO₂ per ship's capacity-mile, which can be expressed as

$$\text{EEDI} = \frac{\text{CO}_2 \text{ emissions}}{\text{transport work}}. \quad (1.2)$$

A smaller EEDI gives a more energy efficient ship. The requirements are differentiated for different ship types and size segments.

An attained EEDI factor is calculated for each ship (see Appendix B for details regarding calculations). The attained EEDI shall be less than or equal to the required EEDI for the ship type. According to IMO (2011), the required EEDI for the different ship types is found by

$$\text{Required EEDI} = (1 - x/100) \cdot \text{Reference line value}, \quad (1.3)$$

where x is the reduction factor for the given ship type as specified in Table 1.8.

The reference line for each ship type is used to determine the required EEDI. According to IMO (2012c), the reference line is a curve representing an average index value fitted on a set of individual index values for a defined group of ships. The reference line value for a ship is calculated as

$$\text{Reference line value} = a \cdot \text{DWT}^{-c}, \quad (1.4)$$

where the parameters a and c are according to ship type, and are listed in Table 1.9.

The ship reference levels will be tightened every five years in three phases. Reduction factors are set until 2025, when a 30 % reduction from the reference line value is mandated (IMO, 2014b).

Table 1.8: EEDI reduction factors (in percentage) for the EEDI, relative to the EEDI reference line for selected ship types. Source: IMO (2011)

Ship type	Size	Phase 0 ^a	Phase 1	Phase 2	Phase 3
		2013-01-01/ 2014-12-31	2015-01-01/ 2019-12-31	2020-01-01/ 2024-12-31	2025-01-01 and onwards
Bulk carrier	20,000 DWT and above	0	10	20	30
	10,000-20,000 DWT	n/a ^b	0-10*	0-20*	0-30*
Gas carrier	10,000 DWT and above	0	10	20	30
	2,000-10,000 DWT	n/a	0-10*	0-20*	0-30*
Tanker	20,000 DWT and above	0	10	20	30
	4,000-20,000 DWT	n/a	0-10*	0-20*	0-30*
Container ship	15,000 DWT and above	0	10	20	30
	10,000-15,000 DWT	n/a	0-10*	0-20*	0-30*

^aReduction factor to be linearly interpolated between the two values dependent upon vessel size. The lower value of the reduction factor is to be applied to the smaller ship size.

^bn/a means that no required EEDI applies.

Table 1.9: Parameters for determination of reference line values for the ship types in Table 1.8. Source: IMO (2011)

Ship type	<i>a</i>	<i>c</i>
Bulk carrier	961.79	0.477
Gas carrier	1120.00	0.456
Tanker	1218.80	0.488
Container ship	174.22	0.201

The Ship Energy Efficiency Management Plan (SEEMP)

According to IMO (2011), each ship shall keep on board a ship specific Ship Energy Efficiency Management Plan (SEEMP). The SEEMP is a mechanism for operators to improve energy efficiency in the operation of ships. It provides the operators with an approach to monitor ship and fleet efficiency performance over time, and options to consider when seeking to optimise the performance of the ship (IMO, 2012a). The SEEMP is ship-specific, but can be linked to a broader corporate energy management policy.

The IMO has developed guidelines for ship operators and owners for developing a SEEMP (see IMO (2012a)). There are many ways of improving energy efficiency for ships, some of those recommended by the IMO are listed in Table 1.10. As a part of the SEEMP, the IMO recommends that the energy efficiency of a ship's operation is monitored and thus can be evaluated and improved. The EEOI may be used as a tool for monitoring the energy efficiency of the ship's operation.

Table 1.10: Technologies for reducing the EEDI and SEEMP related measures. Source: Bazari and Longva (2011)

EEDI reduction measure	SEEMP related measure
Optimised hull dimensions and form	Engine tuning and monitoring
Lightweight construction	Hull condition
Hull coating	Propeller condition
Hull air lubrication system	Reduced auxiliary power
Optimisation of propeller-hull interface and flow devices	Speed reduction (operation)
Contra-rotating propeller	Trim/draught
Engine efficiency improvement	Voyage execution
Waste heat recovery	Weather routing
Gas fuelled (LNG)	Advanced hull coating
Hybrid electric power and propulsion concepts	Propeller upgrade and aft body flow devices
Reducing onboard power demand (auxiliary system and hotel loads)	
Variable speed drive for pumps, fans, etc.	
Wind power (sail, wind engine, etc.)	
Solar power	
Design speed reduction (new builds)	

The Energy Efficiency Operational Indicator (EEOI)

The Energy Efficiency Operational Indicator (EEOI) was developed by the IMO to assist ship owners and operators to evaluate the performance of their ship and/or fleet with regard to CO₂ emissions during operations (IMO, 2009). As the amount of CO₂ emitted from a ship is directly related to the consumption of bunker fuel oil, the EEOI can also provide information on the ship's performance with regard to fuel efficiency.

The information in the following paragraphs is taken from the IMO's "Guidelines for voluntary use of the ship Energy Efficiency Operational Indicator (EEOI)".

The indicator is defined as the ratio of mass of CO₂ emitted per unit of transport work:

$$\text{EEOI} = \frac{M_{\text{CO}_2}}{\text{transport work}} \quad (1.5)$$

The EEOI is applicable for all ships performing transport work, and is calculated based on data from the operation of the ship. The indicator can be calculated for one voyage or for a period or number of voyages.

The basic expression for EEOI for a voyage is defined as

$$\text{EEOI} = \frac{\sum_j FC_j \cdot C_{F,j}}{m_{\text{cargo}} \cdot D}, \quad (1.6)$$

where index j is the fuel type, FC_j is the mass of consumed fuel j , $C_{F,j}$ is the fuel mass to CO₂ mass conversion factor (see Table 1.11), m_{cargo} is cargo carried (tonnes) or work done (number of TEU or passengers) or GT for passenger ships and D is the distance in nautical miles corresponding to the cargo carried or work done.

For a period or for a number of voyages, the average EEOI is calculated as

$$\text{Average EEOI} = \frac{\sum_i \sum_j (FC_{ij} \cdot C_{F,j})}{\sum_i (m_{cargo,i} \cdot D_i)}, \quad (1.7)$$

where index i is the voyage number (so FC_{ij} is the mass of consumed fuel j on voyage i , etc.).

Ballast voyages should also be included in the EEOI calculations. Where $m_{cargo} = 0$, the fuel consumption for the voyage should still be included in the summation in the nominator.

As a result of the different definition of the transport work done, the unit of EEOI differs from the different ship types.

Table 1.11: The values of the fuel mass to CO₂ mass conversion factor C_F . Source: IMO (2009)

Type of fuel	Reference	Carbon content	C_F (t-CO ₂ /t-fuel)
Diesel/Gas Oil	ISO 8217 Grades DMX through DMC	0.875	3.206000
Light Fuel Oil (LFO)	ISO 8217 Grades RMA through RMD	0.86	3.151040
Heavy Fuel Oil (HFO)	ISO 8217 Grades RME through RMK	0.85	3.114400
Liquified Petroleum Gas (LPG)	Propane	0.819	3.000000
	Butane	0.827	3.030000
Liquified Natural Gas (LNG)		0.75	2.750000

1.9.3 Discussion on emission controls

As Regulation 13 emission limits on NO_x is based on the engine's rated speed, the regulations are not able to address situations where vessels which are operating outside the design conditions.

Under ideal conditions, main engine load is correlated with vessel speed (Lack and Corbett, 2012). For lower ship speeds, due to reduced fluid resistance on the hull (as a cubic function) result in a decrease in fuel consumption. Marine diesel engines are often tuned for maximum energy output at minimum fuel consumption during operation at the most common engine load conditions expected. When engines operate outside the tuned engine load, fuel efficiency decrease and emissions increase as a consequence of variations in conditions away from ideal combustion.

Operation in Arctic Seas often entails highly variable engine loads, as safe travel speeds vary with ice conditions and ship construction (McCallum, 1996). Lack and Corbett (2012) estimate that transits in Polar waters would span loads from approximately 10 % to 100 % with the lower load range required for approximately 20 % to 50 % of the distance of the transit. Therefore the actual emissions from vessels operating in Arctic waters could be substantially higher than the emission limits.

Bazari and Longva (2011) studied the effects of the energy efficiency regulations, and found that the reduction measures will lead to significant emission reductions by the shipping industry. The estimates show that the regulations lead to an average of 152 million tonnes of CO₂ reductions by 2020, compared to a "business as usual" scenario. By 2050, the annual CO₂ reductions were estimated to 1013 million tonnes.

The EEDI is a performance-based mechanism, so as long as the required energy efficiency standards are met, the choice of technologies is up to the ship designers and builders. This makes it possible to choose the most cost-efficient solutions, such as those listed in Table 1.10. According to Bazari and Longva (2011), ship hydrodynamic and main engine optimisation can bring energy savings of up to 10 % with no significant additional cost of shipbuilding. In addition, main and auxiliary engines are already available with reduced specific fuel consumption of about 10 % compared to the values used in the study's calculations. Hence,

cost of compliance to the first phases (0 and 1, see Table 1.8) will not be significant. Cost of compliance for phase 2 and 3 (beyond 2020) may be higher and will involve design-speed reduction. Still, the overall life-cycle fuel economy will be positive due to the high savings in fuel costs.

The SEEMP is mandatory to have on board, but the actual use of the plan is not mandatory. It is hoped that the procedural framework will lead the shipping companies to recognise the importance of the operational energy-saving activities, and a positive cultural change. However, no measures are currently in place to make the operators utilise the SEEMP.

1.9.4 Regulatory consequences for shipping operations

Ships operating in ECAs will have to take measures to comply with emission regulations. There are several ways of complying with the regulations (see section 1.10).

MARPOL Annex VI states that ships trading both within and outside ECAs are allowed to perform a fuel switch-over when entering and leaving ECAs. This means that ships can operate on residual fuel while at sea, and switch to distillate fuels when approaching ECAs. This requires additional space for secondary fuel tanks and piping, which will occupy space that could otherwise be utilised for cargo. As an alternative to fuel switching, exhaust cleaning technologies may be installed and operated only during ECA sailing. Another options for ship operators is to utilise alternative technologies with lower emission levels such as LNG. As a consequence, operation inside and outside ECAs will be the same. This could possibly save time and reduce the chance of operational complications due to fuel change-over. Additionally, separate fuel arrangements are not needed.

1.10 Measures for emission abatement

The abatement of harmful emissions from combustion engines is a considerable technical challenge. Current technology allows significant reduction of air emissions. Miola et al. (2010) claims that emissions reductions of NO_x by up to 80 %, PM up to 70 %, SO_x by up to 90 % and CO₂ by up to 70 % are possible by utilizing new technology and “greener” fuels.

According to Andreoni et al. (2008) it is common to distinguish between three categories when discussing emission abatement measures: pre-treatment, primary (or internal) methods and secondary (or after-treatment) methods.

Pre-treatment methods involve modification of the fuel to reduce its quantity of pollutants. By decreasing the amount of pollutants in the fuel, fewer pollutants are produced. Use of alternative fuels may also be included in this category.

Primary methods are means which change the combustion process directly within the engine. They are generally referred to as Internal Engine Modification (IEM). The goal is to optimise combustion, improve air charge characteristics or alter the fuel injection systems through engine modification. There are many parameters who influence the combustion process, so there are many IEM methods where the technological solutions differ widely.

Secondary methods reduce emission levels without changing engine performance settings. Equipment that is not a part of the engine itself is used to treat the engine exhaust gas, either by reburning the gas or passing it through a catalyst or plasma system.

Ship owners and operators may utilise one or more of these methods in combination to meet regulation limits.

In the following sections, the main emission abatement technologies and measures for SO_x, NO_x and CO₂ are presented. The main emission reduction measures are summarised in Table 1.12.

Table 1.12: Emission reduction measures

Reducing measure	Associated emissions	Possible abatement measures
Fuel	CO ₂ , SO _x , PM	Lowering fuel sulphur content, alternative fuels (LNG, hydrogen, etc.)
Combustion process	NO _x , HC, PM	Better design of combustion process and engines, technical improvements
Exhaust gas cleaning	SO _x , PM, NO _x	After treatment technologies

1.10.1 CO₂ reduction measures

CO₂ emissions are proportional to the content of carbon in the fuel. Therefore, the key to reducing CO₂ emissions are increased energy efficiency and use of alternative fuels.

There are many measures to increase energy efficiency, some of which are listed in Table 1.10. Substantial savings can be achieved if topics such as ship dimensions, hull and appendage design and total ship concepts are introduced in the beginning of the ship design process (Wärtsilä, 2010). Also topics related to propulsion and machinery systems are important to consider. Further, operational measures such as voyage planning, speed reduction can yield savings in CO₂ emissions. Lastly, means related to maintenance and service of the vessel such as hull and propeller cleaning, automation adjustments and condition based maintenance are relevant.

1.10.2 SO_x reduction measures

Sulphur oxide emissions are directly proportional to the sulphur contents of the fuel. The main method to reduce emissions is to burn fuel with less sulphur, though exhaust gas cleaning devices can also be used to remove sulphur from the exhaust.

In the following sections, the following abatement measures are described:

- Fuel switching,
- Sea Water Scrubbing (SWS) and
- Fresh water scrubbing.

Fuel switching and alternative fuels

The most practical way of reducing SO_x emissions are by simply reducing the sulphur content of the fuel oil. As SO_x emissions are directly related to the sulphur content in the fuel, the reduction efficiency on SO_x emissions is also directly related to the sulphur content in the fuel. Low-sulphur fuels or alternative fuels may be used. Generally, the vessels can operate by switching entirely to alternative fuels or operating on dual-fuel mode with separate storage tanks and handling systems for each fuel.

In addition to reducing SO_x emissions, a switch to low-sulphur fuel will also reduce PM emissions. Entec UK Ltd. (2005b) refers to a 2003 US EPA study that reports a 18 % decrease in PM emissions by switching from 2.8 % to 1.5 % sulphur fuel. According to the same source, switching to marine distillate yields PM emission reductions of 63 %.

Modern diesel engines can burn low-sulphur fuels⁶ without difficulties, providing that attention is given to the cylinder lubricating oil grade and feed rate, and the jacket cooling water temperatures (Wärtsilä, 2005). Therefore, it may be necessary to have additional arrangements for storing and handling a second grade of cylinder lubricating oil.

⁶Less than 1.5 % sulphur

For ships with two types of storage and settling tanks, fuel switching is relatively straightforward. The process is costly and time consuming for ships with only one settling tank.

Distillate fuels are typically 30 % to 50 %, more expensive than HFO (Acciaro, 2014). Production capacity is limited and as the demand will most likely rise as a consequence of more ECAs being introduced world wide. Hence, the prices will probably increase more rapidly in the future.

Alternative fuels such as biofuels, natural gas (LNG) or hydrogen can be used instead of diesel fuels. The limited availability and high costs of biofuels is still an issue (Karila et al., 2004). Hydrogen technology requires the application of fuel cells. A few installations exist on smaller ships (15 kW), but for large vessels with substantial power demands (60 MW), the application of fuel cells is still not possible (Eyring et al., 2005).

The use of LNG is both a fuel switch and an alternative technology. LNG does not require cleaning technologies to comply with ECA regulations. SO_x emissions are negligible, and NO_x emissions are below Tier III limits (Acciaro, 2014). Additionally, GL (2012) reports of CO₂ reductions of up to 20 % to 25 %,. However, as mentioned in subsection 1.8.2, availability may be an issue. Costs of retrofitting LNG facilities are considerable. Moreover, substantial engine, fuel tank and piping modifications may be necessary. The NO_x reduction potential has been demonstrated in four-stroke engines, but has yet to be established for large two-stroke engines (Buhaug et al., 2009).

Sea Water Scrubbing (SWS)

The use of liquid scrubbers is a well established practice, and has been used on land-based combustion units since the 1930s. The SWS is a cleaning technology that allows the ship to operate within a SECA with regular sulphur fuel and without operating on a more expensive fuel that is potentially difficult to locate. SO_x emission reductions of up to 95 % has been reported with SWSs (Entec UK Ltd. 2005b; US EPA, 2009; Nikopoulou et al., 2013). Additionally, other exhaust emissions can be reduced. Nikopoulou et al. (2013) reports of NO_x reductions of up to 10 % to 20 %, 80 % of PM and 10 % to 20 %, of HC.

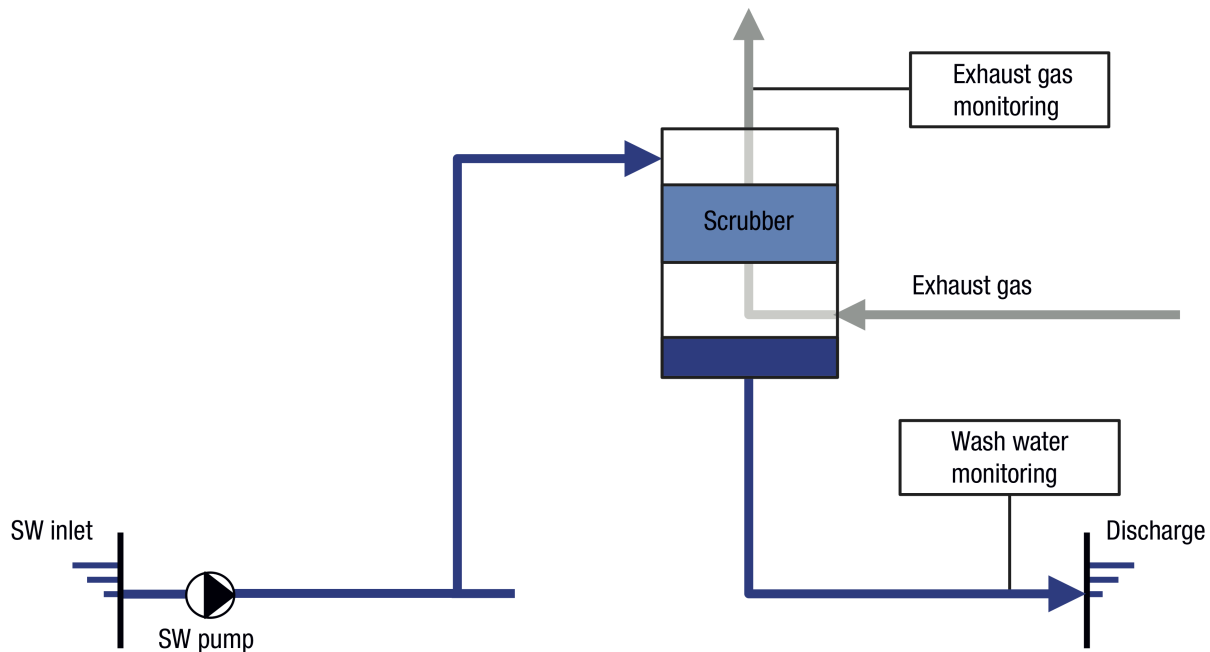
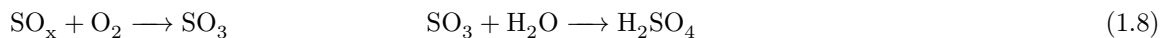


Figure 1.10: Open loop sea water scrubber system. Source: MAN B&W (2014)

Due to sea waters natural alkalinity, the sea water scrubber is one of the most versatile, available and cost-effective scrubbing processes. The water is taken directly from the sea and fed to the scrubber. Leaving the scrubber, the water is discharged into the sea without any further treatment. Sea water naturally contain large quantities of sulphur, and is therefore considered a safe sulphur reservoir.

Figure 1.10 illustrate the open loop system in a sea water scrubber. The hot exhaust gases are sprayed or passed through a tank filled with sea water. The SO_x in the exhaust gas reacts with oxygen to form sulphur trioxide (SO₃). The SO₃ then reacts with water to form sulphuric acid (H₂SO₄):



The solid particles removed from the exhaust gas are trapped in a sludge tank for disposal. The remains may either be burned in the ship's incinerator or disposed of ashore. The scrubbed water is diluted with more water before discharge, and is discharged with a pH of 6.5 to the sea (Nikopoulou et al., 2013).

Concerns have been raised regarding the disposal of acidic water in enclosed waters such as ports and bays. Furthermore, the volume of water required to filter the exhaust is an issue (Nikopoulou et al., 2013). The required consumption of water is non-linear with the level of reduction achieved. However, these issues are mostly relevant ships operating in enclosed water and not for sea going ships.

There are large volume requirements, especially in the funnel (Yang et al., 2012). Figure 1.11 illustrate the dimensions of the system. Also corrosion issues due to the sulphuric acid may arise. Installation costs may be substantial.

The system is simple and the cheapest solution in regards to installation and operating cost (MAN B&W, 2014). However, an open loop system lacks flexibility when local regulations prevent or limit the use of the system due to low alkalinity or restricted discharge criteria.

Scrubbers reduce the exhaust gas temperature. Therefore, scrubbers in combination with SCR technology (see section 1.10.3), which requires high exhaust gas temperature and at the same time low sulphur and PM content, is considered infeasible (Buhaug et al., 2009).

Fresh water scrubbing

A fresh water scrubber has a cleaning efficiency of over 90 %. The scrubber works on fresh water in a closed-loop design. A caustic soda (NaOH) solution is added to the water to increase the alkalinity. As a result the water is able to remove SO₂ from the exhaust gases by the same principles as described for the SWS. The washing solution is pumped from the process tank through a system cooler to the scrubber. The solution returns to the process tank by gravity (Andreoni et al., 2008).

1.10.3 NO_x reduction measures

This section will discuss methods to reduce NO_x emissions from ship exhaust. One of the best ways to lower NO_x emissions are to lower peak combustion temperatures. Removing nitrogen in the fuel by denitration can only reduce NO_x emissions to a small degree, as the nitrogen in the fuel contributes only marginally to emissions. To reach Tier III level reductions, "end of pipe" technologies may be necessary to utilise (Brynnolf et al., 2014).

According to Wartsila (2005), there is always a trade-off between fuel consumption and NO_x emission levels. Due to the underlying laws of combustion chemistry, when one decreases, the other increase, and vice-versa.

Key strategies to reduce NO_x in the engine involve reducing peak temperatures, reducing the time for which gases are at high temperatures and reducing the concentration of oxygen in the charge air (Buhaug et al., 2009). There are a wide range of approaches to achieve this.

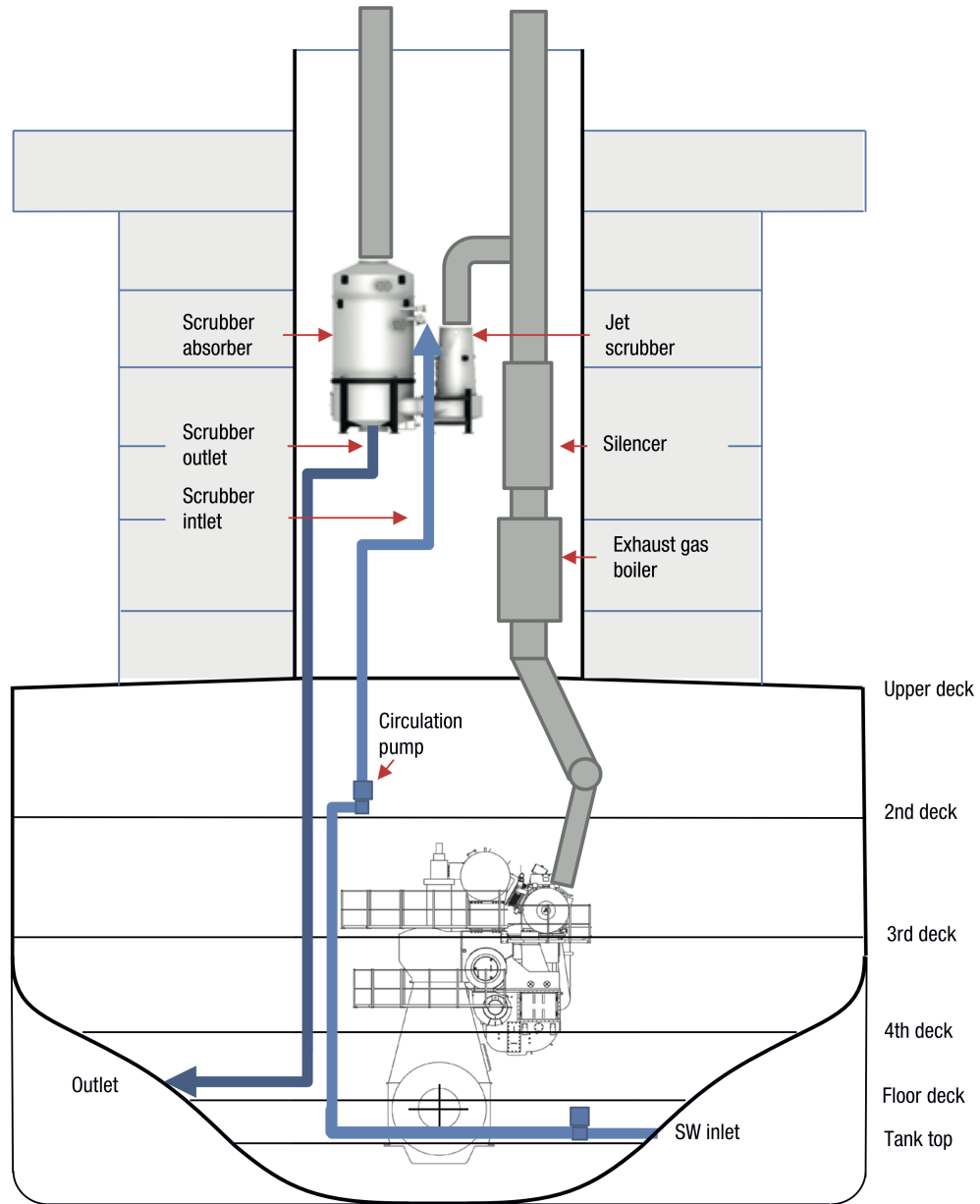


Figure 1.11: Schematic arrangement of an open loop SOx scrubber system (SWS). Source: MAN B&W (2014)

Methods can be divided in dry and wet methods. Dry methods involve methods which alter the physical properties in and around the combustion process. Wet methods are when water is introduced into the combustion chamber. Both methods may be directly included in newbuildings, or retrofitted on existing engines.

The following sections contain technical descriptions of the following NO_x reduction methods:

- Internal Engine Modification (IEM),
- Direct Water Injection (DWI),
- Humid Air Motors (HAM),
- Exhaust Gas Recirculation (EGR) and
- Selective Catalytic Reduction (SCR).

Internal Engine Modification (IEM)

NO_x reductions can be achieved through modification of the combustion process in the engine with no additional equipment installed. There are a wide range of measures available. The methods aim to either optimise combustion, improve air charge characteristics or alter the fuel injection system (Entec UK Ltd. 2005a). The measures can be applied in various combinations according to achieve the desired NO_x reduction appropriate for each specific engine type. The solutions are often simple and effective, and has no detrimental effect on engine reliability. Fuel consumption is increased only minimally (Wärtsilä, 2005).

Entec UK Ltd. (2005a) divides IEM methods in “basic” and “advanced” methods:

Basic IEM refers to the exchange of conventional fuel valves with low-NO_x fuel valves of the sliding type. The slide valves are designed to optimise spray distribution in the combustion chamber. The method is only applicable for slow-speed two stroke engines. According to Entec UK Ltd. (2005a), the manufacturers claims that slide valves can reduce NO_x emissions by up to 20 %. Also PM and VOC may be reduced, however this is unconfirmed and dependent on fuel type. Entec UK Ltd. (2005a) claims that slide valves are usually fitted as standard in engines delivered after 2000, as means of meeting the IMO NO_x standard. Retrofit installations are no issue, as the original valves may easily be replaced.

Advanced IEM methods include a variety of other modification methods, depending on the manufacturer. Means include retard injection, Miller cycle valve timing, higher compression ratio, increased turbo efficiency, higher maximum cylinder pressure, etc. Advanced IEM is still in development (Entec UK Ltd. 2005a).

Direct Water Injection (DWI)

Introducing water into the combustion chamber reduces NO_x formation by lowering the combustion temperature. Direct water injection utilise a separate water valve that injects water into the cylinder. Water injection may occur either during or right after the fuel injection. Unlike other technologies that introduces water (e.g. fuel emulsion, where water and fuel is mixed before injection), DWI allows the water injection to occur at the right time and place to ensure the greatest NO_x reduction.

The quantity of injected water can vary. An addition of 20 % to 50 % water is anticipated, but water fuel ratios are not restricted. With about 70 % water to fuel ratio, DWI has been shown to reduce NO_x emissions down to around 8 g/kWh or to some 50 % below IMO Tier II limits (Wärtsilä, 2005).

Wärtsilä and MAN B&W are the main producers of water injection technologies (Andreoni et al., 2008).

Water injection can be combined with other measures to achieve higher reductions. DWI combined with internal exhaust gas recirculation (EGR) may reduce NO_x emissions up to 70 % below the IMO

limits (Wärtsilä, 2005). However, water injection methods increase fuel consumption and smoke emissions (Eilts and Borchsenius, 2001).

Because the water and fuel systems are separate, the DWI system needs separate pumps and handling systems. Storage and bunkering or production of freshwater is also necessary. Providing sufficient fresh water needs to be considered, as the quantities of water will be substantial. In addition, the consumption and purity of the water are issues in wet methods in general.

Also, these systems have relatively short lifetimes and elevated costs.

Humid Air Motors (HAM)

A HAM introduce evaporated seawater in the charge air. This decreases combustion temperatures, and can reduce NO_x formation up to 80 %. The seawater is evaporated in a humidifier. About three times as much vapour as fuel is introduced into the engine (Entec UK Ltd. 2005a).

There are high initial costs related to installation of the humidifier, due to the need for significant pre-installation work as it needs to be integrated with the engine. The system also have large surface and volume requirements. Additionally, since engine waste heat is used for hot water generation, a HAM could lead to capacity problems which would require extra boiler capacity (Entec UK Ltd. 2005a).

Exhaust Gas Recirculation (EGR)

Exhaust gas recirculation reduces NO_x formation by reducing the oxygen available in the engine cylinder and increasing the heat capacity of the cylinder charge (Wärtsilä, 2005). A portion of the exhaust gases is filtered, cooled and circulated back to the engine charge air. By decreasing the peak temperature of the combustion, this method reduces the formation of NO_x during the combustion process. The NO_x reduction is almost linear to the ratio of recirculated exhaust gas (MAN B&W, 2014). Subfigure 1.10.3 shows the principles of an EGR.

According to MAN B&W (2014), two different layouts are available for the EGR systems: EGR with bypass matching, normally with only one turbocharger (TC), and EGR with TC cut-out matching, having two or more turbochargers. Both layouts have both Tier II and Tier III modes, to switch between operation in and outside ECAs. The choice of layout is in principle determined by the number of turbochargers. Usually, engines with a bore of 80 and above will be configured with TC cut-out matching, and engines with a bore of 70 and less will be configured with bypass matching. MAN B&W (2014) claims that there is no significant difference regarding engine performance of the two methods. In both configurations, the EGR components are integrated on the engine.

Internal recirculation increases the thermal load of the engine. Combining EGR with DWI or other water introducing measures are desired to keep the thermal loads much the same as running without EGR.

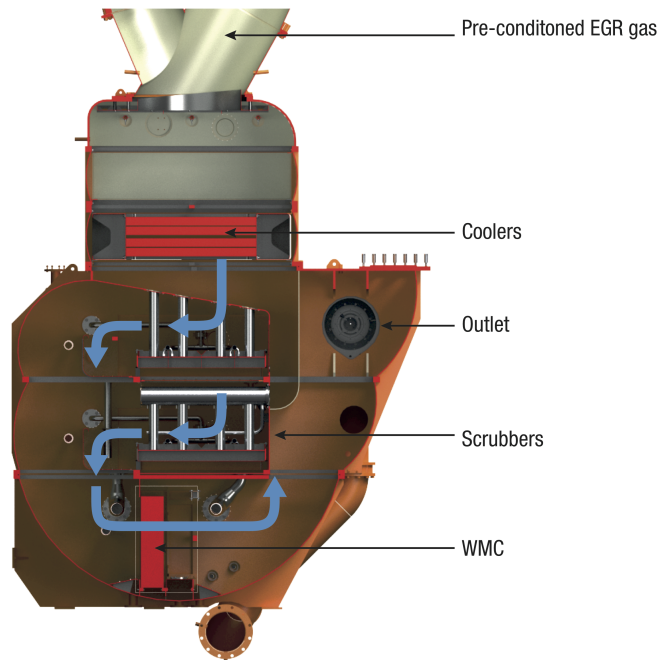
Entec UK Ltd. (2005a) reports NO_x emission reductions of 35 % with EGR. However, smoke and PM tend to increase due to the reduced amount of oxygen and longer burning time. Furthermore, there are issues with long installation time, large space requirements and accelerate degradation of the combustion chamber (Entec UK Ltd. 2005a).

A benefit of EGR is that exhaust gas temperatures are raised, which is helpful for heat recovery systems.

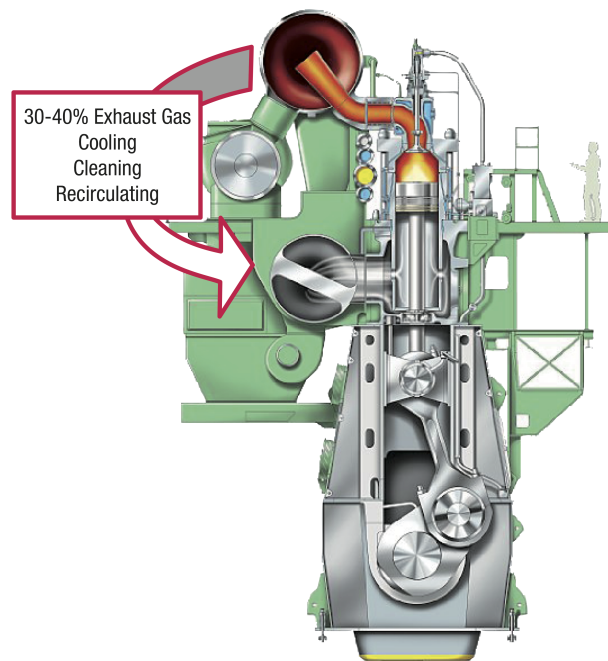
EGR is not yet a mature technology, and capital costs can be difficult to estimate (Entec UK Ltd. 2005a).

Selective Catalytic Reduction (SCR)

Where minimum NO_x emissions are required, SCR is a good alternative. SCR is a well proven technology that makes it possible to remove up to 95 % of the NO_x in the exhaust gas (Er, 2002; Wärtsilä, 2005). The method is not limited to ship type, and has been installed on both low and medium speed diesel engines.



(a) Gas flow in the EGR unit



(b) The chemical principles of the EGR system

Figure 1.12: Illustrations of the EGR system. Source: MAN B&W (2014)

A SCR catalyst reduces NO_x to N₂ and water by using ammonia as a reducing agent. The most common way to supply ammonia (NH₃) is to add urea (CO(NH₂)₂) to the exhaust gas before it enters a catalytic converter (US EPA, 2009). The warm exhaust gas (greater than 250 °C) cause the urea to hydrolyze and form ammonia and CO₂. Figure 1.13 illustrate the principles in the SCR.

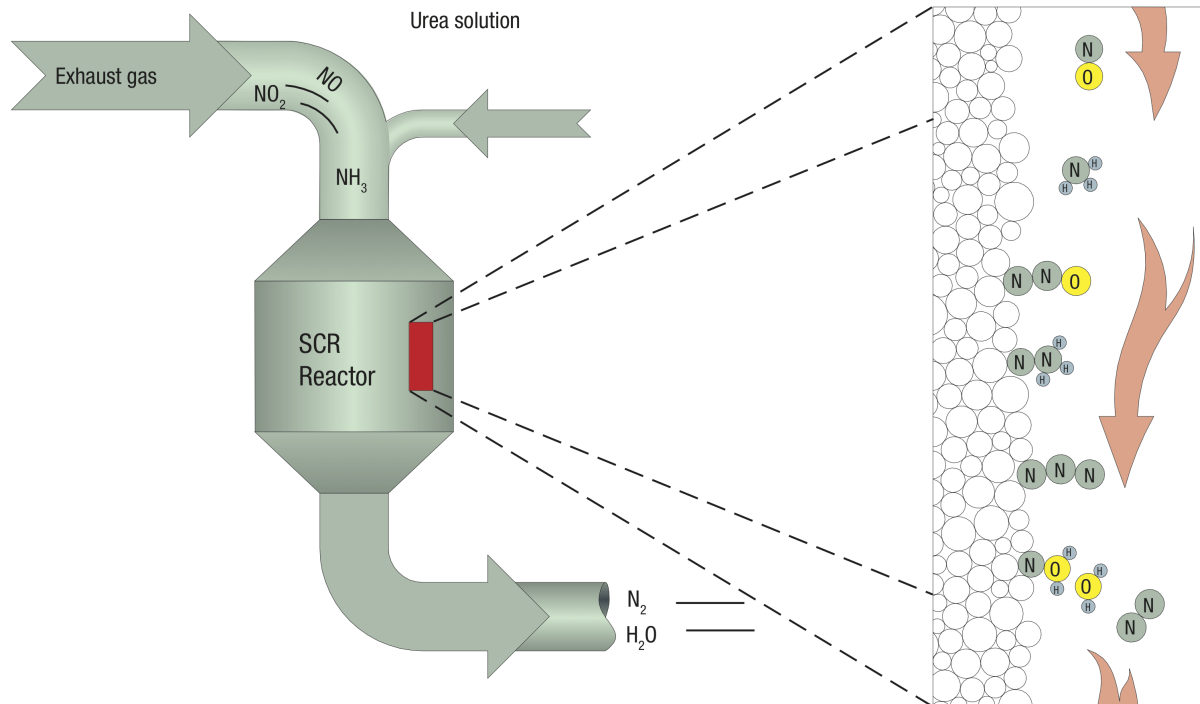


Figure 1.13: The working principles of the SCR system. Source: MAN B&W (2014)

Equation 1.9 gives the chemical reaction in the catalyst, where NO_x reacts with the ammonia. To reduce NO_x emissions by 90 %, a consumption of approximately 15 g of urea is needed per kWh (Cooper and Gustafsson, 2004).



The system requires space for catalyst elements and ammonia/urea storage tanks. Investment and operational costs are sizeable. Urea can be delivered with a road tanker directly to the ship, but the related transport costs can be significant (Entec UK Ltd. 2005a). The lifetime of the system is relatively long, but it depends on the fuel. Clean fuel will lengthen the life of the catalyst and decrease the maintenance necessary.

1.10.4 Previous work on emission control and ECA compliance

Andreoni et al. (2008) performed an analysis on cost effectiveness of emission abatement in the shipping sector. They found that many methods are available for reduction of NO_x and SO_x emissions, while few technologies exist for CO₂ reduction. The “size factor” is reported to be an important aspect of the cost efficiency evaluation, as a bigger ship has a lower specific fuel consumption per unit of growth weight than a lighter one. Internal engine modification and sea water scrubbing resulted to be the most cost effective technologies to reduce NO_x and SO_x emissions respectively, both economically and environmentally. To reduce CO₂ emissions, energy efficiency measures and switching to alternative fuels was the key means.

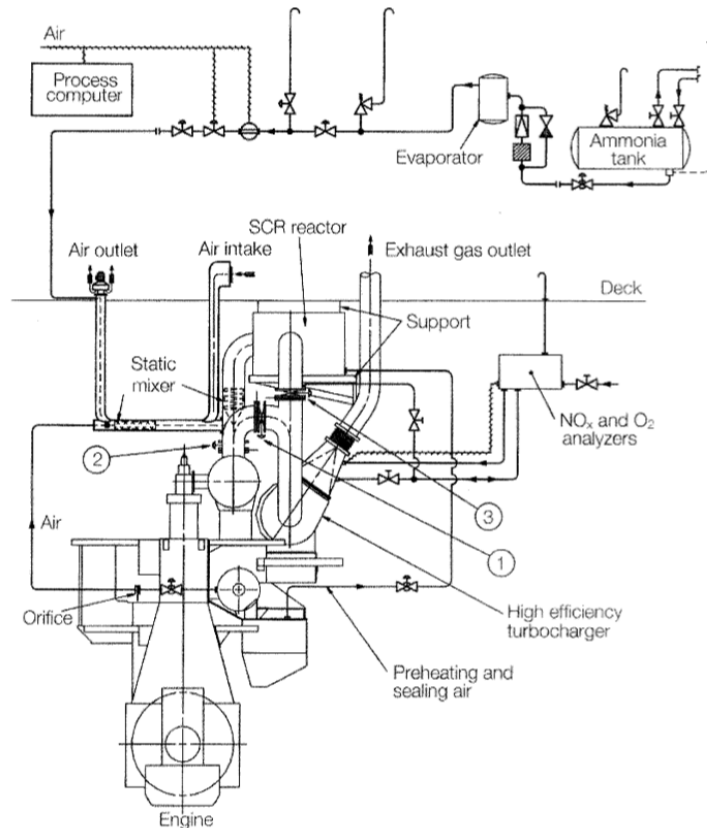


Figure 1.14: Schematic layout of a SCR system for a low-speed diesel engine. Source: Er (2002)

Madsen and Olsson (2012) sought to find the most cost effective strategy for complying with the Baltic Sea ECA in reducing SO_x and NO_x emissions. They considered both newbuilds and retrofitting of existing vessels. Tier II limits was used for NO_x emission limits. In the study, they considered several compliance strategies:

1. MGO with 0.1 % sulphur, and no abatement measures installed;
2. HFO with 2.7 % sulphur and scrubber and SCR;
3. MGO with 0.1 % sulphur with SCR, and
4. LNG, single fuel and duel fuel.

They found that the second scenario was the most cost effective compliance strategy, both for newbuilds and retrofit vessels. This scenario had the lowest fuel costs and also the lowest present value of all scenarios. They conclude that to run on MGO is not desired, as MGO prices are high and increase costs significantly. Further, they claim that LNG is cost effective in terms of reducing emissions, but are costly to retrofit. Their further claim that their comparison depend largely on the development of fuel prices, as the total costs largely consist of fuel costs.

Chapter 2

Modeling of simulations

A case study was performed in order to compare the economic potential of utilising the NSR in parts of the year, given an introduction of an ECA in Arctic waters. To compare the different feasible methods for achieving exhaust emission regulatory compliance in ECAs, different abatement scenarios were defined. In addition, a base case scenario was defined. This chapter will describe the vessel used in the study and the different scenarios that were compared. Further, the development and implementation of the simulations are also explained. Lastly, the simulation model is explained.

2.1 Vessel model

One ship was selected as basis for the case study. The ship was based on the specification of bulk carrier *Nordic Orion* (IMO no. 9529463), retrieved from Sea-Web (2014). *Nordic Orion* has ice class 1A, and sailed the NSR in 2011 with assistance of one icebreaker (NBC, 2011). In the study, the vessel is assumed to be escorted by icebreaker along the the route.



Figure 2.1: Nordic Orion on the North West Passage in 2013. Source: (George, 2013)

The specifications for the vessel used in the case study was defined as in Table 2.1. The vessel was assumed delivered in 2011, and has FS ice class 1A.

Table 2.1: Characteristics of the vessel used in the case study based on the vessel *Nordic Orion*. Source: Sea Web.

Dimension	Symbol	Unit
Length over all	LOA	225 m
Length between perpendiculars	LPP	220 m
Breadth	B	32.3 m
Draught	T	14.1 m
Dead weight	DWT	75,603 tonne
Gross tonnage	GT	40,142
Net tonnage	NT	25,265
Max speed	V_m	15.4 knot
Service speed	V_s	14.5 knot

The propeller diameter D_p was estimated based on measurements from the general arrangement for a typical Panamax bulk carrier in Levander (2009, p. 163). The ratio D_p/T were found to be 0.53, so D_p for the case ship were calculated as

$$D_p = 0.53 \cdot T = 7.5 \text{ m} \quad (2.1)$$

The water line length was assumed to be 221 m.

The vessel's volume displacement was estimated based on bulk carrier statistics from Levander (2009). Expected lightweight for a 75,000 DWT bulk carrier was found to be approximately 14,375 tonnes. However, this statistic is not based on ice classed ships. As described in sec:iceclass (subsection 1.6.1), the lightweight of the ship will increase with ice class. An increase of 4 % in lightweight was assumed. The assumption were based on numbers from DNV ('DNV ARCON-project'), for a container ship of >4,200 TEU with ice class PC5 (see Figure 1.3). Accordingly, the case ship's lightweight were calculated as follows:

$$\text{WLS} = 104\% \cdot 14.375 \text{ tonne} = 14.950 \text{ tonne} \quad (2.2)$$

When the lightweight had been determined, the weight and volume displacements (Δ respectively ∇) were determined as:

$$\Delta = \text{WLS} + \text{DWT} = 90.553 \text{ tonne} \quad (2.3)$$

$$\nabla = \frac{\Delta}{\rho_{sw}} = 88.344 \text{ m}^3 \quad (2.4)$$

The block coefficient, C_B were found from the following relation:

$$C_B = \frac{\nabla}{L_{wl} \cdot B \cdot T} = 0.878 \quad (2.5)$$

The midship area coefficient, C_M were assumed as 0.98. Hence, the prismatic coefficient C_P can be determined from the relationship in Equation 2.6:

$$C_P = \frac{C_B}{C_M} = 0.896 \quad (2.6)$$

Based on the block coefficient, the longitudinal centre of buoyancy (LCB) were determined based on a method from Watson (1998, p. 242). It was found from the diagram that the LCB was approx. 3 % of the ship's length forward from amidships, or 6.63 m from amidships.

The calculated and estimated values for the case vessel are given in Table 2.2. These were later used in hull resistance calculations.

Table 2.2: Estimated vessel characteristics for the case vessel

Dimension	Symbol		Unit
Length in waterline	L_{wl}	221	m
Propeller diameter	D_p	7.5	m
Lightweight	WLS	14 950	tonne
Weight displacement	Δ	90,553	tonne
Volume displacement	∇	88,344	m ³
Block coefficient	C_B	0.878	
Midship area coefficient	C_M	0.98	
Prismatic coefficient	C_P	0.896	
Longitudinal centre of buoyancy	LCB	+6.63	m

2.1.1 Resistance in open water and ice

The following section describes how the ship resistance was calculated in the model. The total resistance in ice is usually divided in open water resistance and ice resistance components. The method of finding the open water resistance is described first, and then the method for finding the resistance in ice.

Open water resistance

The open water resistance was calculated using Guldhammer and Harvald's method, as described in Amdahl et al. (2005). Some ship parameters were assumed and/or estimated. This is specified where applicable.

In Guldhammer and Harvald's method, the resistance is estimated based on empirical data from model tests. The estimations are later corrected in order to account for special characteristics of the hull.

The total open water resistance can be described as

$$R_{T,OW} = R_F + R_R, \quad (2.7)$$

where $R_{T,OW}$ is the total open water resistance, R_F is the frictional resistance and R_R is the residual resistance.

In order to simplify calculations, resistance forces are usually converted to non-dimensional coefficients. The method in Equation 2.8 can be applied to any resistance component of a ship.

$$C_j = \frac{R_j}{0.5 \cdot \rho \cdot V^2 \cdot S} \quad (2.8)$$

C_j is the non-dimensional resistance coefficient, R_j is the resistance force, ρ is the density of the fluid, V is the ship's speed and S is the wet surface.

Frictional resistance The coefficient of frictional resistance, C_F , are found from the ITTC'57 formula:

$$C_F = \frac{0.075}{(\log(\text{Re}) - 2)^2} \quad (2.9)$$

Re is Reynold's number, as defined as

$$\text{Re} = \frac{V \cdot L}{\nu} \quad (2.10)$$

In Equation 2.10, V is the speed in m/s, L is the characteristic length and ν is the kinematic viscosity of the fluid. Calculations were performed for a range of speeds from 0 to 16 knots, with L equal to the waterline length and a kinematic viscosity of water at 5 °C, $\nu_{5^\circ\text{C}} = 1.519 \times 10^{-6} \text{ m}^2/\text{s}$.

Residual resistance Gulddammer and Harvald describes the coefficient of residual resistance, C_R , as a function of the prismatic coefficient C_P , the Froude number Fn and the slenderness ratio. C_R from ships with similar slenderness ratio are plotted in diagrams as a function of C_P and Fn. Thus, C_R can be estimated empirically from these diagrams.

The slenderness ratio for a ship is defined as

$$\text{Slenderness ratio} = \frac{L}{\nabla^{1/3}} \quad (2.11)$$

Using L equal to the waterline length, the slenderness ratio of the case ship was found to be 4.96. The diagrams are plotted for slenderness ratios between 4 and 8, in steps of 0.5. Accordingly, the diagram for slenderness ratio 5.0 (see Appendix D) was used to find C_R .

The diagram is plotted for values of C_P between 0.5 and 0.8, and for Fn between 0.15 and 0.45. C_P for the case ship was found to be 0.896. Therefore, the curve for the closest value, $C_P = 0.8$, was chosen. The Froude number are found from Equation 2.12:

$$\text{Fn} = \frac{V}{\sqrt{g \cdot L}} \quad (2.12)$$

The ship's maximum speed is 15.4 knots, and using L equal to the waterline length, this equals a Fn of 0.17. For Fn smaller than 0.15, C_R appears to approach a lower limit of 0.6×10^{-3} . Therefore, a constant C_R of 0.6×10^{-3} was assumed for Fn smaller than 0.15. The values for C_R read from the diagram are shown in Table 2.3.

Corrections As previously mentioned, the total resistance coefficient was adjusted by adding correctional coefficients. The corrections were the following:

- Scale effects and coarseness (C_{scale}),
- Breadth/draught (B/T) relationship (C_{BT}),

Table 2.3: Values of the coefficient of residual resistance, C_R

Vessel speed [kn]	Froude number	$C_R \cdot 10^3$
0	0	0
1 to 13	0.011 to 0.144	0.600
14	0.155	0.790
15	0.166	1.000
16	0.177	1.140

- Frame shape (C_{frame}) and
- Bulbous bow (C_{bulb}).

The corrections are chosen according to suggested values and calculation methods as described in Amdahl et al. (2005). Values for the correction coefficients that were used are shown in Table 2.4 and Table 2.5.

Table 2.4: Values for correction coefficients used in resistance calculations

Correction coefficient index i	Calculation method	$C_i \cdot 10^3$
<i>scale</i>	Interpolation ^a	-0.084
<i>BT</i>	$0.16 \cdot (B/T - 2.5)$	0.033
<i>frame</i>	- ^b	0

^aTable 10.1 in Amdahl et al. (2005)

^bNormal frame shape was assumed

C_{bulb} depends on Fn and C_P . Table 10.3 in Amdahl et al. (2005) indicate C_{bulb} for values of C_P between 0.5 and 0.8, and for Fn between 0.15 and 0.36. The correction factor were assumed linear between the data points in the table. For the case ship, values were read from $C_P = 0.8$, and were interpolated between Fn of 0.15 and 0.18. The values are presented in Table 2.5.

Table 2.5: Values for C_{bulb}

Vessel speed [kn]	Froude number	$C_{bulb} \cdot 10^3$
0 to 13	0 to 0.144	0
14	0.155	0.084
15	0.166	0.047
16	0.177	0.011

Total resistance After all the correction factors were determined, the total resistance coefficient was calculated as a function of the vessel speed by adding all the resistance coefficients:

$$C_T = C_F + C_R + \underbrace{C_{scale} + C_{BT} + C_{frame} + C_{bulb}}_{C_{corr}} \quad (2.13)$$

The values of all coefficients are shown in Figure 2.2. When C_T are known, the total resistance were found by using Equation 2.8 solved for the resistance force, as shown in Equation 2.14.

$$R_{T,OW} = C_T \cdot 0.5 \cdot \rho_{sw} \cdot V^2 \cdot S \quad (2.14)$$

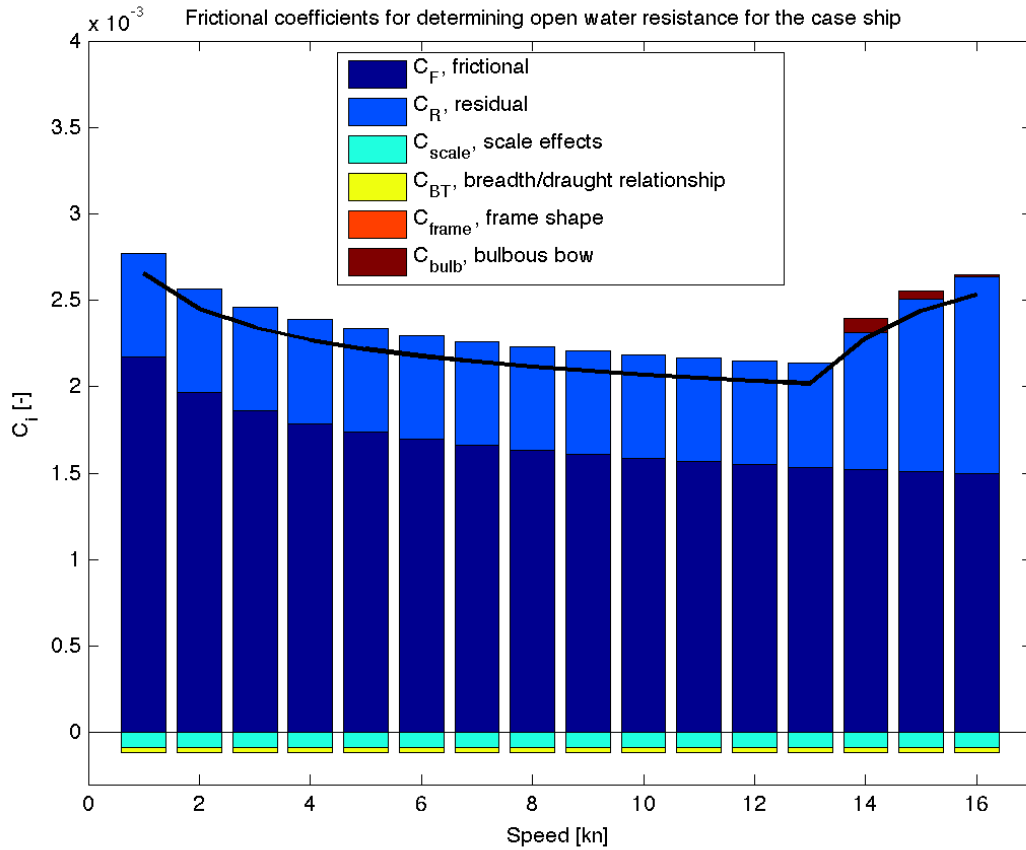


Figure 2.2: Coefficients that were calculated used in Guldhammer and Harvald's method to determine open water resistance. The sum is the vessel's coefficient of total resistance, represented by the black line.

where ρ_{sw} is the density of salt water, 1.025 kg/m^3 , and V is the ship speed in m/s. The wet surface, S , was found from the estimation formula

$$S = k \cdot \sqrt{\nabla \cdot L_{wl}}, \quad (2.15)$$

where k is determined from a diagram as a function of the B/T ratio and the midship area coefficient, C_M (see Appendix E). With $B/T = 2.3$ and $C_M = 0.98$, k was found to be 2.73. Hence, the wet surface were found to be 12.110 m^3 .

Figure 2.3 shows the results of the calculation of the open water resistance of the ship as a function of the ship's speed.

Resistance in ice

Riska et al. (1997) has studied the ice resistance of ships in navigational channels. The total resistance when sailing in ice is normally divided into open water and ice resistance components:

$$R_T = R_{OW} + R_I \quad (2.16)$$

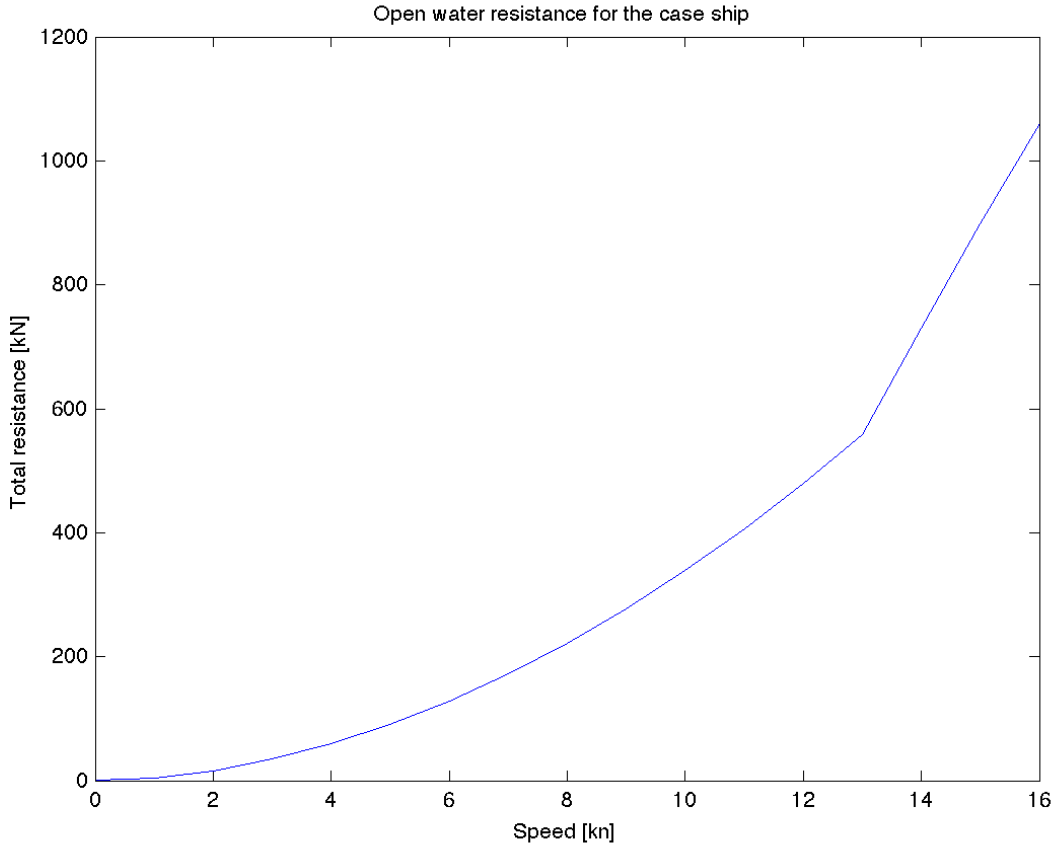


Figure 2.3: Open water resistance for the case ship, calculated with Guldhammer and Harvald's method

where R_T is the total resistance, R_{OW} is the open water resistance and R_I the ice resistance. Ice resistance can be further divided in several types of components. The most significant are level ice and brash ice resistance. Level ice resistance is when a ship breaks ice floes from the intact ice field, turns them parallel to the ship hull and forces them to slide down and eventually up the hull. Brash ice resistance stems from both when the ship breaks the brash ice and also when it pushes the brash ice both down and sideways, leading to friction along the parallel midbody of the ship.

In the study, the ship was assumed to always have icebreaker support when level ice are present. Thus, the ship will only be sailing in navigational channels which are recently broken. No consolidated layer of ice in the channels were assumed. Therefore, only brash ice resistance was calculated.

Brash ice resistance The formula used here is the simplified formula as described in Riska et al. (1997). The full method is described in Appendix F. The simplified formula is given as

$$R_I = C_1 + C_2 + C_3[H_F + H_M]^2[B + C_\psi H_F]C_\mu + C_4 L_{par} H_F^2 + C_5 \left[\frac{LT}{B^2} \right]^3 \frac{A_{wf}}{L_{bp}} \quad (2.17)$$

where H_M is the thickness of the brash ice and H_F describes the thickness of the brash ice layer that is displaced by the bow and is moved to the side along the parallel midbody. For $B > 10$ m and $H_M > 0.4$ m,



Figure 2.4: A typical brash ice channel. Source: Riska (2013)

it can be estimated as

$$H_F = 0.26 + (H_M B)^{0.5} \quad (2.18)$$

Further,

$$C_\mu = 0.15 \cos \phi_2 + \sin \psi \sin \alpha, \quad \min 0.45 \quad (2.19)$$

$$C_\psi = 0.047\psi - 2.115, \quad \min 0.0 \quad (2.20)$$

$$\psi = \arctan \left(\frac{\tan \phi_2}{\sin \alpha} \right) \quad (2.21)$$

C_1 and C_2 apply only for ice class 1A Super, and are to be taken as zero for lower classes.

$$C_3 = 845.576 \text{ kg}/(\text{m}^2 \text{ s}^2) \quad (2.22)$$

$$C_4 = 41.74 \text{ kg}/(\text{m}^2 \text{ s}^2) \quad (2.23)$$

C_5 for ice class 1A is given in Juva and Riska (Table 2 2002) as 825.6 kg/s.

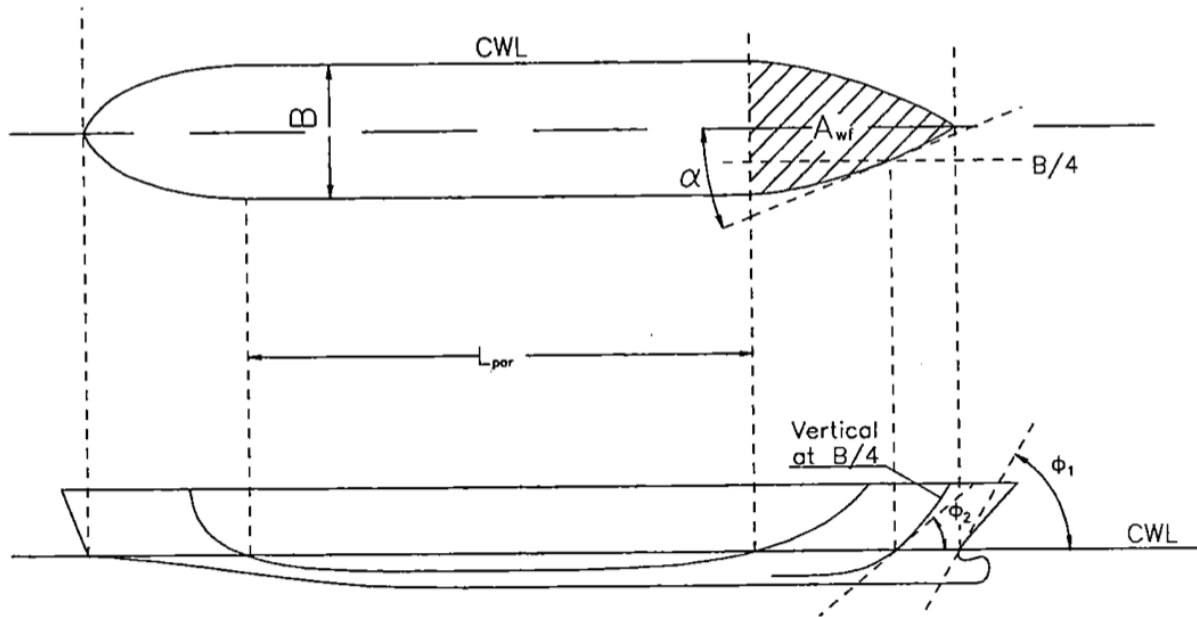


Figure 2.5: Definitions of parameters used in the ice resistance formulation. Source: Riska et al. (1997)

The term $[\frac{LT}{B^2}]^3$ is to be taken as 20 if $[\frac{LT}{B^2}]^3 > 20$ or 5 if $[\frac{LT}{B^2}]^3 < 5$. For the case ship, $[\frac{LT}{B^2}]^3 = 26.29 > 20$, therefore $[\frac{LT}{B^2}]^3 = 20$ was used in the calculations.

The ship specific coefficients A_{wf} is the waterline area of the foreship, L_{par} the length of the parallel midbody at the waterline, α the waterline entrance angle and ϕ_2 the stem angle between the waterline and the vertical at $B/4$. The definitions are shown in Figure 2.5.

L_{par} and α were estimated for the case ship based on direct measurements on the general arrangement (GA) drawing of a typical Panamax bulk carrier (see Appendix A). Thus, for the case ship, $L_{par} = 164.6$ m and $\alpha = 48^\circ$. However, A_{wf} and ϕ_2 are difficult to estimate without line drawings for the ship. According to Juva and Riska (2002), conservative estimates for these coefficients can be taken as $\phi_2 = 40^\circ$ and

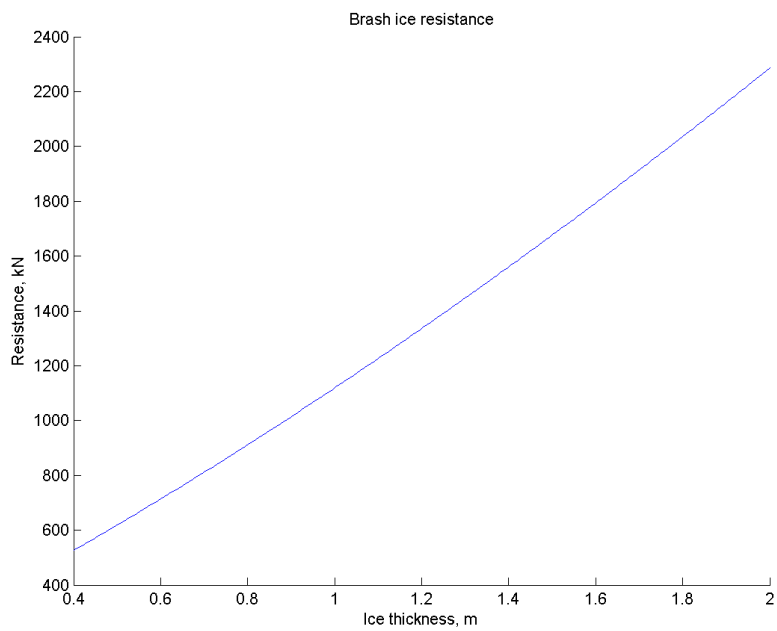
$$A_{wf} = \frac{1}{4}LB \quad (2.24)$$

The ship specific coefficients are listed in Table 2.6. The coefficients that were calculated on the basis on those, and which were used in Equation 2.17 are given in Table 2.7.

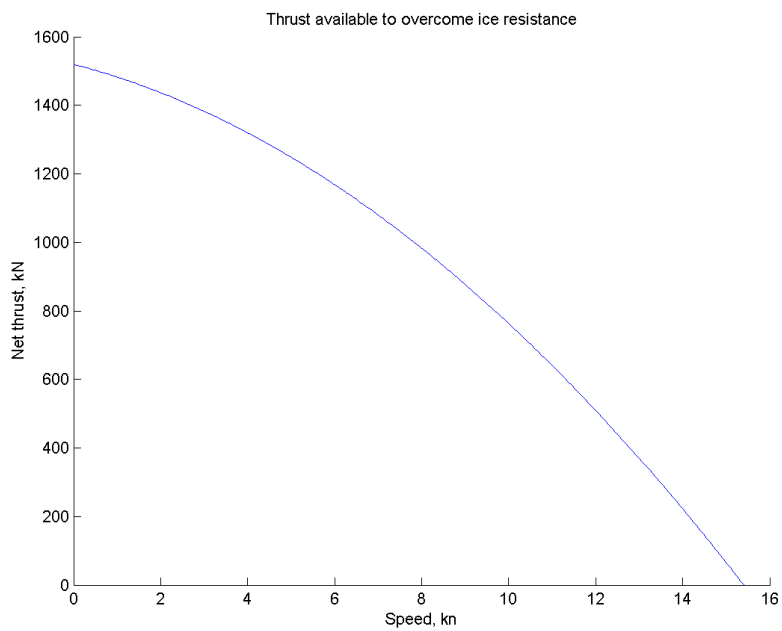
Table 2.6: Ship specific coefficients used to calculate the coefficients in Table 2.7.

Coefficient	Value	Unit
α	48	$^\circ$
ϕ_2	40	$^\circ$
A_{wf}	1776.5	m^2

By analysing Equation 2.17, it can be determined that the resistance in brash ice is only dependent on ice thickness. Thus, increasing speed will not affect the ice resistance on the hull from brash ice. The calculated resistance in brash ice for varying ice thickness is shown in Subfigure 2.6(a).



(a) Resistance in brash ice, as calculated from Equation 2.17



(b) Net thrust available to overcome the ice resistance, calculated from Equation 2.27

Figure 2.6: Ice resistance and net thrust

Table 2.7: Coefficients used in Equation 2.17.

Coefficient	Value	Unit
C_μ	0.67	-
C_ψ	0.165	-
ψ	48.5	°
C_1	0	-
C_2	0	-
C_3	845.576	kg/(m ² s ²)
C_4	41.74	kg/(m ² s ²)
C_5	825.6	kg/s
$[\frac{LT}{B^2}]^3$	20	m
L_{par}	164.6	m

As Equation 2.17 is only valid for ice thicknesses $H_M \leq 0.4$ m, ice resistance for ice thicknesses below this is assumed to be negligible.

2.1.2 Available thrust for overcoming ice resistance

The required power is the power that gives high enough thrust to exceed the ice resistance. Because the speed is low, the efficiency of propulsion must be considered. Thus, the power requirement is derived from the power needed to generate the bollard pull. The bollard pull can be determined as

$$T_{pull} = K_e (P_s D_p)^{2/3} \quad (2.25)$$

where T_{pull} is the bollard pull (kN), P_s is the total propulsion power (kW) and D_p is the propeller diameter (m). The dimensionless coefficient K_e is called the quality constant of the bollard pull. For a single screw vessel with a fixed pitch (FP) propeller, the value of K_e can be used as $0.78 \cdot 0.9 = 0.70$ (Juva and Riska, 2002).

The net thrust T_{net} is the net thrust available to overcome the ice resistance after the thrust used to overcome the open water resistance is taken into account (Juva and Riska, 2002). The net thrust can be determined as

$$T_{net}(v) = f(v) \cdot T_{pull} = \left(1 - \frac{1}{3} \frac{v}{v_{ow}} - \frac{2}{3} \left(\frac{v}{v_{ow}}\right)^2\right) \cdot T_{pull} \quad (2.26)$$

where v is the ship speed and v_{ow} is the maximum open water speed. Combined with Equation 2.25, Equation 2.26 gives

$$T_{net}(v) = K_e (P_s D_p)^{2/3} \cdot \left(1 - \frac{1}{3} \frac{v}{v_{ow}} - \frac{2}{3} \left(\frac{v}{v_{ow}}\right)^2\right) \quad (2.27)$$

A transmission efficiency coefficient η_s of 0.99 was assumed, and multiplied with P_s to find the power delivered to the propeller. The speed was varied from 0 to the maximum speed of 15.4 kn.

The net thrust, as calculated from Equation 2.27 is shown in Subfigure 2.6(b).

2.1.3 Attainable speed in ice

When the ice resistance and net thrust is determined, the attainable speed for varying ice thickness can be determined. By setting $T_{net}(v) = R_I(h)$, the attainable speed v for ice thickness h can be found. The results of the calculations are shown in fig. 2.7.

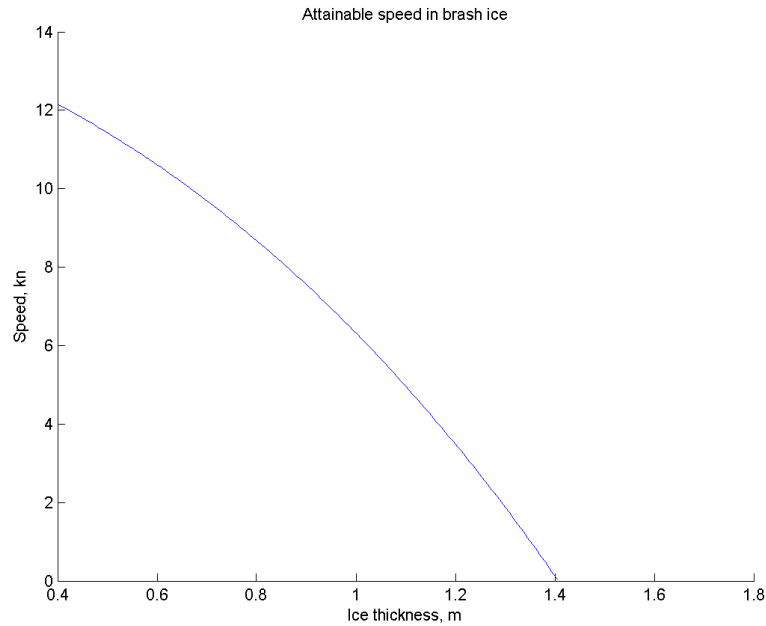


Figure 2.7: Attainable speed in brash ice conditions (h - v curve)

2.1.4 Attained EEDI for the case vessel

As seen in section 1.9.2, the attained Energy Efficiency Design Index (EEDI) for a ship shall be less than or equal to the required EEDI. The required EEDI is found from Equation 1.3, using a reduction factor x and a reference line value according to ship type and size. The reference line value for the case vessel is found by using Equation 1.4, with constant values $a = 961.79$ and $c = 0.477$ from Table 1.8:

$$\text{Reference line value} = 961.79 \cdot \text{DWT}^{-0.477} = 4.53 \quad (2.28)$$

The required EEDI for the case vessel is the reference line value, as the reduction factor x is currently zero (see Equation 1.3). However, from 2015-01-01 the required EEDI is to be reduced by 10 % for the case vessel, to an EEDI of 4.08.

The attained EEDI for the vessel is found from the method described in Appendix B (see also Appendix C for input). The attained EEDI is found to be 4.06. This means that the new required EEDI from 2015 is satisfied, but additional measures must be taken from 2020.

2.2 Route modelling

The routes between Tianjin and Murmansk were plotted in Google Maps, and exported to Matlab. The generated routes are shown in Subfigure 2.9(a). The routes that were plotted in Matlab are shown in Subfigure 2.9(b).

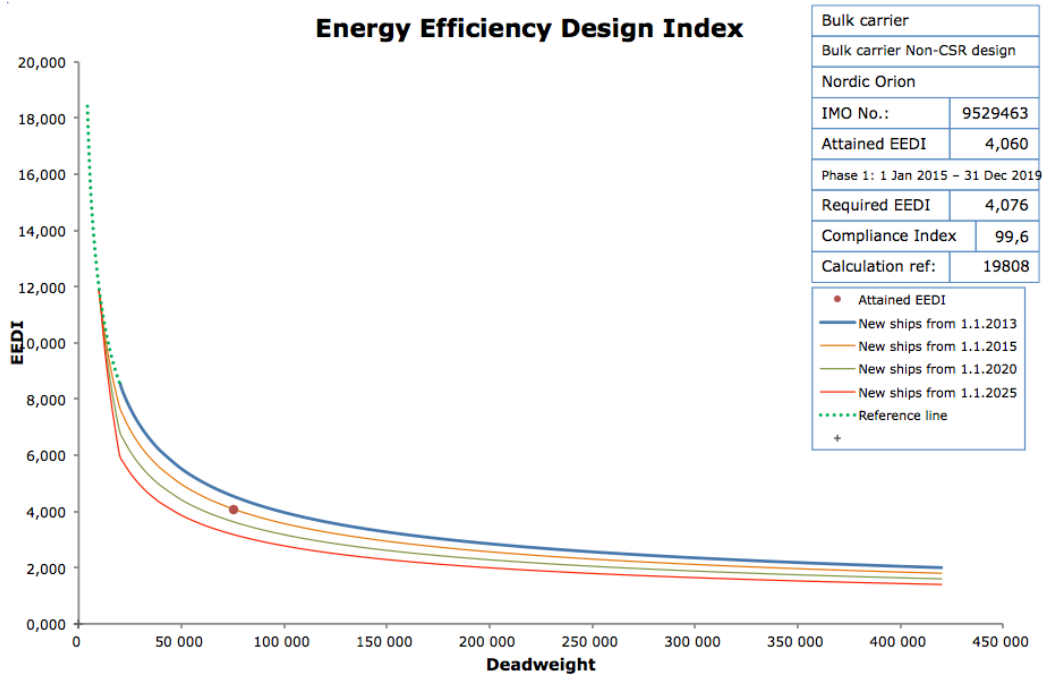


Figure 2.8: Plot of required EEDI's from the Bimco EEDI calculator

Table 2.8: Route properties

	SCR	NSR
Total distance, nm	12 624	6 680
ECA share, %	11	60

2.2.1 Modeling the Suez Canal Route (SCR)

The transit speed limit varies between 5.9 to 8.6 knots, depending on the vessel and also the tidal currents (SCA, 2014b). In the study, the speed limit was set to 5.9 knots for the whole Suez Canal transit.

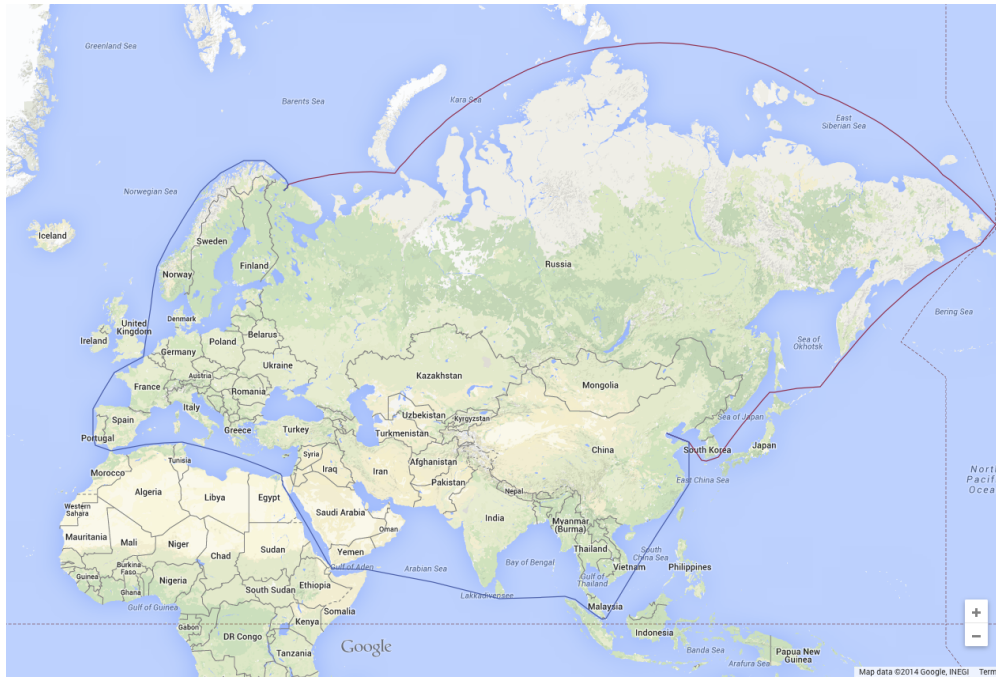
The North European SECA was also taken into account on the SCR modeling. According to IMO (2014f) the area is defined so that vessels on the SCR will enter the area at W 5° in the English Channel and leave the area when sailing north of latitude N 62°. When vessels sail in this area, the appropriate SO_x abatement measures must be used.

The costs of the SCR are found and described in section 2.8.

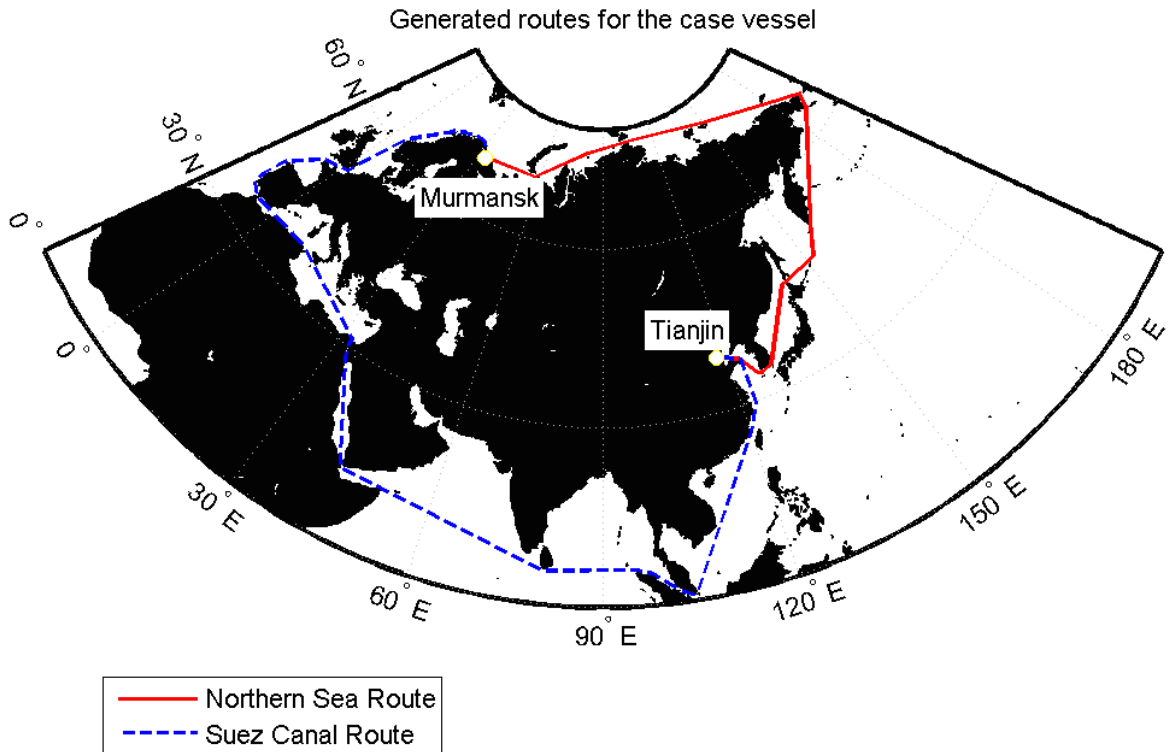
2.2.2 Modeling the Northern Sea Route (NSR)

An Arctic ECA

The study assumed an introduction of an ECA in the Arctic Ocean. The sea area, from now on known as the Arctic ECA (AECA), shall be defined as the area defined as *Arctic waters* by IMO in the *Guidelines for Ships Operating in Polar Waters* (IMO, 2010). The area is shown in Figure 2.10. For ships sailing on the NSR, this means that vessels sailing eastbound from Murmansk will enter the AECA when passing



(a) Illustration of the routes as they were generated in Google Maps. The NSR are displayed in red, the SCR in blue.



(b) The routes as they were plotted in Matlab.

Figure 2.9: Routes used in the simulation

the latitude extending north from Cap Kanin Nos (at E 43.2°¹), and leave the AECA when passing the latitude N 60° in the Bering Sea.



Figure 2.10: The areas north of the black line is defined as *Arctic waters* by IMO. In the case study, the area was modified as shown by the red dotted line. Source: IMO (2010)

Both sulphur and nitrogen emissions were assumed to be regulated in the AECA. A limit of 0.1 % sulphur content in the fuel (or utilization of emission abatement technologies which provide equivalent emission reductions) was assumed. This is according to the limits which will be introduced from 2015-01-01 in existing SECAs. For regulation of NO_x emissions, Tier III controls were assumed (see section 1.9.1) for all ships operating in the area.

Consequently, ships operating on the NSR would have to introduce appropriate measures to comply with emission limits for both SO_x and NO_x.

Retrieval of ice data

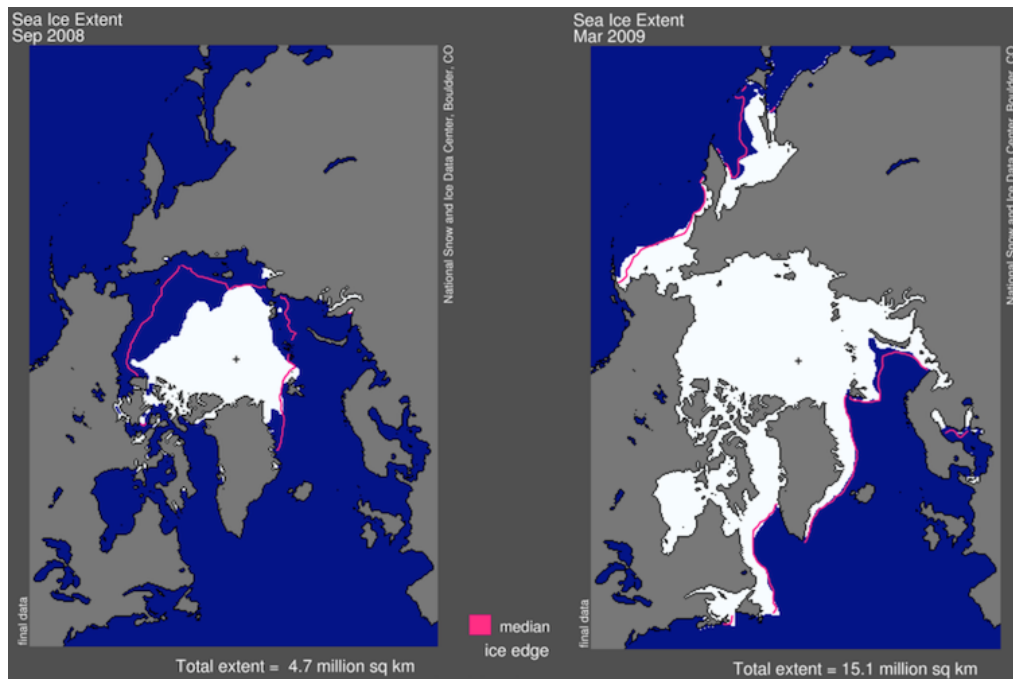
Data for ice conditions along the NSR were obtained from Tõns (2014). The data originates from satellite data provided by the U.S. National Ice Center from 2008 and 2009 (US NIC, 2014).

The coordinate points for the retrieved data are plotted in Subfigure 2.11(b). Both data for ice concentration and thickness was obtained for each point. Both the maximum and minimum limits for ice thickness and concentration were retrieved.

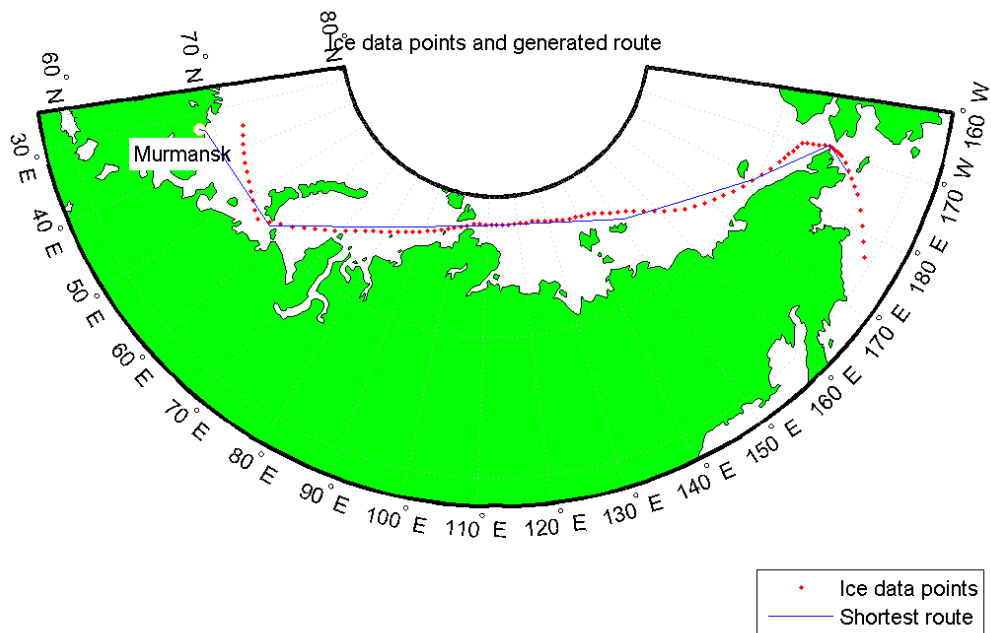
The ice data were collected for the year 2008-07-13 to 2009-07-13. Subfigure 2.11(a) shows the sea ice extent for September 2008 and March 2009.

The minimum limit scenario was used in the study to simulate the current ice conditions. As subsection 1.6.2 described, Arctic sea ice extent has decreased significantly the last decades, and the minimum scenario is thought to best represent the outlook in coming years.

¹Arctic waters is defined in IMO (2010) as “waters located north of [...] a great circle line from the Island of Bjørnøya to Cap Kanin Nos”. In the study the Arctic ECA was set to be restricted by the latitude extending north from Cap Kanin Nos for practical reasons.



(a) Sea ice extent for September 2008 and March 2009. Source: NSIDC (2014)



(b) Ice data points vs the originally plotted route

Figure 2.11: Ice data used in the study

Ice thickness assumed linearly increasing between data points in time and distance.

Route modification

The NSR route, as shown in Subfigure 2.9(b), was modified to correspond with the ice data point measurements. The originally plotted route vs the ice data points are shown in Subfigure 2.11(b). The route waypoints were replaced by the ice data points from Cape Kanin Nos in the west (at E 43.2°) to the end of the ice measurements.

2.3 Simulation time period

The simulation time period for the model was set to one year. The start of the simulation time period was set to the start time for the ice data measurements, 2008-07-13. The end date for the simulations are one year after this date, on the 2009-07-13.

2.4 Operation profile

Full loads of iron ore (75,600 tonnes) was assumed for each trip from Murmansk to Tianjin. Ballast conditions were assumed for each return leg.

Maneuvering in harbour areas, waiting time in canals and ports or loading and unloading times in port is not taken into account in the simulations.

Figure 2.12 presents the maximum ice thickness at any point of the NSR route for the whole simulation time period. As the figure shows, the max ice thickness does not fall below the maximum limit for sailing after this date. From this, the operating window on the NSR is found to be from 2008-07-13 to 2008-09-21, in total 70 days. After 2008-09-21 the vessel must sail on the SCR for the rest of the simulation time period.

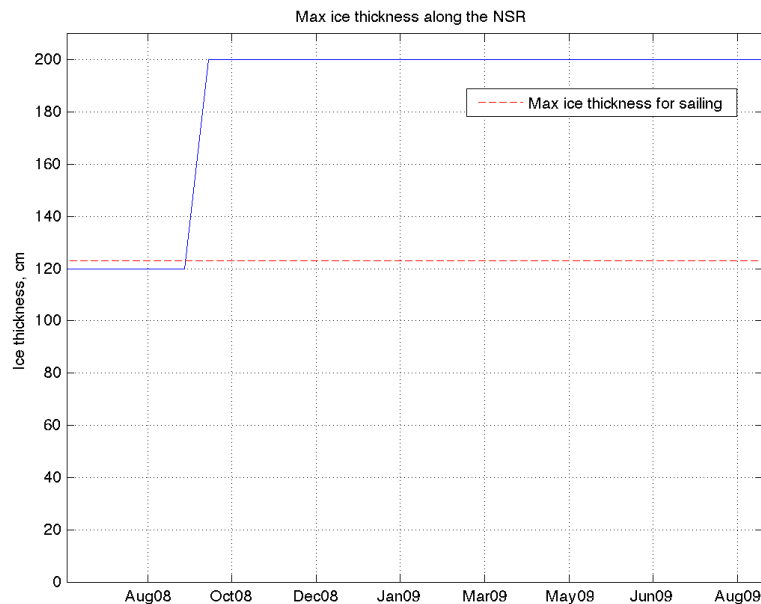


Figure 2.12: Maximum ice thickness along the NSR

2.5 Definition of scenarios in study

This section describes the different scenarios for compliance that were compared in the study. A base case scenario was defined in order to have a base line cost scenario to compare with. Several alternative scenarios were defined for different ways of fulfilling ECA emission limits.

2.5.1 Selection of abatement technologies

The available technical measures for emission abatement were discussed in section 1.10. The feasible alternatives for complying with both sulphur and nitrogen emission regulations were found to be the following:

- Fuel switch to low sulphur fuel,
- Exhaust gas cleaning systems, and/or
- Alternative fuels and/or technologies.

No measure meet requirements for both SO_x and NO_x reductions. Therefore, at least two of the measures above must be combined in the scenarios.

To reduce SO_x, two approaches was considered: Fuel switch in ECAs and installation of a sea water scrubber.

For reduction of NO_x, only two of the technologies described in section 1.10 are mature enough to consider in the study, according to MAN B&W (2014). This is the selective catalytic reduction (SCR) and exhaust gas recirculation (EGR) technologies. As previously mentioned, EGR is an internal engine process that prevent the formation of NO_x by controlling the combustion process. SCR is an after-treatment method using an additive to reduce the NO_x generated in the combustion process. Figure 2.13 shows the layout of an EGR and SCR configured engine.

Thus, the following scenarios were identified as feasible approaches to ECA regulatory compliance:

1. Burn only high sulphur fuel (HFO with less than 3.5 % sulphur). Use scrubber to reduce SO_x and catalyst (SCR) to reduce NO_x in ECAs;
2. Burn HFO in open seas, and switch to low sulphur fuel (MGO) in ECAs. No SO_x abatement technology is necessary. Use SCR in ECA to reduce NO_x emissions;
3. Convert machinery to dual fuel LNG machinery. Burn HFO in open seas, switch operation to burn LNG when operating in ECAs. Use EGR for NO_x abatement.

The base case burns HFO while in open seas, and switch to MGO when sailing in the North European SECA. There are no abatement measures installed.

The following sections describe the scenarios in more detail.

2.5.2 The base case scenario

In order to evaluate the vessels' performance on the NSR, they were compared to sailing the Southern route (see subsection 1.5.1) all year. The vessel in the base case burn HFO in open seas. When it enters the North European SECA, it switches to MGO fuel. Thus, the base case vessel does not have any abatement technologies installed.

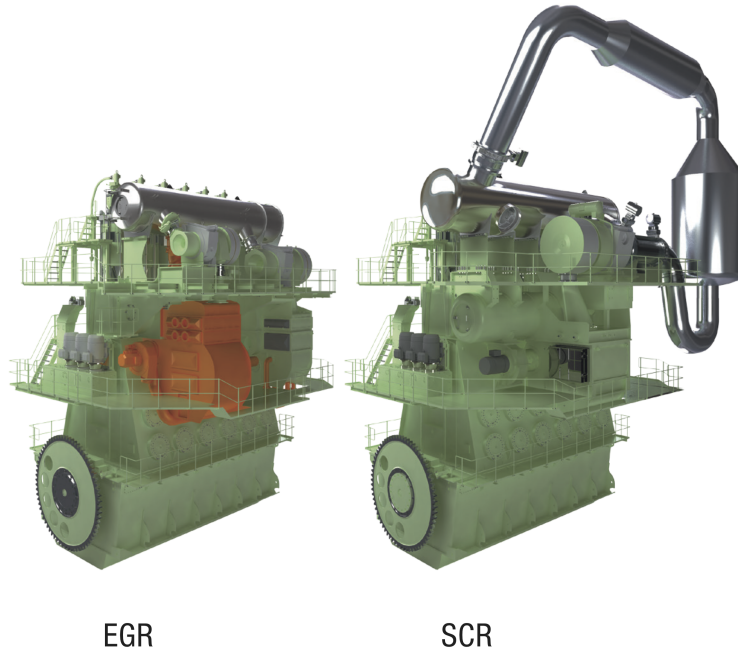


Figure 2.13: EGR and SCR solutions. Source: MAN B&W (2014)

2.5.3 Scenario 1: Exhaust cleaning only

The vessel in scenario 1 utilise exhaust gas cleaning technologies to comply with ECA regulations. The vessel is retrofitted with a scrubber to reduce SO_x emissions combined with SCR technology to obtain the necessary NO_x reduction.

By installing these measures, the vessel can operate on HFO at all times.

2.5.4 Scenario 2: Combine exhaust cleaning and fuel switch

Scenario 2 combine exhaust gas cleaning with fuel switching when operating in an ECA. The vessel operate on HFO in open seas, and switch to the low sulphur fuel MGO in ECAs. Thus, no SO_x abatement technology is necessary. A SCR unit is retrofitted, in order to reduce NO_x emissions. This is utilised in ECAs.

The arrangement implies that the vessel must have separate fuel tanks for the two different fuels.

MGO is a more expensive fuel, but installation costs are saved by only installing one abatement technology.

2.5.5 Scenario 3: LNG conversion and exhaust cleaning

The third scenario is the most extensive in terms of retrofitting. The main engine is converted to be able to run on dual fuel (DF), HFO and LNG. This includes conversion of the mechanically controlled (MC) fuel injection system to an electronic system (ME). Also, the engine must be converted to be able to operate on gas, to a ME-GI type. Figure 2.14 is an illustration of components that needs to be modified and added to the engine.

However, LNG operation is not adequate to satisfy Tier III limits. Therefore an EGR unit is installed in addition to the conversion of the main engine.

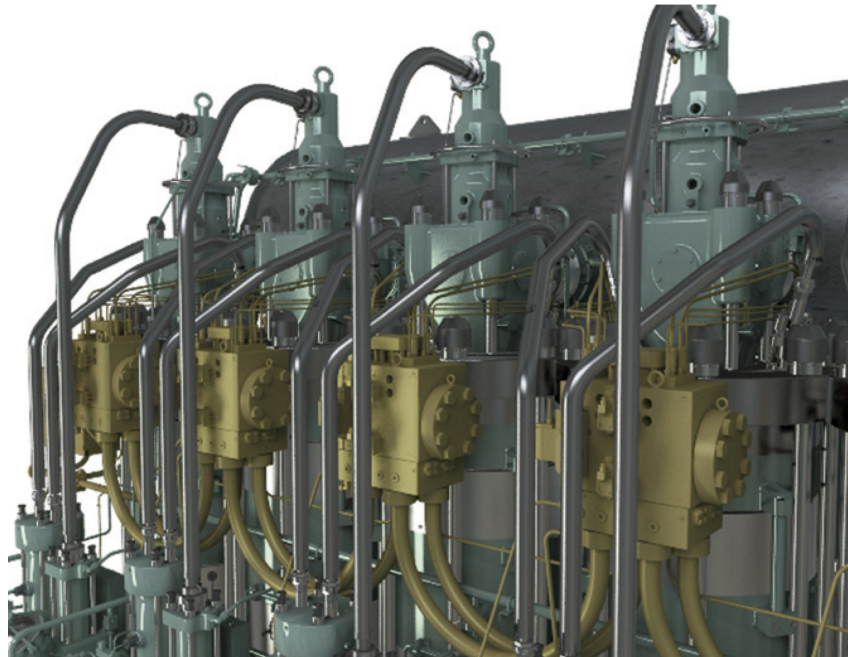


Figure 2.14: Illustration of components which needs to be modified and added to the engine in order to allow it to operate on gas (illustrated in yellow). Source: MAN B&W (2012)

The availability of LNG could be an issue for a vessel like this. However, the study assume that adequate bunkering facilities are available in the ports considered.

2.6 Modeling machinery and abatement technologies

The vessel has one main engine of type MAN B&W 6S60MC-C. The engine is a low speed, 2 stroke, 6 cylinder engine, driving a fixed pitch propeller at 105 rpm. Total installed power is 13 560 kW. The fuel consumption is given as 34 tonnes of HFO per day at 14 knots.

The specific fuel consumption (SFC for HFO were assumed to be 174 g/kWh at a nominal MCR of 80 %, based on info from the technical specification for the engine type (MAN B&W, 2010). For the other fuels SFC at nominal engine load (75 %) were estimated as 154.4 g/kWh for MGO and 126.5 g/kWh for LNG, based on numbers from GL (2011).

Table 2.9: Base line values for specific fuel consumption at optimal load used in the study.

Fuel type	SFC, g/kWh	Optimal load %	Source
HFO	174	80	MAN B&W (2010)
MGO	154.4	75	GL (2011)
LNG	126.5	75	GL (2011)

The SFC varies with engine load. GL (2011) presents typical SFC values for different fuels over varying engine load. These values were used in the study to establish a reference line, in order to describe the relative variation of the fuel consumption over the engine load range. Reference values for SFC were taken from GL (2011) at 30, 50, 75 and 100 % engine load, and modeled over the whole load range as polynomial functions of second degree. For HFO, the reference values were made dimensionless and

thereafter multiplied with the SFC found as shown in Table 2.9. The SFC as a function of engine load for the different fuels are presented in Figure 2.15.

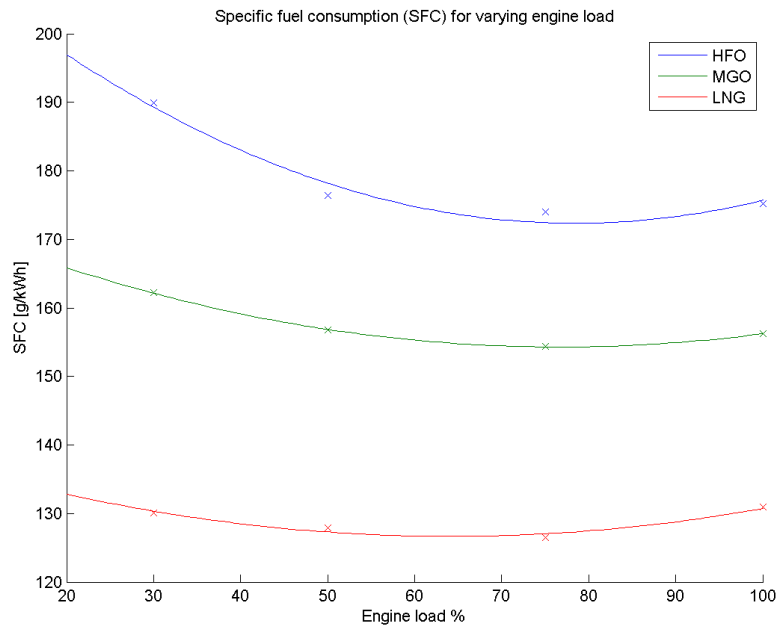


Figure 2.15: Specific fuel consumption for varying engine load. The points marked with x are the reference values used to construct the SFC as a polynomial function.

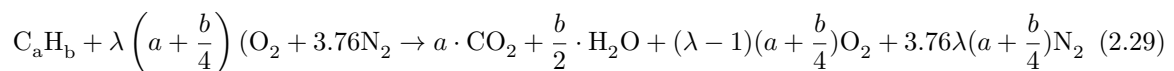
The vessel has three auxiliary engines of type Daihatsu 5DK-20 (4 stroke, 5 cylinder) installed. The high speed engines run on distillate fuel. The engines produce 610 kW each at 720 rpm.

2.7 Modeling of emissions

According to section 1.3, the model should model emissions according to varying operating conditions. This sections discuss how emissions form in marine diesel engines, and how it can be modeled in the simulation model.

2.7.1 Formation of pollutant emissions in marine diesel engines

CO₂ emissions are directly related to the carbon content of the fuel. Therefore CO₂ emission reductions may be achieved by reducing the fuel consumption. Emission ratios for CO₂ can be found from the chemical reaction in the combustion process. Consider the fuel as a pure hydrocarbon with a general chemical composition C_aH_b². The air in the combustion process is considered as dry atmospheric air with composition 79 % nitrogen and 21 % oxygen³, or 3.76 mol N₂ per mol O₂. A complete combustion gives the following reaction:



²For “normal” hydrocarbon types, $b \simeq 2a$, which gives C_nH_{2n}.

³In volume percentage

where λ is the air surplus number, equal to 1 when the combustion is complete.

Sulphur oxides are caused by the oxidation of the sulphur in the fuel into SO_2 and SO_3 (Andreoni et al., 2008). They are formed through the combustion process through the reaction:



Accordingly, SOx is directly related to the sulphur content of the fuel. HFO may contain up to 4.5 % sulphur, light distillates often have around 0.1 % to 0.5 % sulphur.

Nitrogen oxides (NO, NO_2 and to some degree N_2O) are collectively referred to as NOx. The quantity produced is a function of temperature, oxide concentration and fuel used. Atmospheric nitrogen (N_2) forms NO at the high temperatures during combustion in the cylinder. The NO transforms to NO_2 outside the engine. Nitrogen in the fuel also transforms to NO. However, the nitrogen content in the fuel is low, especially for distillates. High temperatures are required to form NOx, therefore the best way to reduce NOx generation is to lower combustion temperatures.

Other pollutants such as unburnt hydrocarbons (UHC or HC, sometimes called VOC for Volatile Organic Compounds), carbon monoxide (CO), soot and particulate matter (PM) are due to incomplete combustion, and may be reduced by improved design of the combustion system.

Table 2.10 lists the sources of all emission components, and indicate some possible control methods.

Table 2.10: Overview of pollutants and their control. Source: Er (2002)

Pollutant	Control
NOx	Function of peak combustion temperatures and oxygen concentration. Reduction can be achieved by utilizing primary and secondary methods.
SOx	Function of fuel oil sulphur content. The most effective means of reduction is to lower the sulphur content in the fuel.
CO	Function of the air excess ratio and combustion temperature and air/fuel mixture. Very low for 2 stroke diesel engines.
HC	During the combustion process a very small part of the fuel and lube oil is left unburned. Depends on fuel and lube oil types.
Particle emission	Originate from partly burned fuel, ash content in fuel/cylinder lube oil, partly burned lube oil/dosage, deposits peeling off in the combustion chamber/exhaust gas system.

Two parameters are usually used to quantify the emissions from an engine; the specific pollutant emissions, *spe* (in g/kWh), and the pollutant emission ratio, *per* (in g/kg). The definition for specific pollutant emission is

$$\text{spe} = \frac{\dot{m}_{pe}}{P_B} \quad (2.31)$$

where \dot{m}_{pe} is the mass flow of pollutant emission (expressed as g/hr) and P_B is the brake power of the engine (in kW).

The pollutant emission ratio express the relation between the production of pollutants and the actual combustion of fuel. The *per* is defined as the ratio between the pollutant emission and the fuel consumption \dot{m}_f (in kg/hr):

$$\text{per} = \frac{\dot{m}_{pe}}{\dot{m}_f} \quad (2.32)$$

The pollutant emission ratio and the specific pollutant emission are related with the specific fuel consumption SFC as follows:

$$\text{spe} = \text{per} \cdot \text{SFC} \quad (2.33)$$

Typical emission values are listed in Table 2.11, and can also be seen in Figure 2.16. The specific pollutant emissions are often part of the engine specification from the manufacturer.

Table 2.11: Typical diesel engine exhaust emissions. The values are calculated using a specific fuel consumption between 160 and 220 g/kWh. Source: Woud and Stapersma (2002)

	Pollutant Emission Ratio (<i>per</i>) in g/kg	Specific Pollutant Emission (<i>spe</i>) in g/kWh
CO ₂ (86 % C in fuel)	3200	500-700
SOx per % S in fuel	20	3.2-4.4
NOx	40-100	6-22
HC (gaseous)	0.5-4	0.1-0.9
CO	2-20	0.3-4.4
Particulates (depending on fuel)	0.5-2	0.1-0.4

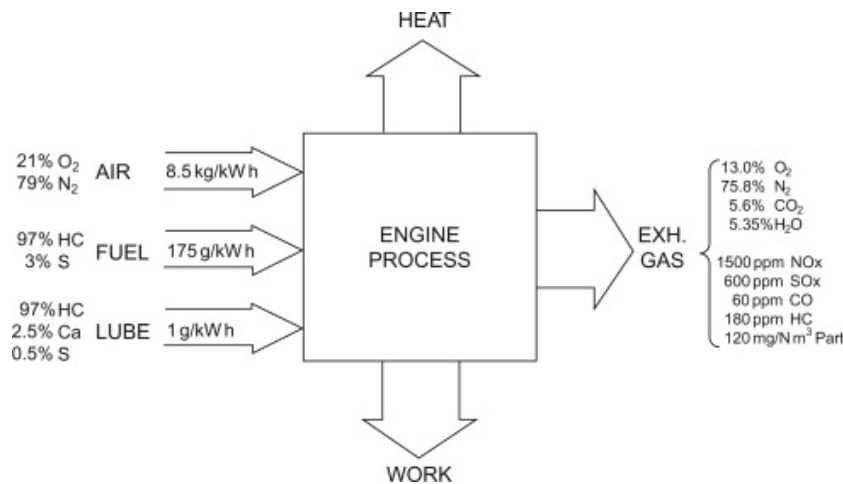
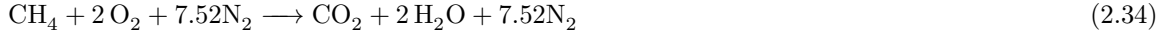


Figure 2.16: Typical exhaust emission values for a marine diesel engine. Source: Woodyard (2009)

2.7.2 Modeling of emissions in study

Emissions depend on type of fuel, fuel consumption and engine load. As determined in subsection 2.7.1, CO₂ and SO_x emissions are directly determined by the fuel composition and consumption. NO_x and PM emissions additionally depend on the combustion process and the machinery.

In fossil fuels, the pollutant emission ratio (*per*) of CO₂ is relatively constant at 3200 g CO₂ per kg fuel. This emission ratio was used in the emission calculations for the HFO and MGO fuels. The chemical composition of LNG is different, and the CO₂ emission ratio was found using Equation 2.29. The balanced chemical reaction equation for burning methane is:



Thus, the ratio of mol CH₄ to CO₂ is 1:1. The molecular weight of CH₄ is 16.043 g/mol and for CO₂ 44.010 g/mol. Consequently, the *per* for CO₂ for LNG fuel is approximately 2743 g CO₂ per kg LNG.

The *per* for sulphur oxide emissions from fossil fuels is approximately 20 g SOx per kg fuel per % S in the fuel. LNG contains only negligible amounts of sulphur, so SOx emissions from burning LNG is negligible.

The *per* values for CO₂ and SOx for the different fuels used in the study are listed in Table 2.12.

Table 2.12: Pollutant emission ratios (*per*) for CO₂ and SOx for the different fuels used in the study.

Fuel type	<i>per</i> CO ₂ , g/kg fuel	Sulphur in fuel, %	<i>per</i> SOx, g/kg fuel
HFO	3200	2.1	42
MGO	3200	0.05	1
LNG	2743	0	0

In order to model change in NOx emissions when operating on loads outside of the optimum operation point, the relative change in emissions found by Æsøy et al. (2013) were used. Æsøy et al. (2013) tested alternative fuel oils and their effect on engine emission characteristics. The test engine used was a one-cylinder loop-scavenged 2-stroke Wärtsilä WX 28B with maximum power output of 300 kW at 600 rpm. It is a turbocharged medium-speed direct-injection marine diesel engine with cylinder bore of 280 mm and piston stroke of 360 mm. Among the tested fuels were HFO with a fuel sulphur content (FSC) of 2.1 % and MGO with a FSC of 0.05 %. For each of the fuels, the test engine was operated on 25 %, 50 %, 75 % and 100 % load, and the emissions were measured for each operating point. Assuming 75 % MCR as the optimum operational point, the relative values are given in Table 2.13.

Table 2.13: Relative change in NOx specific emissions [g/kWh] for varying engine load, compared to the optimum operational point at 75 % MCR. Derived based on data from Æsøy et al. (2013)

Load	HFO	MGO
25 %	1.36	1.45
50 %	1.15	1.20
75 %	1	1
100 %	0.89	0.86

The relative change in *spe* were used as reference values, and modeled as polynomial functions of second degree. As no data was available for LNG fuel, the reference line for MGO were also used to model LNG NOx emissions in this study.

To determine specific NOx emissions for the fuels, the reference values were multiplied with a reference value for the particular fuel at optimum load point. At 75 % load, the *spe* values for HFO, MGO and LNG were chosen as 9, 8 and 5 g/kWh respectively, based on data from Æsøy and Stenersen (2013). Multiplied with the reference value functions, the results are shown in Subfigure 2.17(a).

As discussed in section 1.9.1, the NOx Tier II and Tier III limits for slow speed engines are limited to 14.4 and 3.4 g/kWh respectively (see Table 1.7). All fuels comply with Tier II limits. This is as expected,

as the vessel's engine is built according to Tier II regulations. However, to comply with Tier III limits Subfigure 2.17(a) illustrates that fuel switch alone is not enough. Therefore, all scenarios in the study must use end of pipe technology to clean exhaust emissions for NO_x.

Also particle matter (PM) emissions are dependent on both fuel properties and the combustion process. The PM *spe* were based directly on the measured results from *Æsøy et al. (2013)* for HFO and MGO fuels. For LNG, no published figures exist. Therefore, the *spe* values were guesstimated as 5 mg/kWh at 100 % load and 10 mg/kWh at 50 % load for LNG. The *spe* values (see Table 2.14) was plotted over the engine load range, and the *spe* were modeled as polynomial functions of 3rd, 2nd and 1st degree, respectively.

Table 2.14: PM specific emissions [mg/kWh] for varying engine load. Source: *Æsøy et al. (2013)*

Load	HFO	MGO	LNG
25 %	233	79	
50 %	254	76	10
75 %	267	83	
100 %	299	108	5

2.7.3 Emission reductions from abatement technology

The efficiencies of the abatement technologies was assumed in the study as listed in Table 2.15. The figures are based on the findings of *Entec UK Ltd. (2005a)* (see section 1.10).

Table 2.15: Emission reduction efficiencies. Emission reductions are indicated with a negative sign, increases are indicated with a positive sign.

	Reductions, %			
	CO ₂	SO _x	NO _x	PM
Scrubber	0	-75	-10	-25
SCR	0	0	-90	-30
EGR w/LNG	0	0	-35	+10

2.8 Costs used in study

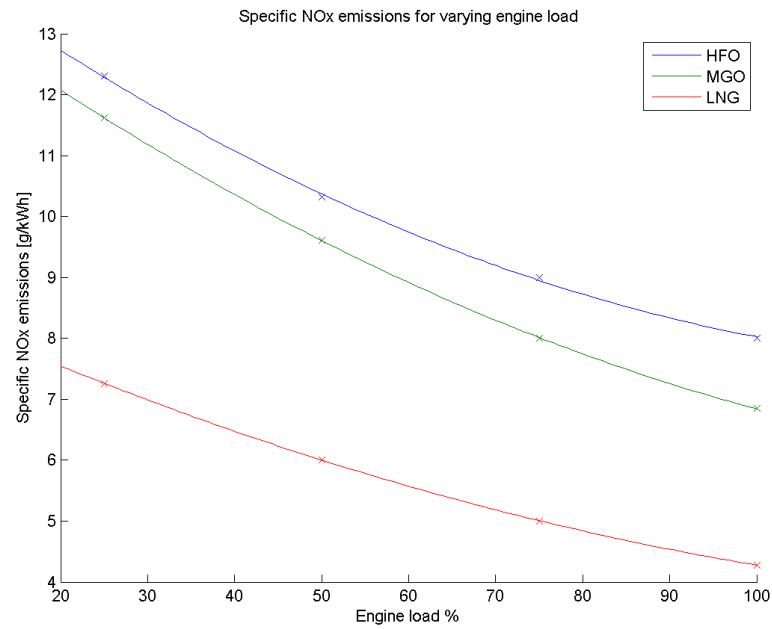
This section discuss the factors influencing the cost and operational factors influencing the cases. Both ice class and emission abatement measures have an influence on both investment costs and operational costs. In addition, voyage costs will also differ depending on route.

The abatement measures were evaluated based on investment costs (CAPEX) and operating costs (OPEX). The sections below describe the costs considered in the study. The figures are retrieved from a ship owner operating a fleet of LPG tankers. Note that the figures are approximations, and should be treated as such.

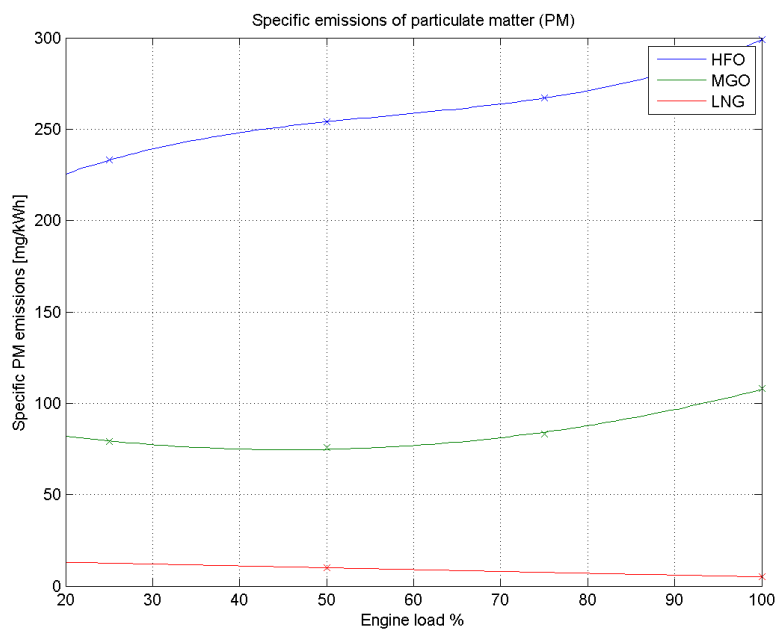
Since the study considers retrofitting an existing vessel with ice class and not a newbuild, added costs for ice classification, winterization etc. (as discussed in subsection 1.6.7) will not be considered in the study.

2.8.1 Direct add to costs from abatement technologies

For the abatement technologies, the capital costs include costs of retrofitting and/or modification. CAPEX for the different scenarios are listed in Table 2.16. Off hire costs are not included in these CAPEX.



(a) NOx emissions



(b) PM emissions

Figure 2.17: Change in emissions for varying engine load. The points mark the reference values of which the functions are extrapolated based on.

Table 2.16: Assumed CAPEX for retrofitting and/or modifying the abatement technologies on the case vessel.

Abatement technology	CAPEX, MUSD
Scrubber installation	3
SCR	3
EGR	1.6 ^a
LNG retrofit ^b	20

^aAssuming an exchange rate of 1 USD = 0.8 EUR.

^bIncluding installation of 2000 m³ LNG tank

The abatement technologies' influence on operational costs are listed in Table 2.17. All technologies give an increase in fuel consumption. The cost of the urea consumption of the SCR is modeled as a 10 % increase in fuel consumption.

Table 2.17: Approximation of the abatement technologies' influence on OPEX for the vessel.

Technology	Influence on OPEX	
	Add to fuel consumption, %	Add to maintenance costs
Scrubber	3	10 % of CAPEX
EGR	3	
SCR	10	
LNG	1	

Another relevant measure is off hire cost for periods in docking and/or in yard. To retrofit a vessel with the emission abatement technologies itself means that the vessel must be taken out of operation. This cost depend on the freight rate of the cargo and the length of the docking period. This is not included in the study.

2.8.2 Fuel prices

The fuel prices used in the case study were chosen based on figures from Levander (2009), and are listed in Table 2.18.

Table 2.18: Fuel costs used in the case study. Source: Levander (2009) and Acciaro (2014)

Fuel type	Cost USD/ton
HFO	450
MGO	750
LNG	650

2.8.3 Route tariffs

Both the NSR and the SCR have tolls or fees. The NSR has tariffs paid to the Russian government for passage on the NSR, and the SCR has tolls for passing the Suez Canal. These are calculated as voyage costs. The SC fees for the case vessel are found from SCA (2014a), listed in Table 2.19. The NSR fees are more difficult to estimate, as discussed in subsection 1.5.2. In the study, the NSR tariffs are estimated as 10 % higher than the SC fees. Costs for icebreaker support is assumed to be included in the NSR tariff. Furthermore, the vessel is always assumed to be loaded when sailing southbound and always in ballast condition when sailing northbound. Therefore, the average fee was used in the calculations.

Table 2.19: Route tariffs used in the case study. The NSR fee is calculated as 10 % higher than the SC fees.

Location	Laden fee, USD	Ballast fee, USD	Average fee, USD
Suez Canal	222 091	188 901	205 496
NSR	244 300	207 790	226 050

2.9 Methods for comparing different scenarios

2.9.1 Equivalent annual costs (EAC)

Two common methods to compare investment proposals are the net present value (NPV) method or the equivalent annual costs (EAC) method. According to Jones and Smith (1982), the NPV method discounts cash flows to the present while the EAC method converts cash flows into an equivalent series of uniform annual amounts. The EAC is often considered easier to comprehend, as it gives an amount that is more relatable to companies that report activities on a yearly basis. The NPV method gives a dollar amount of high magnitude, that may be misleading. In addition, the EAC method allows for comparison of alternatives with unequal lives, unlike the NPV method. Therefore, the EAC method were chosen to compare the costs of the scenarios in the study.

The equivalent annual costs are derived from the following formula:

$$\text{EAC} = \text{CAPEX} \cdot f_{AP} + \text{OPEX}, \quad (2.35)$$

where CAPEX is the total fixed cost expenditure and OPEX is the annual operating costs. f_{AP} is the annualisation factor:

$$f_{AP} = \frac{i \cdot (1 + i)^n}{(1 + i)^n - 1} \quad (2.36)$$

In Equation 2.36, n is the lifespan of the measure, and i is the discount rate. In the study, a discount rate of 4 % and a lifespan of 20 years was assumed for all abatement technologies.

2.9.2 Cost effectiveness ratio (CER)

Cost effectiveness analysis can be used to relate the cost of a measure to the outcome or benefit. According to Cellini and Kee (2010), the cost effectiveness ratio (CER) is obtained by dividing costs by *units of effectiveness* :

$$\text{CER} = \frac{\text{Total cost}}{\text{Units of effectiveness}}, \quad (2.37)$$

In the study, the cost used to calculate the CE ratio was the EAC for the scenario, thus Equation 2.37 becomes

$$\text{CER} = \frac{\text{EAC}}{\text{Units of effectiveness}} \quad (2.38)$$

The units of effectiveness can be a measure of any quantifiable outcome. In the study, the measures of effectiveness was primarily defined as the amount of emissions reduced for the scenarios on the NSR, and the cost per tonne freight.

The reduced emissions per year by applying abatement measures was calculated as

$$\text{Reduced emissions} = \text{Emissions without measure} - \text{Emissions with measure} \quad (2.39)$$

where the emissions are measured in tonnes per year. Thus, the CER for emission reduction was found from Equation 2.40:

$$\text{CER}_{\text{emissions}} = \frac{\text{EAC}}{\text{Reduced emissions}} \quad (2.40)$$

The cost per tonne freight was calculated as

$$\text{CER}_{\text{cargofreight}} = \frac{\text{EAC}}{\text{Number of laden trips} \cdot \text{DWT}} \quad (2.41)$$

2.10 Description of MATLAB model

This section presents the simulation model that was developed in order to produce the results.

2.10.1 General description

The model that performed the calculations was made in MATLAB (v 2013b). Some files in the model requires the *Mapping Toolbox*. These files were tested in MATLAB version 2012b. All files are listed below. The most important files are described in detail later in this chapter (see subsection 2.10.2). All files are presented in full in the appendices.

The MATLAB simulation model includes one main file and calls on several sub-files. Figure 2.18 is a flow chart demonstrating the flow of the main files in the model. The main files of the model with their descriptions are listed in Table 2.20.

Table 2.20: Main files of the MATLAB model and their functions

File name	Function
<code>emissions_calc.m</code>	Calculate the emissions of CO ₂ , NO _x , SO _x and PM
<code>findice.m</code>	Calculate the ice conditions for a given date and location on the NSR
<code>sailNSR.m</code>	Simulates the sailing for a voyage on the NSR route
<code>sailSCR.m</code>	Simulates the sailing for a voyage on the SCR route
<code>sail_ice.m</code>	Calculates time, fuel consumption and emissions for a given distance with ice present
<code>sail_ow.m</code>	Calculates time, fuel consumption and emissions for a given distance in open water
<code>simulate_sailing.m</code>	Main file. Simulates for all scenarios for the whole time period

The model files read variables saved in MATLAB format files. The contents of the format files are defined and calculated by supporting files. The files that define the variables are listed in Table 2.21. The

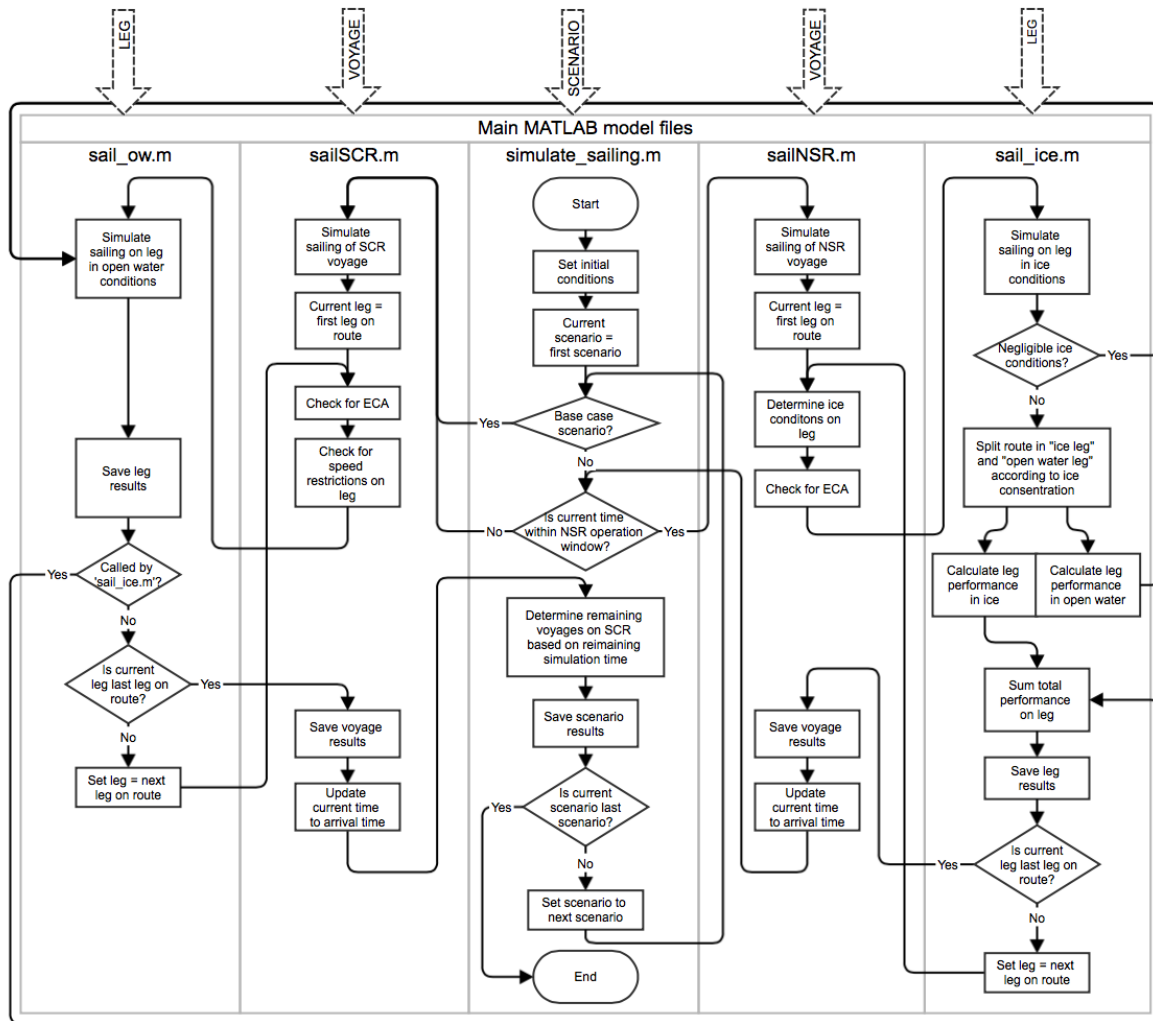


Figure 2.18: Flowchart illustrating the main flow of the main files of the model. Note! Not all subprocesses are shown. See detailed descriptions of file processes and flow charts in subsection 2.10.2.

files' dependencies of other files are also shown. Files that are not a part of the main model, but are required to calculate the input variables are listed in Table 2.22. The MATLAB format files in which the required variables are stored in are listed in Table 2.23.

Table 2.21: Files in the MATLAB model directory who define input variables for the simulation model. The table also lists if the file reads variables from a format file, if it calls on other functions, and in which format file the calculated and/or defined variables are stored.

File name	Define	Format file read	Calls on	Format file write
abatement_tech.m	Properties of the abatement technologies			abatementtech.mat
costs.m	All costs			costs.mat
engine_data.m	Properties of fuels and engine characteristics			enginedata.mat
hv_input.m	Input required for file HV.m	variables.mat	hv.m	hv.mat
maindim.m	Main parameters of the case vessel	ow_resistance.m	shipdata.mat	
read_ice.m	Ice condition and thickness data (read from input files)			icedata.mat
routedata.m	Route properties (read from input files)	icedata.mat		routedata.mat
routegen.m	Special geographical areas on the routes (ECAs, speed limits)	routedata.mat, icedata.mat, shipdata.mat		routedata.mat
scenarios.m	Scenario specifications (fuel type, abatement technology, etc.)			scenarios.mat

Table 2.22: Supporting files in the MATLAB model directory and their functions

File name	Function	Calls on
hv.m	Calculates the ship performance in brash ice	ice_resistance.m
ice_resistance.m	Calculate the resistance in ice	
ow_resistance.m	Calculate open water resistance	

As seen from Table 2.21, some files read data from input files. The input files used in the model are listed in Table 2.24.

2.10.2 Descriptions of main files in model

This section presents the main files of the simulation model in detail. All files are presented in full in the appendices.

Table 2.23: MATLAB format files in the model directory

File name	Contents
<code>abatementtech.mat</code>	Properties of the abatement technologies
<code>costs.mat</code>	Costs data
<code>routedata.mat</code>	Route properties
<code>enginedata.mat</code>	Properties of fuels and engine characteristics
<code>scenarios.mat</code>	Scenario specifications
<code>hv.mat</code>	Resistance in ice and net thrust curve
<code>shipdata.mat</code>	Vessel specification and open water resistance
<code>icedata.mat</code>	Ice dataset contents

Table 2.24: Data files in the directory ‘data’

File name	Contents
<code>NSR_waypoints.gpx</code>	Waypoints on the NSR route (from Tianjin to Murmansk)
<code>SCR_waypoints.gpx</code>	Waypoints on the SCR route (from Tianjin to Murmansk)
<code>icedata_ct.xlsx</code>	Ice concentration data for points along the NSR
<code>icedata_thicknesses.xlsx</code>	Ice thickness data for points along the NSR

`simulate_sailing.m`

This is the main file of the simulation model. The process in the file is illustrated in Figure 2.19 and Figure 2.20.

The file loads the necessary format files. Initial conditions for the simulations, such as start and stop time are defined. Because the ice data is based on a specific time series, the simulation start time is set to the start date for the ice measurements, 2008-07-13. The stop time is defined as one year after this date.

The file determines the maximum possible ice thickness the vessel can sail when the minimum speed is set to 3 knots from the h - v -curve. From this, the operational window on the NSR can be found. The condition is defined so that when the ice thickness at any point on the NSR is greater than the maximum found value, the vessel must sail on the SCR. This check is performed when the vessel is in harbour, and ready to sail. This means that the vessel can risk getting stuck on the route, if the ice thickness grows while underway. Fortunately this does not occur for the ice data used in the simulations, but it is good to be aware of. Also, since the max ice thickness never decrease again after initial operational window closes (see Figure 2.12), the sailing pattern in the simulations is defined so that the vessel sails the NSR until this date, and then sails on the SCR for the rest of the simulation time period. The model cannot switch back to the NSR. Thus, for other ice data, the model input must be reformulated.

After the operational window on the NSR is found, the file locates the legs on the route where ice may occur. A position vector is defined, so that the file know whether the vessel is headed north or south bound at any trip.

The sailing simulations are performed as a series of nested for-loops. The outermost loop runs for all defined scenarios. For each scenario, a trip counter is reset and the position vector is set to Murmansk. The fuel specification for normal sailing and sailing in ECAs for the scenario is read from the format file `scenarios.mat`. Via an if-condition, the file tests if the current scenario is the base case scenario or not. If this is the case, the simulations on the NSR are skipped, and simulations are performed on the SCR only. For the other scenarios, a while-loop makes the vessel sail the NSR via the file `sailNSR.m` while the current simulation time is less than the stop date for the operational window on the NSR. When the time

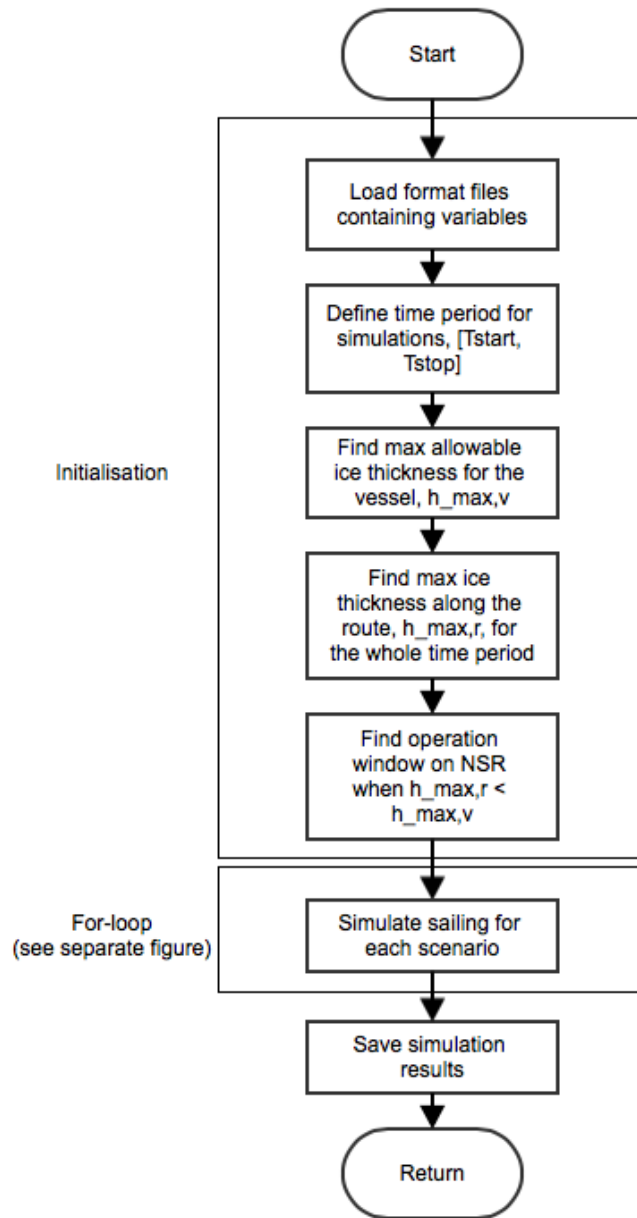


Figure 2.19: Flowchart for `simulate_sailing.m` file. See Figure 2.20 for description of the simulations per scenario.

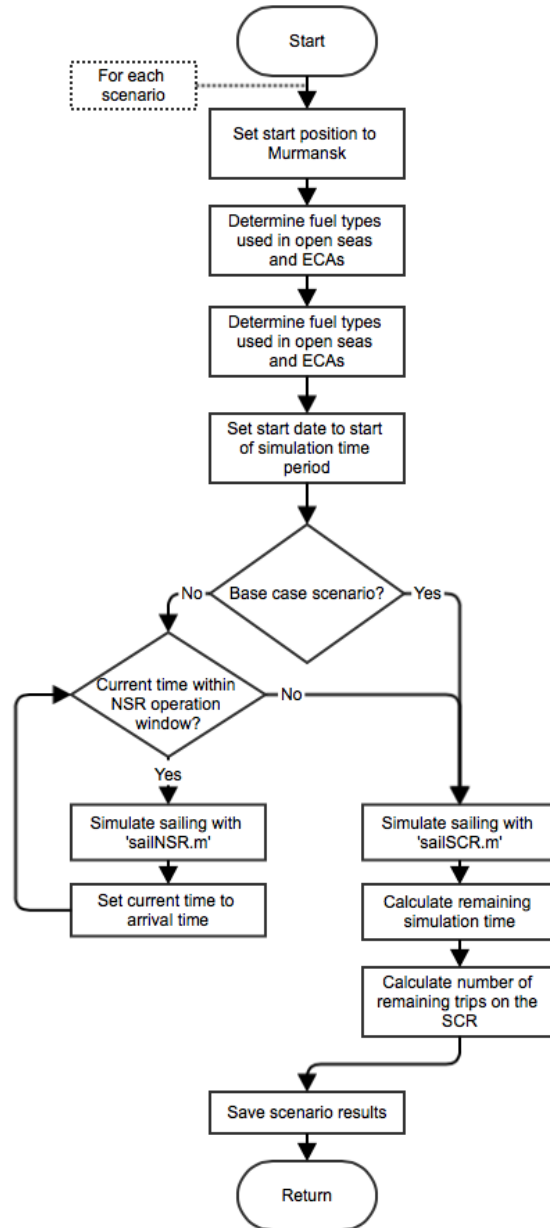


Figure 2.20: Flowchart for the simulation of each scenario in the `simulate_sailing.m` file (see Figure 2.19)

passes this date, vessel sails on the SCR for the remaining time of the simulation time period. The SCR voyages are simulated using the file `sailSCR.m`.

After the sailing simulations are performed for the current scenario, the data is stored as structures in a format file exclusively for the results. A new results file is generated for each run of the file, dated according to the time for the simulations. The results file is named `results_YYYYMMDDThhmmss.mat`, where ‘YYYYMMDDThhmmss’ is the date format for the current date. A field named ‘revision’ allows the user to specify a text string explaining what has been changed in this revision/run of the file.

`sailNSR.m`

This file simulates the sailing of one voyage on the NSR route, as a part of the file `simulate_sailing.m`. The process in the file is illustrated in Figure 2.21 and Figure 2.22.

The file runs once for each voyage on the NSR. The file checks the position vector to see which way the voyage is taken (North to South or vice versa). If the vessel sails from Tianjin, the index for the for-loop is switched, so the for-loop runs from large indexes to small (as the route vector is defined from Murmansk to Tianjin).

The voyage simulations are performed with a for-loop for each leg. For each iteration, the file determines the distance of the leg and the ice conditions (concentration and thickness). The ice conditions are determined by using the file `findice.m` to calculate the ice concentration and thickness between the two nearest dates where these are measured. The ice conditions are assumed to grow linearly with time. If the found ice thickness be thicker than the max ice thickness found in `simulate_sailing.m`, the file returns an error.

Further, the file checks whether the vessel is near or in an ECA. The file defines that the vessel must switch to ‘ECA conditions’⁴ from the leg before it enters the ECA and until the first leg after it has exited the ECA. Therefore, if the vessel is near or in an ECA, the fuel type is set to the fuel specified for use in ECAs for the current scenario. It also reads whether there is abatement technology installed for abating SOx and/or NOx emissions. If the vessel is outside ECAs, these are set to ‘none’.

For the simulation of the sailing, the file calls `sail_ice.m`. This file returns the time, fuel consumption, emissions and energy used on the leg. Then, the abatement technologies are considered. The file calculates the increase in fuel consumption and change in emissions based on the properties of the abatement technologies, as defined in the format file `abatementtech.mat`. Because several of the abatement technologies have effect on more than one emission type, the file uses the total reducing efficiency of the emission by adding the total efficiencies together. It also checks for negative emissions (in case of >100 % efficiency). In that case, the emissions are set to zero.

Lastly, the file switch position (from Murmansk to Tianjin, or opposite) and adds to the total trip counters.

`sailSCR.m`

This file simulate the sailing of one voyage on the SCR route, as a part of the file `simulate_sailing.m`. The file has an identical structure as `sailNSR.m`, see Figure 2.21. Figure 2.23 describes the subprocess in the for-loop simulating each leg on the route. Because this files highly resembles the file `sailNSR.m`, only the differences will be described in the following sections. For more details, readers are referred to the description in section 2.10.2.

Unlike the file `sailNSR.m`, this file does not check for ice conditions on the leg, as there are no ice on the SCR. The file checks for ECA, but only for SOx technologies, as the North European ECA (the only ECA on the SCR voyage) only has limits on sulphur. If this area is redefined in the future, the file should be modified to be similar to `sailNSR.m` for the ECA check.

⁴Either switch fuel or use the installed abatement technology or both

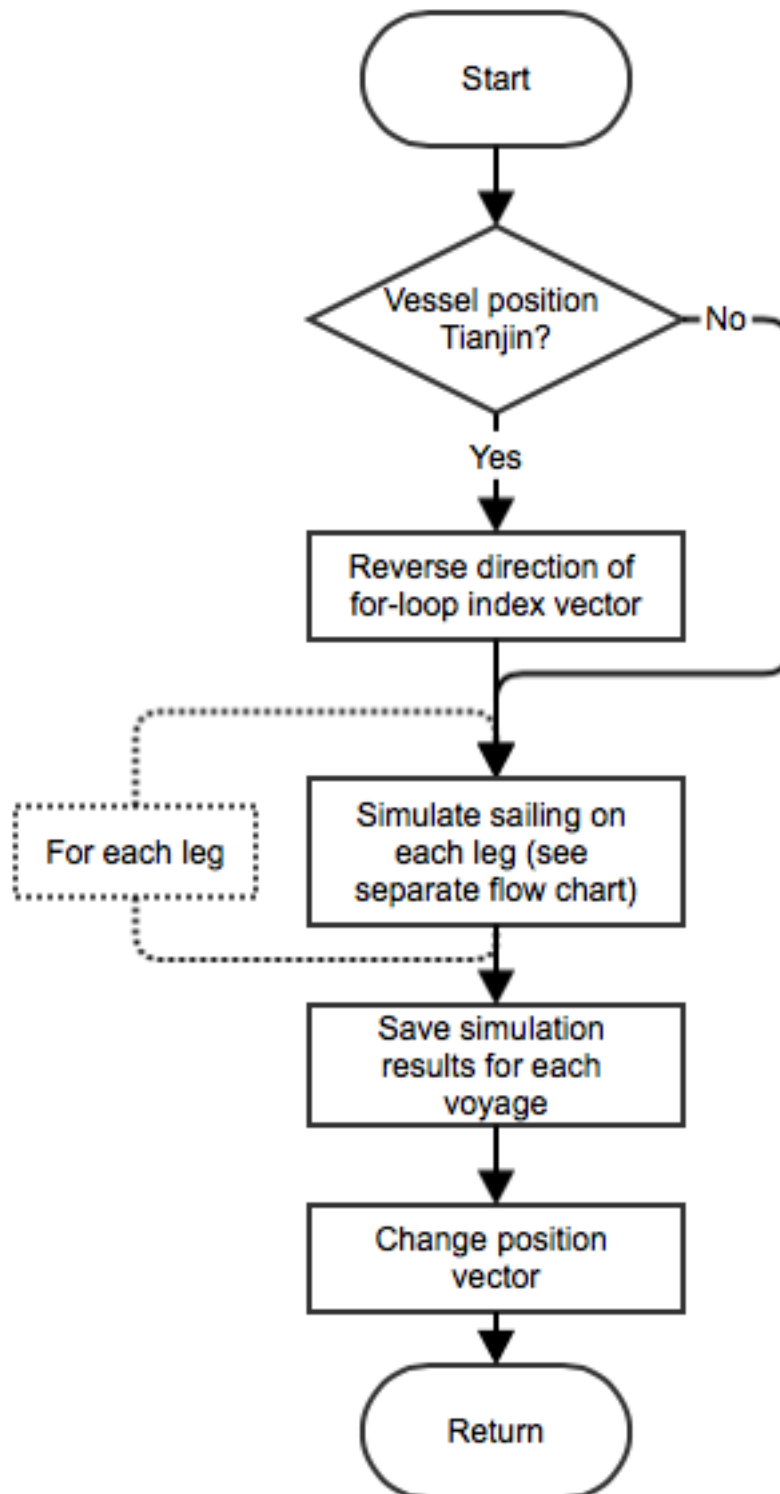


Figure 2.21: Flowchart for both the `sailNSR.m` and `sailSCR.m` files. See Figure 2.22 for description of the simulations per leg for the NSR, and Figure 2.23 accordingly for the SCR legs.

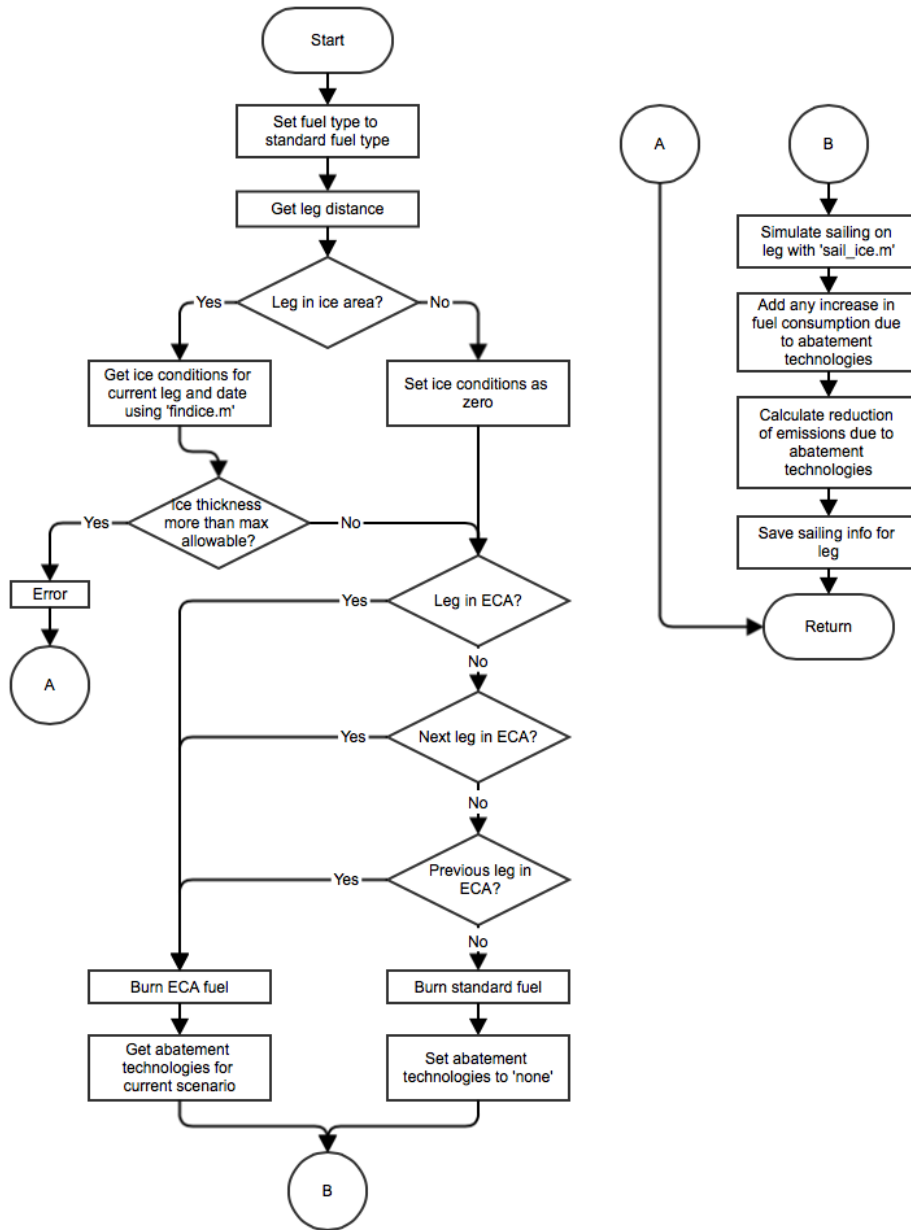


Figure 2.22: Flowchart for the simulation of each leg in the `sailNSR.m` file (see Figure 2.21)

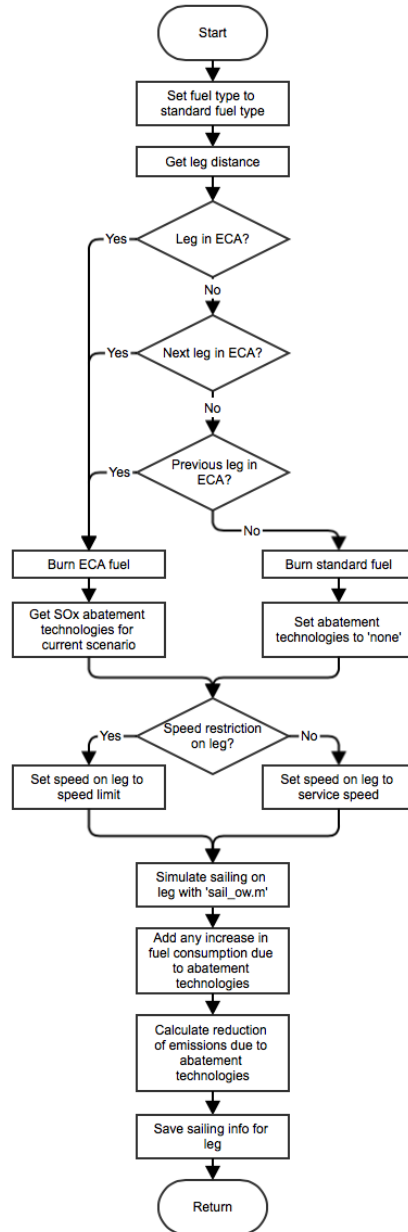


Figure 2.23: Flowchart for the simulation of each leg in the `sailSCR.m` file (see Figure 2.21)

During the for-loop that simulates sailing on the legs, file checks for legs with speed restrictions. Currently, only the Suez Canal has such a restriction. However, the file may easily be modified in the future, to accommodate reduced speeds on other legs, i.e. when approaching ports and canals or when navigating in narrow straits heavy trafficked channel lanes. The speed restrictions are defined for each leg in the format file `routedata.mat`.

For the sailing simulations, the file calls `sail_ow.m`. This file returns the same as `sail_ice.m` (as used in `sailNSR.m`). From here, the file has no differences in function from the file `sailNSR.m`.

`sail_ice.m`

This file is a function that calculates time, fuel consumption, emissions and energy consumption for a given distance with ice present. It is called by the file `sailNSR.m` for each leg in icy waters. The input is the distance, ice concentration and ice thickness for the leg, and also the fueltype used. The output is the time, fuel consumption, emissions and energy consumption on the leg. Figure 2.24 shows a flowchart of the function.

Firstly, the function checks the ice conditions. If the ice thickness is less than 40 cm or the ice concentration is zero, open water sailing conditions is assumed (see section 2.1.1). The function then calls the file `sail_ow.m` to calculate the output, and returns.

For not negligible ice conditions, the leg is divided in an open water and an ice part, as weighted by the ice concentration. I.e. if the leg distance is 100 nm and the ice concentration is 40 %, the distance in ice is set to 40 nm and the distance in open water as 60 nm. The output for each part is found separately for the open water and the ice part. The time, fuel consumption and emissions for the distance in open water is calculated using `sail_ow.m`⁵, while for the distance in ice conditions the file calculates the output for this distance. The total time, fuel consumption and emissions are then summed and given as output.

Maximum attainable speed in the current ice conditions is determined by interpolating using data from the *h-v*-curve, which values are stored in `hvdata.mat`. Cubic interpolation is used to find the value. The file checks that the attainable speed is in the allowed range, between the required minimum speed of 3 knots and the service speed of 14.5 knots. If the attained speed is outside this range, the file returns an error. The maximum attainable speed is set as the sailing speed for the distance in ice.

Knowing the speed for the distance, the sailing time is found.

Further, the resistance in ice for the current ice thickness is found from the `hvdata.mat` format file, which stores R_i as a function of ice thickness. Open water resistance is found from the format file `shipdata.mat`, which stores R_{ow} as a function of speed. The total resistance is found by summing resistance in ice and open water resistance.

The required power for the current conditions is found by multiplying the total resistance by the attainable speed. Knowing the required power, the engine load is found by dividing the required power by the vessel's total brake power. The file checks that the engine load is in the range 0 % to 100 %, and returns an error otherwise.

Total energy consumption for the ice part of the leg is found by multiplying the required power with the sailing time for that part.

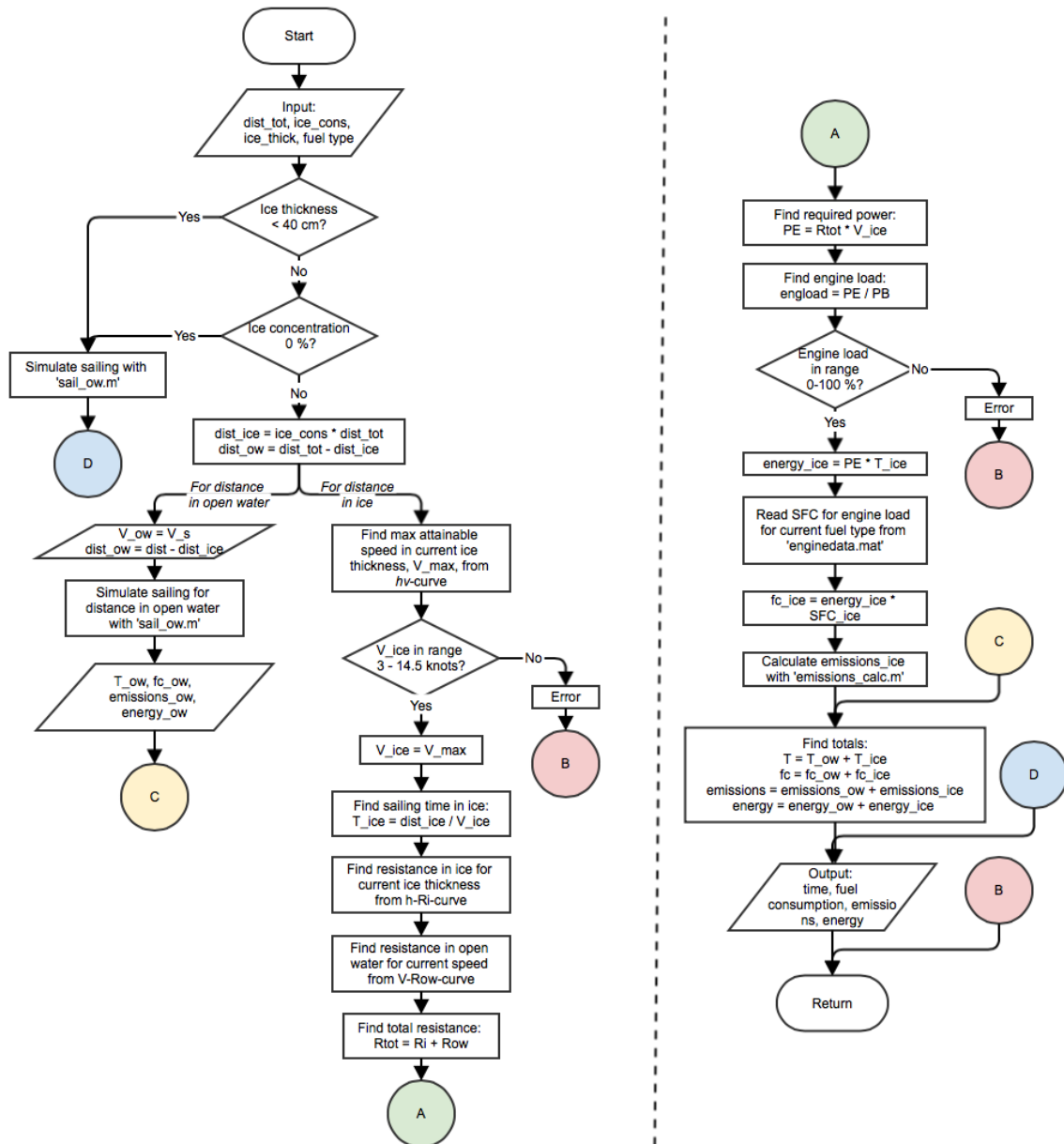
The engine load is used to determine the SFC for the leg for the current fuel type. The SFC is found from the polynomial function stored in `enginedata.mat`.

Fuel consumption on the leg is found from multiplying the energy with the current SFC.

Emissions for the leg is found by calling the file `emissions_calc.m`, giving in the fuel consumption, the energy, the MCR and the fuel type for the leg.

Lastly, the time, fuel consumption, emissions energy consumption for the ice part and open water part is summed to produce the final output of the function.

⁵See section 2.10.2

Figure 2.24: Flowchart for function `sail_ice.m`

`sail_ow.m`

This file calculates time, fuel consumption and emissions for a given distance in open water. It is called by `sailSCR.m` to simulate sailing for all legs on the SCR. It is also called by `sail_ice.m`, to simulate sailing on legs with no ice. The input is the speed, distance and fuel type used on the leg. The output is the total sailing time, fuel consumption, emissions and energy consumption on the leg. The file bears resemblance to `sail_ice.m` (see section 2.10.2). Figure 2.25 shows a flowchart of the function.

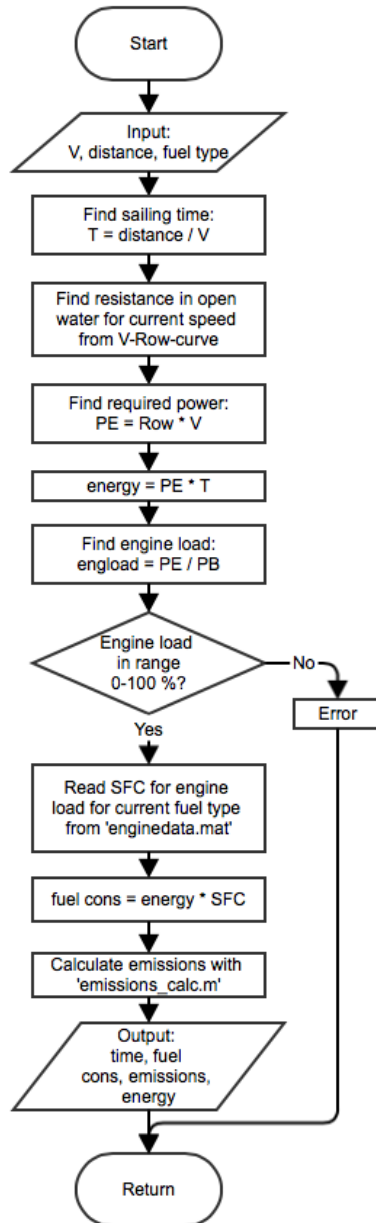


Figure 2.25: Flowchart for function `sail_ow.m`

Firstly, the total sailing time for the leg is determined by dividing the distance by the speed. The open water resistance is found from interpolation of R_{ow} , stored in `shipdata.mat`, for the current speed.

Necessary power to attain the given speed is found from multiplying the resistance with the speed. Thus, the energy can be found from multiplying the necessary power with the time on the leg, giving total kWh on the leg. The file finds the engine load for the current power by dividing with the vessel's total brake power. It returns an error if the load is outside the range of 0 to 100 %. Specific fuel consumption for the current load condition is found by evaluating the polynomial storing the SFC for the current fuel type in the format file `enginedata.mat`. The fuel consumption is found by multiplying the energy with the SFC. Emissions are found by calling the file `emissions_calc.m` with the fuel consumption, energy, engine load and fuel type. Lastly, the sailing time is converted to days and the emissions to tonnes before returning.

`findice.m`

This file is a function that calculate the ice conditions for a given date and location on the NSR. It is called by the file `sailNSR.m`, to determine the ice conditions for the current leg while simulating the sailing. The input is the leg number and the current date. The output is the ice thickness and concentration on the leg on the current date.

The process of the file is described in Figure 2.26.

First, the file checks if the current date is outside the date range for ice measurements. If so, the file returns an error.

The file finds the date in the date vector for the ice data that is closest to the current date (d_1). It then checks if the current date is before or after d_1 , and sets d_2 to the date before or after d_1 accordingly. Thus, the date interval in which the current date is in is determined as d_1, d_2 .

The ice thickness on the given leg in d_1 and d_2 , T_1 and T_2 , is obtained. To find the current ice thickness, T_c , linear interpolation is used. The method to obtain the current ice concentration is the same as for ice thickness.

`emissions_calc.m`

This file calculate the emissions of CO₂, NO_x, SO_x and PM for a given fuel consumption and energy use. The file is called by `sail_ice.m` and `sail_ow.m` to calculate the emissions for a given leg. The file does not consider emission abatement technology. The input is fuel consumption in kg, energy in kWh, engine load in percent and fuel type.

The process of the file is described in Figure 2.27.

The file loads the polynomial functions for specific emissions of NO_x and PM, the fuel sulphur percentage ($S\%$), and the emission rates for CO₂ and SO_x from the file `enginedata.mat`. To find the current specific emissions (spe) for NO_x and PM, the polynomial functions are evaluated at the current engine load.

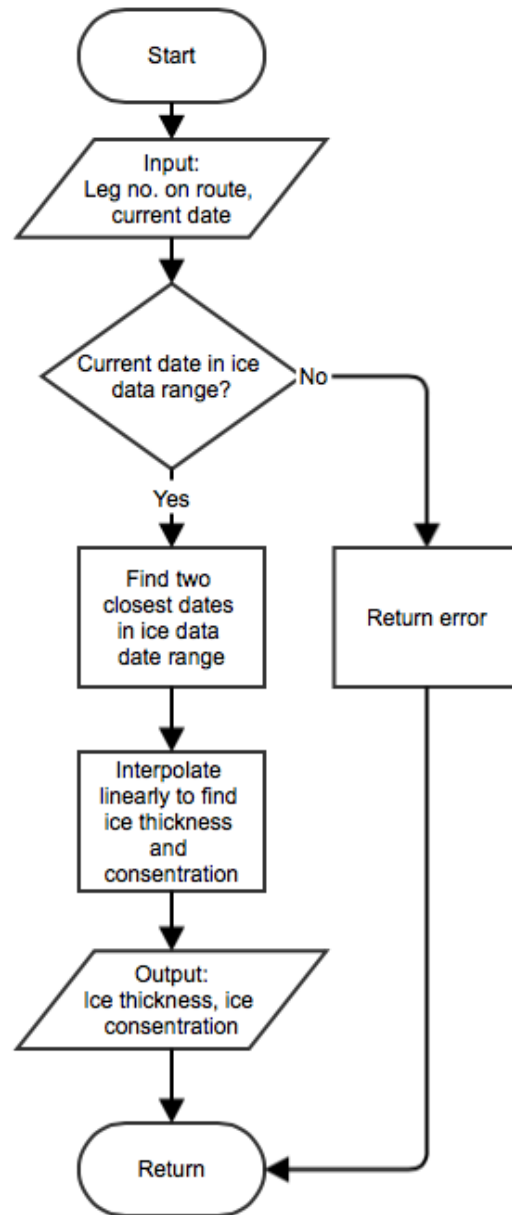
The emissions are found from the following relations

$$M_{CO_2} = per_{CO_2} \cdot fc \quad (2.42)$$

$$M_{SO_x} = per_{SO_x} \cdot S\% \cdot fc \quad (2.43)$$

$$M_{NO_x} = spe_{NO_x} \cdot E \quad (2.44)$$

$$M_{PM} = spe_{PM} \cdot E \quad (2.45)$$

Figure 2.26: Flowchart for `findice.m` file

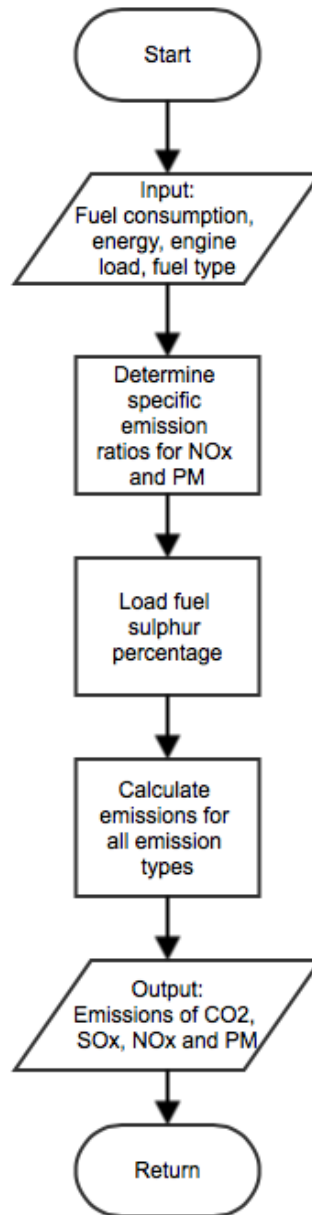


Figure 2.27: Flowchart for `emissions_calc.m` file

where M_e is the total emission for emission type e , per_e is the per emission ratio for emission type e in g emissions per kg fuel, fc is the fuel consumption in kg, $S\%$ is the fuel sulphur percentage, spe_e is the specific emission ratio in g/kWh and E is the energy in kWh.

`engine_data.m`

This file define and calculate the properties of the different fuels and also the engine characteristics. The file is a part of the model initiation procedure of the model. The file generates polynomial functions for SFC and emission rates, and coefficients of the polynomial functions as variables to the format file `enginedata.mat`. Plots of SFC, NOx and PM over the engine load range may also be produced (optional).

`ice_resistance.m`

This file is a function who calculates the resistance in ice with the method of Juva and Riska (2002), as described in section 2.1.1. The file is called by `hv.m`. The input is ice thickness H_M (can be a vector or a scalar), the vessel's angle between the bow and the waterline at $B/4$ (ϕ_2), the waterline entrance angle (α), ship length, breadth and draught, and the length of the parallel midbody of the vessel at midships. The output is the resistance in ice, either as a scalar or as a vector, depending on the format of input H_M . As the calculation method in the file is directly as described in section 2.1.1, the function will not be elaborated further here.

`ow_resistance.m`

This file calculates open water resistance with Gulddammer and Harvald's method, as described in section 2.1.1. The input is the vessel's length on waterline, breadth, draught, maximum speed, wet surface and also two binary indicators for whether to plot the resistance curve and/or the coefficients used in the formula. The output is the open water resistance vector and the corresponding speed vector. The process of the file is described in Figure 2.28.

`hv.m`

This file is a function that determine the ship performance in brash ice. In addition to the essential data (h & v) for generating ship performance in ice ($h-v$) curves, the algorithm can optionally return the information on net thrust and brash ice resistance (R_i) for a desired vessel. Finally, computed $h-v$ plot is readily available. The file is called by the file `hv_input.m`, who generate the required input for the function. The file calls the function `ice_resistance.m` (see section 2.1.1) to calculate the resistance in ice. The input is speed, length, breadth, draught, parallel midbody length, stem angle at $B/4$ (ϕ), waterline entrance angle (α), brake power, propeller diameter and the empirical factor for bollard pull, K (see Chapter 6 of Juva and Riska (2002)). The output is vectors for ice thickness, speed, net thrust and ice thickness.

The process of the file is described in Figure 2.29.

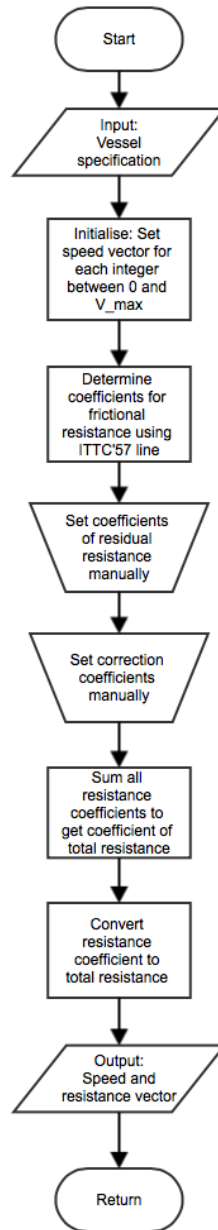
The file sets a transmission efficiency coefficient to 0.99. The delivered power to the propeller is set as the brake power multiplied with the transmission efficiency coefficient.

Vectors for ice thickness h and speed v are defined.

The net thrust is calculated using Equation 2.27. A polynomial curve fit function is used to model the net thrust as a polynomial of second degree as a function of the speed.

The brash ice resistance is found using `ice_resistance.m`. Polynomial curve fitting is applied also here.

The file runs a for-loop to determine the $h-v$ -curve values. For each ice thickness h_i , the ice resistance is found. To determine the attainable speed v_a , the file sets $R_i(h_i) = T_{net}(v_a)$. The corresponding h_i and v_a values is saved in a vector. Thus, the $h-v$ -curve can be produced.

Figure 2.28: Flowchart for `ow_resistance.m` file

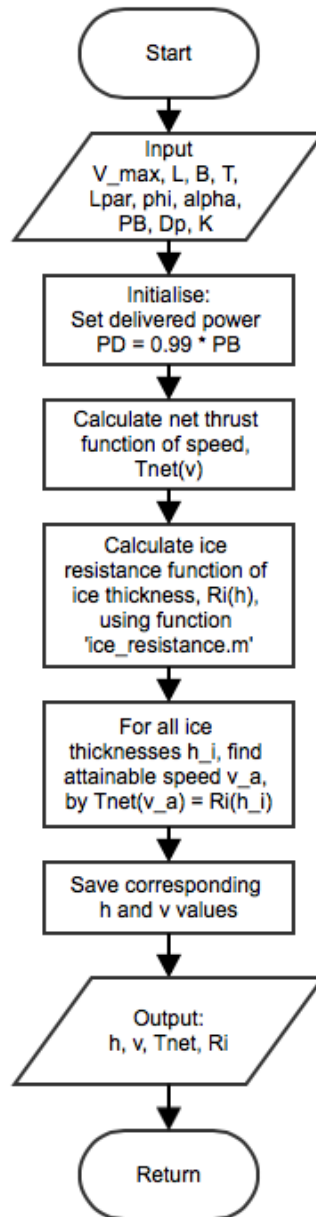


Figure 2.29: Flowchart for hv.m file

Chapter 3

Results from simulations

This chapter presents the results from the model and framework presented in chapter 2. The results are first presented per scenario, with the relevant figures for emissions and costs. Later, the voyages and routes are compared.

3.1 Note on presented results

Before the results are presented, the reader should be aware that the results in the following chapter were produced before an error in the model was discovered. Due to time limitations, the results are not reproduced with corrected results.

The error in the model lead to an overestimation of the speed on some legs on the NSR. This lead to an over-optimistic time estimate for the NSR voyages. In the corrected model, one less NSR voyage are performed for the scenarios utilising the NSR.

A few of the presented results are presented based on the corrected version of the model. This will be indicated where it applies. Unless otherwise specified, the reader should assume that the results are produced from the erroneous model.

The impact of the error is discussed further in section 4.4.

3.2 Results from scenario simulations

This section presents the results of the simulations for each scenario. For comparisons of routes, voyages and scenarios, see section 3.4.

3.2.1 Results for the base case scenario

The base case sails only on the SCR and uses fuel switch to low sulphur MGO fuel to reduce SOx emissions when sailing in the North European ECA. No abatement technologies are installed. The vessel makes 9.93 trips on the SCR during the simulation time period of one year.

Table 3.1: Total emissions per year (tonnes) for the base case scenario

CO ₂	SOx	NOx	PM
29 563	709	742	12

Table 3.1 lists the calculated total emissions from the base case scenario for the simulation period of one year.

Table 3.2: Total fuel consumption per year (tonnes) for the base case scenario.

	HFO	MGO
Fuel consumption	810	121

In Table 3.2, the total fuel consumption for both fuels used in the base case scenario is listed. MGO are only used in ECAs, which only makes up 11 % of the distance on the SCR. Therefore, the MGO consumption is relatively low, compared to HFO consumption.

Table 3.3: Total fuel costs in USD for the base case scenario.

	HFO	MGO	Total fuel cost
Fuel cost	364 308	90 632	454 940

The total fuel costs for the base case scenario are given in Table 3.3. Fuel costs for each fuel is according to Table 2.18. Note that even though MGO is only used for 11 % of the total distance, the MGO cost makes up approximately 20 % of the total fuel cost. This is due to the higher price of MGO.

Table 3.4: Total costs in USD, base case

	CAPEX	OPEX	EAC
	0	2 495 393	2 495 393

Total costs for the base case scenario are specified in Table 3.4. CAPEX include total capital expenses for installing abatement technology. No abatement technologies are installed in the base case scenario, therefore the CAPEX is zero. The OPEX include fuel costs and fees in the Suez Canal. The equivalent annual costs are calculated according to Equation 2.35. In the base case scenario, the CAPEX is zero, therefore the EAC are the same as the OPEX.

3.2.2 Results for scenario 1 (exhaust cleaning only)

The first scenario burns only HFO. The vessel in this scenario uses a scrubber to abate SO_x emissions and a catalyst (SCR) to abate NO_x emissions.

Table 3.5: Total emissions per year (tonnes) for scenario 1. The first row (gross emissions) is the “base line”, the total emissions from the engine. The net emissions is what is actually released to the atmosphere. The net reduced emissions is the difference between the gross and net emissions, and is what is abated with the abatement technology installed.

	CO ₂	SO _x	NO _x	PM
Gross emissions	29 110	802	722	13
Net emissions	29 110	669	637	12
Net reduced emissions	0	133	84	1

Table 3.5 lists the calculated total emissions from scenario 1 for the simulation period of one year. The gross emissions are the total emissions produced by the main engine. The net emissions are the emissions actually released to the atmosphere. The net reduced emissions are the emissions reduced by the scrubber and SCR.

In Table 3.6, the total fuel consumption for both fuels used in scenario 1 is listed. The fuel consumption increase with the use of abatement technology, and the net increase due to the scrubber and SCR is shown.

Table 3.6: Total fuel consumption (fc) per year (tonnes) for scenario 1. The net increase in fc is the increase in fuel consumption due to use of scrubber and SCR.

	HFO
Fc without abatement	2714
Fc with abatement	2842
Net increase fc	127

Table 3.7: Total fuel costs in USD for scenario 1. The cost with and without abatement is according the fuel consumption (without and with use of the scrubber and SCR). The net increase in fuel cost is the direct cost of using the scrubber and SCR due to the increase in fuel consumption. The cost increase is also given in percent.

	Total fuel cost
Fuel cost, without abatement	1 221 477
Fuel cost, with abatement	1 278 812
Net increase, cost	57 335
Cost increase (%)	4.7

The total fuel costs for scenario 1 is given in Table 3.7. Fuel costs for each fuel is according to Table 2.18. The cost increase due to the emission abatement is given directly. The cost increase in percent is also given.

Table 3.8: Total costs in USD, scenario 1

CAPEX	OPEX	EAC
6 000 000	4 494 701	4 744 301

Total costs for scenario 1 is given in Table 3.8. CAPEX include total capital expenses for installing the scrubber and the SCR unit. The OPEX include fuel costs and total yearly fees in the Suez Canal and on the NSR, according to the number of trips made. Consumption of urea in the SCR is modeled as an additional 10 % increase in fuel cost (costs without abatement), and is also included in the OPEX. The equivalent annual costs are calculated according to Equation 2.35.

3.2.3 Results for scenario 2 (exhaust cleaning and fuel switch combined)

Scenario 2 burns HFO in open seas. In the ECAs, it switches to MGO to relieve SOx emissions and utilise a catalyst (SCR) to remove NOx emissions.

Table 3.9: Total emissions per year (tonnes) for scenario 2. The first row (gross emissions) is the “base line”, the total emissions from the engine. The net emissions is what is actually released to the atmosphere. The net reduced emissions is the difference between the gross and net emissions, and is what is abated with the abatement technology installed.

	CO ₂	SOx	NOx	PM
Gross emissions	28 294	625	715	11
Net emissions	28 294	625	646	11
Net reduced emissions	0	0	69	0

Table 3.9 lists the calculated total emissions from scenario 2 for the simulation period of one year. The gross emissions are the total emissions produced by the main engine. The net emissions are the emissions actually released to the atmosphere. The net reduced emissions are the emissions reduced by the SCR.

Table 3.10: Total fuel consumption (fc) per year (tonnes) for scenario 2. The net increase in fc is the increase in fuel consumption due to use of the catalyst (SCR).

	HFO	MGO
Fc without abatement	1628	947
Fc with abatement	1628	1030
Net increase fc	0	83

In Table 3.10, the total fuel consumption for both fuels used in scenario 2 is listed. The fuel consumption increase with the use of abatement technology, and the net increase due to the SCR is shown.

Table 3.11: Total fuel costs in USD for scenario 2. The cost with and without abatement is according the fuel consumption (without and with use of the SCR). The net increase in fuel cost is the direct cost of using abatement technologies due to the increase in fuel consumption. The cost increase is also given in percent.

	HFO	MGO	Total fuel cost
Fuel cost, without abatement	732 637	710 514	1 443 151
Fuel cost, with abatement	732 637	772 503	1 505 139
Net increase, cost	0	61 988	61 988
Cost increase (%)	0.0	8.7	4.3

The total fuel costs for scenario 2 is given in Table 3.11. Fuel costs for each fuel is according to Table 2.18. The cost increase due to the emission abatement is given directly. The cost increase in percent is also given.

Table 3.12: Total costs in USD, scenario 2

CAPEX	OPEX	EAC
3 000 000	4 443 196	4 567 996

Total costs for scenario 2 is given in Table 3.12. CAPEX include total capital expenses for installing the SCR unit. The OPEX include fuel costs and total yearly fees in the Suez Canal and on the NSR, according to the number of trips made. Consumption of urea in the SCR is modeled as an additional 10 % increase in fuel cost (costs without abatement), and is also included in the OPEX. The equivalent annual costs are calculated according to Equation 2.35.

3.2.4 Results for scenario 3 (LNG conversion and exhaust cleaning)

Scenario 3 is converted to DF and an EGR is installed. HFO is burnt in open seas. In ECAs, the vessel switches fuel to LNG. If NOx emissions are regulated in the area, EGR technology is used in addition.

Table 3.13 lists the calculated total emissions from scenario 3 for the simulation period of one year. The gross emissions are the total emissions produced by the main engine. The net emissions are the emissions actually released to the atmosphere. The net reduced emissions are the emissions reduced by the EGR.

In Table 3.14, the total fuel consumption for both fuels used in scenario 2 is listed. The fuel consumption increase with the use of abatement technology, and the net increase due to the EGR is shown.

Table 3.13: Total emissions per year (tonnes) for scenario 3. The first row (gross emissions) is the “base line”, the total emissions from the engine. The net emissions is what is actually released to the atmosphere. The net reduced emissions is the difference between the gross and net emissions, and is what is abated with the abatement technology installed.

	CO ₂	SO _x	NO _x	PM
Gross emissions	26 566	625	631	10
Net emissions	26 566	625	620	10
Net reduced emissions	0	0	12	0

Table 3.14: Total fuel consumption (fc) per year (tonnes) for scenario 3. The net increase in fc is the increase in fuel consumption due to use of the EGR.

	HFO	LNG
Fc without abatement	1628	766
Fc with abatement	1628	794
Net increase fc	0	28

Table 3.15: Total fuel costs in USD for scenario 3. The cost with and without abatement is according the fuel consumption (without and with use of the EGR). The net increase in fuel cost is the direct cost of using abatement technologies due to the increase in fuel consumption. The cost increase is also given in percent.

	HFO	LNG	Total fuel cost
Fuel cost, without abatement	732 637	497 918	1 230 555
Fuel cost, with abatement	732 637	515 928	1 248 565
Net increase, cost	0	18 010	18 010
Cost increase (%)	0.0	3.6	1.5

The total fuel costs for scenario 3 is given in Table 3.15. Fuel costs for each fuel is according to Table 2.18. The cost increase due to the emission abatement is given directly. The cost increase in percent is also given.

Table 3.16: Total costs in USD, scenario 3

CAPEX	OPEX	EAC
21 600 000	3 742 307	4 640 867

Total costs for scenario 2 is given in Table 3.12. CAPEX include total capital expenses for retrofitting and converting the main engine to DF LNG operation and also retrofitting with EGR. The OPEX include fuel costs and total yearly fees in the Suez Canal and on the NSR, according to the number of trips made. The equivalent annual costs are calculated according to Equation 2.35.

3.3 Route and voyage results

The following section compares the performance for the different routes.

Table 3.17: Total number of voyages for the scenarios

Scenario	NSR	SCR	Total
Base case	0	9.93	9.93
Scenario 1-3	4	7.74	11.74

Table 3.18: Total number of laden voyages for the scenarios

Scenario	NSR	SCR	Total
Base case	0	5	5
Scenario 1-3	2	4	6

3.3.1 Voyage duration and freight potential

In the base case scenario, the vessel performs 9.93 voyages on the SCR during the simulation time period. Starting in Murmansk fully laden, this equals five laden voyages during the year.

For the scenarios that sails on the NSR (scenario 1-3), four voyages are made on the NSR in the simulation time period, thereof two laden voyages. Outside the NSR operation, the vessel makes 7.74 voyages on the SCR, thereof four laden voyages.

Thus, in scenario 1-3 six laden voyages can be performed during the simulation time period. The base case scenario makes only five laden voyages during the year.

Table 3.19: Comparison of route transit times

Route	Transit time, days
SCR	37
NSR, average	20

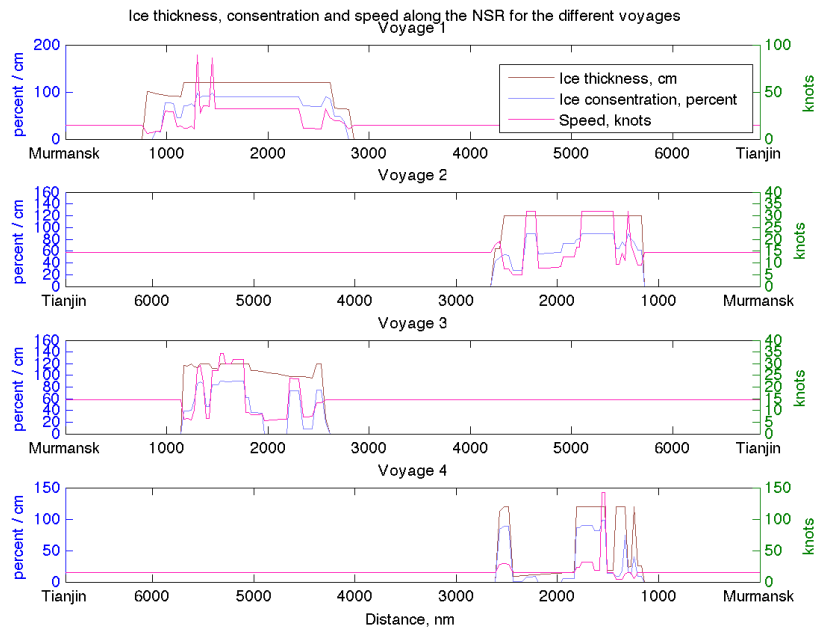
Table 3.20: Transit times on the NSR. Start and end dates are the dates the vessel leaves port in either Murmansk or Tianjin.

Transit no.	Transit time, days	Date (start/end)
NSR1	18.57	2008-07-13/2008-07-31
NSR2	20.76	2008-07-31/2008-08-21
NSR3	21.38	2008-08-21/2008-09-11
NSR4	19.95	2008-09-11/2008-10-01

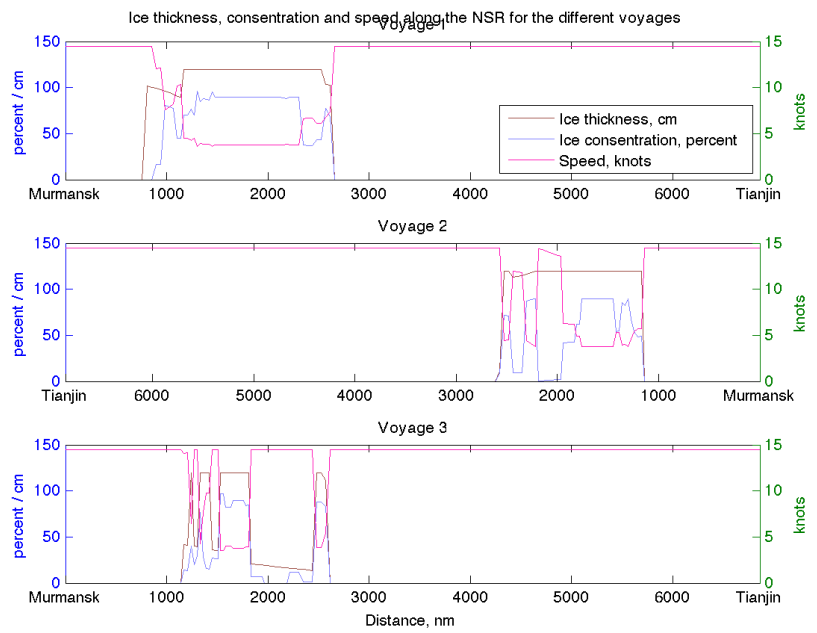
As shown in Table 3.19, the vessel spends approximately 37 days on the voyage from Murmansk to Tianjin on the SCR. For the scenarios sailing the NSR, the vessel makes four voyages on the NSR during the simulation period (see Table 3.20). The averaging transit time was approximately 20 days.

3.3.2 Ice conditions and speed for the voyages

Figure Subfigure 3.1(a) and Subfigure 3.1(b) illustrate the difference in speed calculations on the legs from the erroneous model and the corrected model. In Subfigure 3.1(a), the speed increase above the service speed for certain legs in ice conditions. In Subfigure 3.1(b), the speed decrease according to ice concentration and thickness along the route.



(a) With error



(b) Corrected error

Figure 3.1: Ice conditions and speed along the NSR with and without error in the model (see note in section 3.1). Note that only three voyages are performed on the NSR in the corrected model.

The vessel sails with service speed for legs outside the NSR. A new speed is calculated for each leg, based on the ice conditions. The speed is the weighted average for attainable speed in current ice thickness and the service speed for the “open water portion” of the leg (see section 2.10.2 for details about leg speed calculations).

3.4 Performance comparison

The following section compares the performance in the scenarios to each other and also the base case scenario, which sails only on the SCR.

3.4.1 Emissions performance

The emission performance for the scenarios are presented in this section.

Compliance to NOx Tier III limits in Arctic ECA

The specific emissions for NOx for the scenarios when sailing in the Arctic ECA is shown in Figure 3.2. In addition to the specific emissions for the scenarios, the Tier III limit for NOx emissions in ECAs are shown. From the figure it can be seen that scenario 3 is not compliant with Tier III limits with the current configuration of fuel and abatement technology. Scenarios 1-2 have NOx emissions well below the limit.

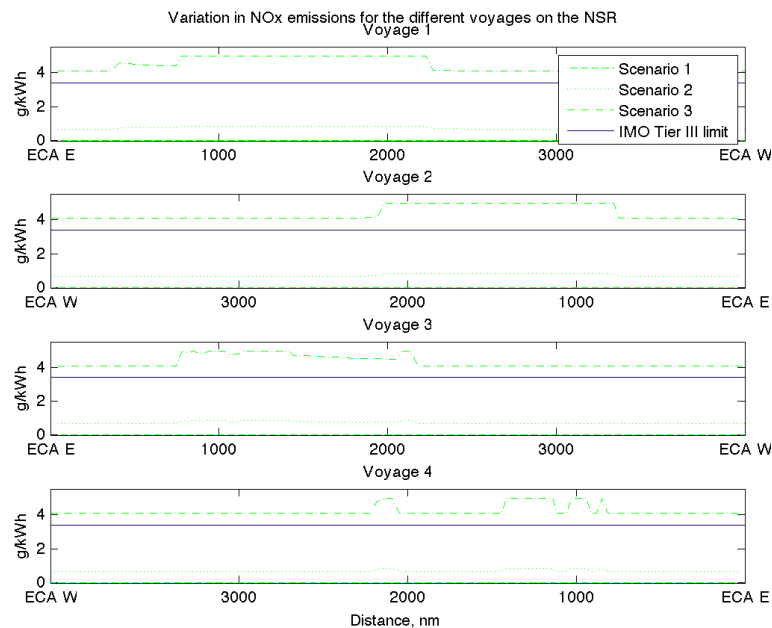


Figure 3.2: Variation in specific NOx emissions in the ECA on the NSR

Voyage emission profiles

The variation in emission rates along the different voyages are shown in Subfigure 3.3(a) to Subfigure 3.4(b). All NSR voyages are plotted for scenario 1-3, as the emission rates differ with ice conditions along the route. Additionally, emission rates for a voyage on the SCR are shown. The emission rates for SCR passage are constant, so only one voyage is plotted.

As some of the scenarios have the same fuel configuration, the emission rates are equal for Emission rates are constant and equal for all scenarios outside of the ECAs. The reason for this is that all scenarios operate on HFO in open seas.

The location of ECAs along the routes can be clearly seen in all figures, as all scenarios have decreases in some or all emission rates in these areas. For the SCR, the decreased emissions from around 500 nm to 2500 nm marks the location of the SECA. The vessels only utilise SO_x abatement technology in this area. The base case scenario switch from HFO to MGO in the SECA, as it has no abatement technology installed. Further, a great part of the NSR is located in the Arctic ECA. As opposed to the SECA in the North Sea, both SO_x and NO_x abatement technology is used here.

Also the location of the Suez Canal can be determined from the plots. The drop in emission rates just before the 5000 nm mark on the SCR gives the location of the canal. Due to the low speed limit in the canal, the fuel consumption is greatly reduced and therefore all emission rates decrease.

The variation in CO₂ emissions are directly proportional to fuel composition and consumption. Variations in fuel consumptions occur here due to variations in speed and/or in ice conditions. The effects of sailing in ice is clearly visible for the CO₂ emission rates on the NSR voyages.

The CO₂ emissions are only affected by ECAs if the vessel switches to a different fuel in these areas. This is the case for the base case scenario (seen in Subfigure 3.3(a) for the SCR route only) and scenario 2, which both switch from HFO to MGO in ECAs. Also in scenario 3, who switch from HFO to LNG in ECAs, a reduction in CO₂ emissions can be seen in ECAs. Scenario 1 runs exclusively on HFO, and will therefore not experience a reduction in CO₂ emission rates in ECAs.

SO_x emissions are also directly related to the fuel composition and consumption. SO_x emissions are abated in ECAs through fuel switch and/or abatement technology. For scenario 3, the SO_x emissions in ECAs are zero, as LNG fuel contains only negligible amounts of sulphur. Also for the base case scenario and scenario 2, using MGO with 0.05 % S in ECAs, the SO_x emissions are negligible. Scenario 1 utilise a scrubber to remove SO_x emissions. As the scrubber only removes 75 % of the SO_x emissions, scenario 1 have the highest SO_x emission rates.

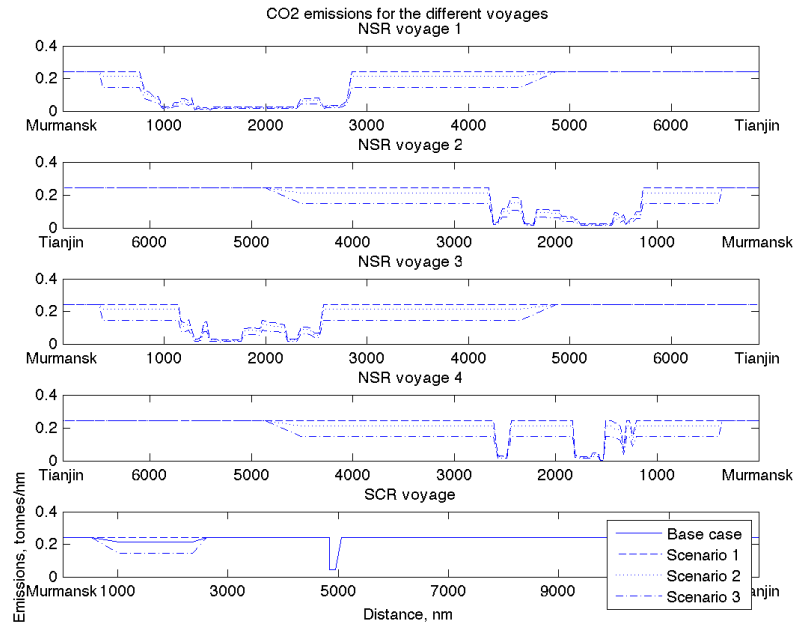
NO_x emissions depend on both fuel consumption and engine load. For the Arctic ECA, NO_x abatement technologies are used for all scenarios. Scenario 1-2 utilise a catalyst (SCR) and scenario 3 have an EGR unit installed. In the SECA, no NO_x abatement technologies are utilised. The base case have no NO_x abatement technology installed.

Reduced NO_x emissions in the SECA can be seen for scenarios that switch to low sulphur fuel to abate SO_x emissions (base case and scenario 2-3). As seen in Subfigure 2.17(a), both MGO and LNG fuels have a lower specific emission factor then HFO. Therefore, these scenarios have reduced NO_x emissions in the SECA due to the fuel switch only. Scenario 1 uses a scrubber to abate SO_x emissions in the SECA. However, the scrubber also have a reducing effect on NO_x emissions (−10 %). Therefore, also scenario 1 experience a reduction of NO_x emissions in the SECA, even though no fuel switch is performed.

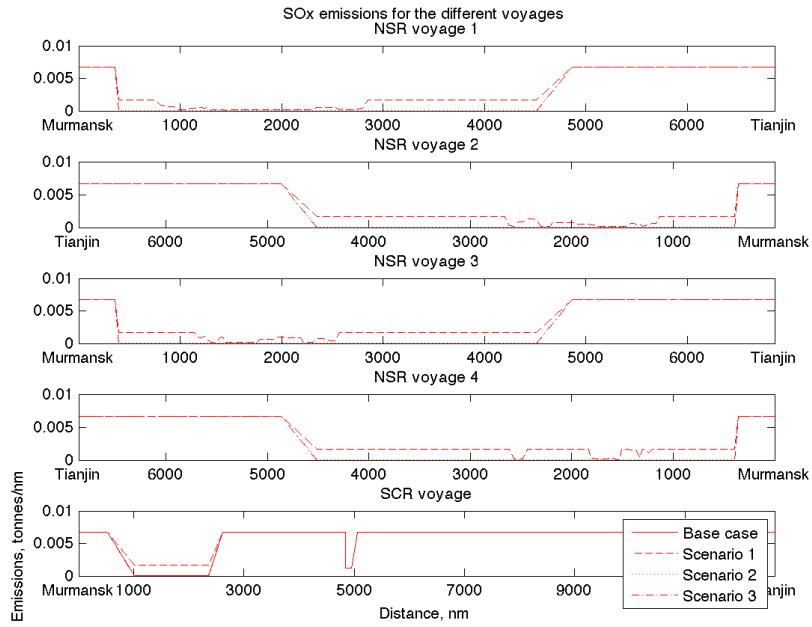
For scenario 1, the reduction in NO_x emissions are only due to the installed SCR. For scenario 2-3, the NO_x emission reduction are a combination of the efficiencies of the technologies and also the reduced specific emission factor of the fuel.

Scenario 3 has the highest NO_x emission rates in the Arctic ECA. LNG has a lower specific emission factor for NO_x than both MGO and HFO. However, the installed EGR have a much lower efficiency for NO_x abatement than a SCR (−35 % vs −95 % respectively). Thus, the NO_x emission rates for scenario 3 are still higher than for scenario 1 and 2. Scenario 1 have the lowest NO_x emission rates in the Arctic ECA. The efficiency of NO_x abatement for the scrubber and the SCR in combination is almost 100 %, so the NO_x emissions are negligible.

The PM emissions are also dependent on both fuel composition and engine load. The emissions are also affected by the technologies installed to abate other emissions. As seen in Table 2.15, both scrubber and SCR technology also reduce PM emissions. However, of LNG fuel in combination with EGR increase

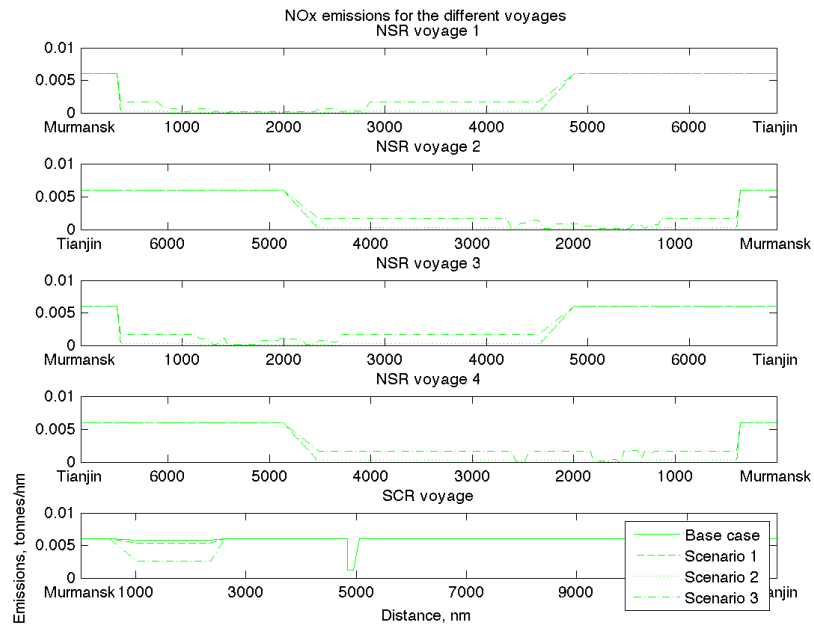


(a) CO₂

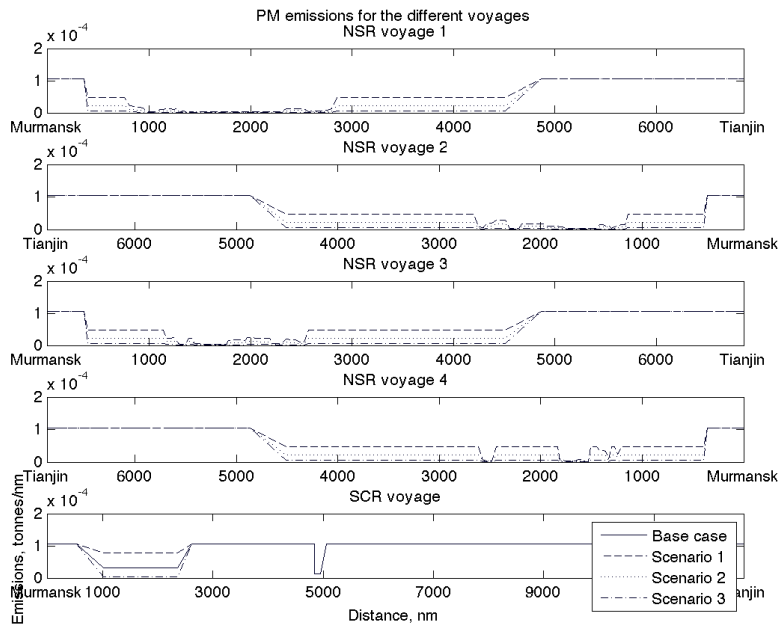


(b) SO_x

Figure 3.3: Variation in CO₂ and SO_x emissions for the different scenarios on the different voyages



(a) NO_x



(b) PM

Figure 3.4: Variation in NO_x and PM emissions for the different scenarios on the different voyages

PM. The total PM emissions are a combination of the influence from the abatement technology, and the specific emission factor for the utilised fuel.

Scenario 1 has the highest PM emissions, even though both technologies that reduce PM emissions are used. However, the HFO fuel used have by far the highest specific emission rate for PM (see Subfigure 2.17(b)). Therefore, scenario 1 still have the highest PM emission rates. Scenario 3 have the lowest PM emissions. Here, the vessel uses an EGR, the NO_x abatement technology with the highest reduction efficiency for PM (−35 %). In addition, the fuel has the definitive lowest *spe* rate for the fuels.

Total emissions for a roundtrip

Total emissions for a roundtrip voyage on the different routes are shown in Figure 3.5. For scenarios 1-3 that does two roundtrips on the NSR, the first of the two NSR voyages is selected for plotting. Total CO₂ emissions for a roundtrip on the NSR are greatly reduced compared to the SCR voyage for scenarios 1-3. This is as expected, as the emissions are proportional with the sailing distance, and the NSR is less than half the distance of the SCR route in the study. Also, scenario 3 utilise LNG, which has even lower CO₂ emission rates than HFO and MGO. The great reductions of SO_x, NO_x and PM emissions are due to a larger portion of the NSR route being defined as an ECA, hence abatement technologies are used on greater parts of the route than for the SCR.

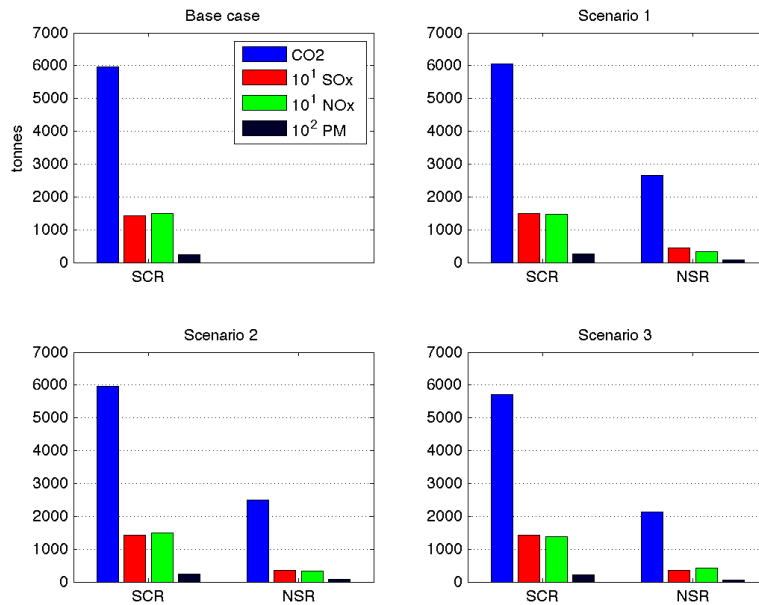
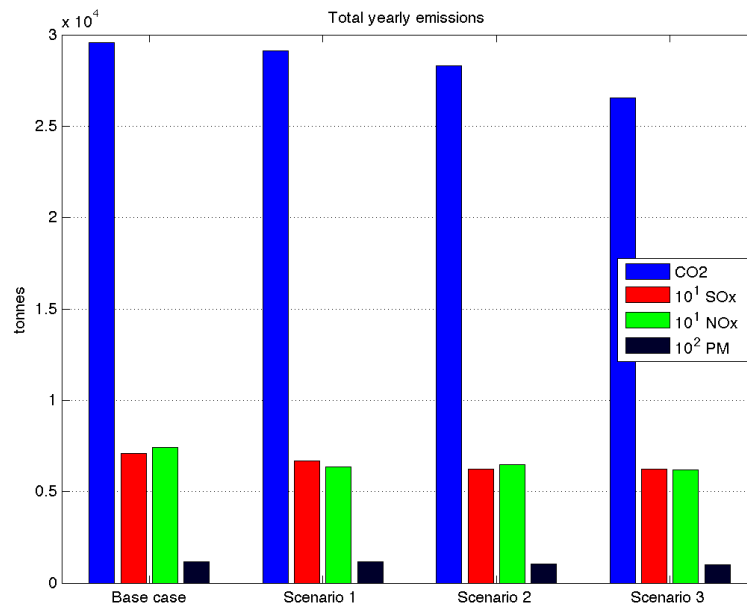


Figure 3.5: Total emissions in tonnes for a roundtrip voyage on the different routes for the scenarios

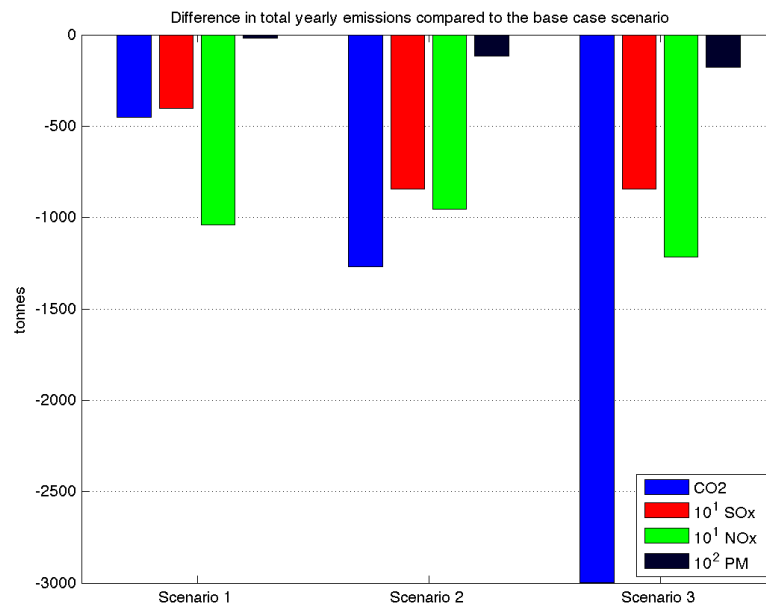
Annual emissions for the scenarios

The total emissions for the different scenarios, listed in Table 3.21 are also shown in Subfigure 3.6(a). The base case scenario have higher emissions than scenario 1-3 for all emission types. The difference in emissions compared to the base case are listed in Table 3.22 and also shown in Subfigure 3.6(b).

As seen from Subfigure 3.6(b), scenario 3 gives the largest reductions in both CO₂, NO_x and PM. Scenario 2 and 3 are equal in terms of SO_x emission reductions. Scenario 1 has the least reductions of the scenarios, compared to the base case.



(a) Total emissions for all scenarios



(b) Difference in total emissions compared to the base case

Figure 3.6: Total yearly emissions

Table 3.21: Total yearly emissions in tonnes for the scenarios

	10^{-4} CO ₂	10^{-3} SO _x	10^{-3} NO _x	10^{-2} PM
Base case	2.96	0.71	0.74	0.12
Scenario 1	2.91	0.67	0.64	0.12
Scenario 2	2.83	0.62	0.65	0.11
Scenario 3	2.66	0.62	0.62	0.10

Table 3.22: Difference in total yearly emissions compared to the base case scenario

	CO ₂	10 ¹ SO _x	10 ¹ NO _x	10 ² PM
Scenario 1	-453	-401	-1041	-20
Scenario 2	-1269	-845	-954	-118
Scenario 3	-2997	-845	-1218	-177

However, the number of trips for the scenarios are not the same. To give a more representative image of the situation, the emissions were calculated as tonnes emissions per tonne cargo. Assuming full ship loads for the laden voyages (as mentioned in the framework), the total yearly emissions were divided by the total tonnage freighted per year for the scenario. Table 3.23 gives the total emissions in kg emissions per tonne freight for the simulation period of one year. The figures are also shown in Subfigure 3.7(a). Table 3.22 give the savings in absolute values and Table 3.25 gives the savings in percent, both compared to the base case scenario. Subfigure 3.7(b) present the total savings in kg emissions per tonne cargo for sailing on the NSR.

Table 3.23: Yearly emissions in kg per tonne cargo

	CO ₂	10 ¹ SO _x	10 ¹ NO _x	10 ² PM
Base case	78.2	18.8	19.6	3.1
Scenario 1	64.2	14.7	14.1	2.5
Scenario 2	62.4	13.8	14.2	2.3
Scenario 3	58.6	13.8	13.7	2.2

Table 3.24: Difference in yearly emissions in kg of emissions per tonne cargo compared to the base case scenario

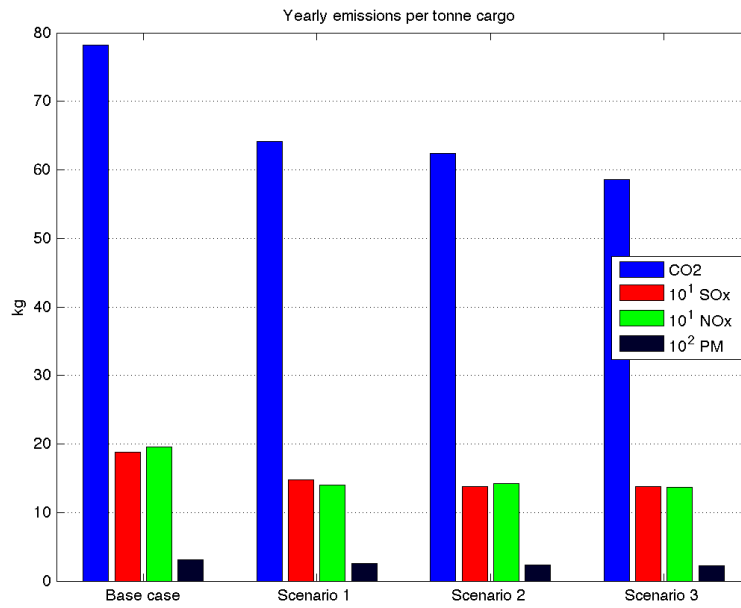
	CO ₂	10 ¹ SO _x	10 ¹ NO _x	10 ² PM
Scenario 1	-14.0	-4.0	-5.6	-0.6
Scenario 2	-15.8	-5.0	-5.4	-0.8
Scenario 3	-19.6	-5.0	-6.0	-0.9

3.4.2 Costs performance

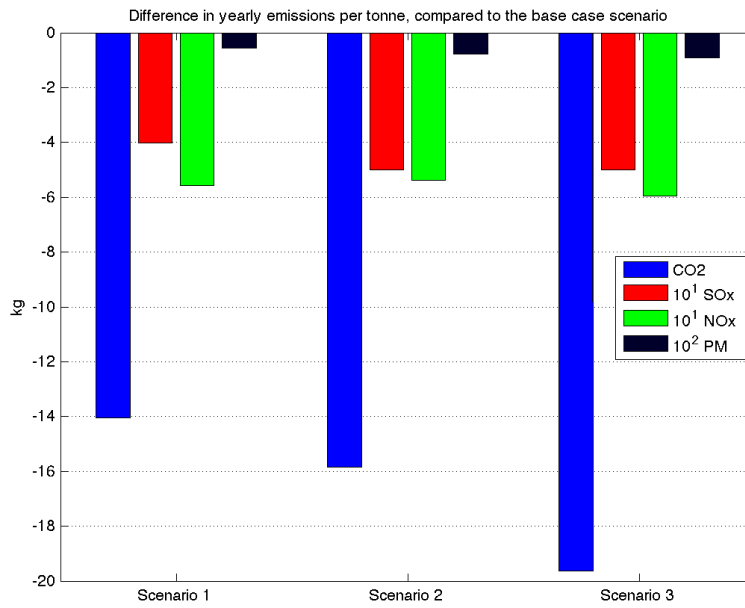
The cost performance for the scenarios are presented in this section.

Fuel costs

Table 3.26 gives the total fuel costs for the scenarios. The increase in fuel costs as a consequence of the increased fuel consumption from the installed abatement technologies are also shown.



(a) Total emissions for the scenarios per tonne cargo in the simulation period



(b) Difference in total emissions per year per tonne cargo compared to the base case scenario

Figure 3.7: Yearly emissions per tonne cargo

Table 3.25: Difference in yearly emissions per tonne cargo in percent compared to the base case scenario

	CO ₂	SO _x	NO _x	PM
Scenario 1	-21.9	-27.2	-39.6	-22.1
Scenario 2	-25.4	-36.2	-37.7	-33.4
Scenario 3	-33.5	-36.2	-43.6	-41.3

Table 3.26: Total fuel costs for all scenarios in USD

	Net increase in fuel costs due to abatement technologies	Total fuel costs
Base case	0	454 940
Scenario 1	57 335	1 278 812
Scenario 2	61 988	1 505 139
Scenario 3	18 010	1 248 565

Total scenario costs

A comparison of the total costs for the different scenarios are listed in Table 3.27 and shown in Figure 3.8. In addition, the relative increase in costs for scenario 1-3, compared to the base case, are shown in Figure 3.9.

Table 3.27: Total costs for all scenarios in MUSD

	CAPEX	OPEX	EAC
Base case	0.00	2.50	2.50
Scenario 1	6.00	4.49	4.74
Scenario 2	3.00	4.44	4.57
Scenario 3	21.60	3.74	4.64

The base case scenario is found to have the lowest EAC. Scenarios 1-3 have higher OPEX due to increased fuel costs and some added maintenance costs for the abatement technology. Also the CAPEX of installing the abatement technologies contribute to increase the EAC. In the base case scenarios, no abatement technologies or alternations are performed, therefore the CAPEX is zero. Clearly, scenario 3 has the highest CAPEX of the alternatives. It is highest due to the magnitude of the cost of LNG conversion of the machinery.

Figure 3.9 shows that the costs increase significantly for all scenarios compared to the base case. For OPEX, scenario 1 and 2 is fairly equal. Scenario 3 has the least increase in OPEX compared to the base case, with only a 50 % increase. Scenario 2 has the least increase in EAC of the alternatives. However, the increase in EAC is fairly equal for all scenarios, all lying between 80 to 90 % increase compared to the base case scenario.

3.4.3 Cost effectiveness performance

The performance on cost effectiveness for the different scenarios are presented in this section.

Cost effectiveness for emission reduction on the NSR

Table 3.28 lists the CER values for the scenarios sailing the NSR compared to each other. The CER value was calculated according to Equation 2.40, with the EAC of the scenario and the total reduced emissions for the scenario by installing the abatement technology.

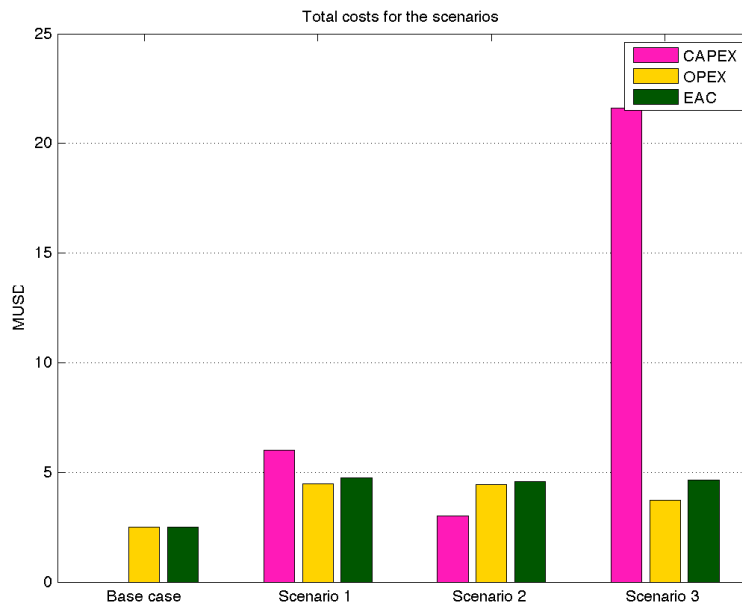


Figure 3.8: Total costs for the scenarios

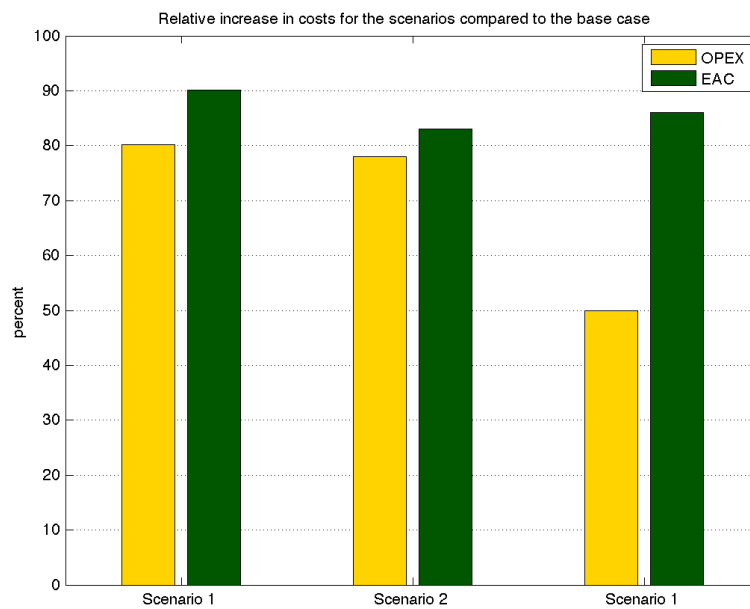


Figure 3.9: Relative increase in total costs for scenario 1-3, compared to the base case scenario

Table 3.28: CER values for the scenarios sailing on the NSR (USD/tonne reduced emissions)

	CO ₂	SOx	NOx	PM
Scenario 1	Inf	35 573	56 300	4 377 467
Scenario 2	Inf	Inf	65 931	38 842 129
Scenario 3	Inf	Inf	399 980	-828 575 435

Scenario 1 has the lowest CER value for both SOx and PM emission reduction. Scenario 2 have the lowest CER value for NOx emission reduction. No scenario reduce CO₂ emissions, so none of the scenarios have a CER value for CO₂.

For scenario 3, PM emissions are actually increased when abatement technology is used. Therefore the CER is negative.

Cost effectiveness for emission reductions compared to the base case

Table 3.29 lists the CER values for the scenarios compared to the base case scenario. The CER value was calculated according to Equation 2.40, with the EAC of the scenario and the total reduced emissions as the total emissions from the scenario minus the total emissions for the base case scenario.

Table 3.29: CER values in USD per tonne reduced emissions compared to the base case scenario

	CO ₂	SOx	NOx	PM
Scenario 1	10 473	118 358	45 579	23 700 707
Scenario 2	3 598	54 089	47 906	3 865 346
Scenario 3	1 548	54 895	38 106	2 616 347

Scenario 3 is the most cost effective for reducing CO₂, NOx and PM emissions. Scenario 2 is the most cost effective for reducing SOx emissions.

Cost effectiveness per tonne freight

Table 3.30 lists the CER values for the different scenarios, calculated as USD per tonne cargo freighted per year. The relative increase in CER compared to the base case scenario is also given for scenario 1-3. The results are also shown in Figure 3.10. The CER was calculated with Equation 2.41.

The base case scenario has the lowest CER value by far. Scenario 2 comes out as the most cost effective of the scenarios, but only marginally. All three scenarios utilising the NSR comes out fairly equal.

Table 3.30: CER values for the scenarios in USD/tonne cargo per year. The increase in % compared to the base case is also shown.

	CER	Increase in CER, %
Base case	6.60	0.0
Scenario 1	10.46	36.9
Scenario 2	10.07	34.4
Scenario 3	10.23	35.5

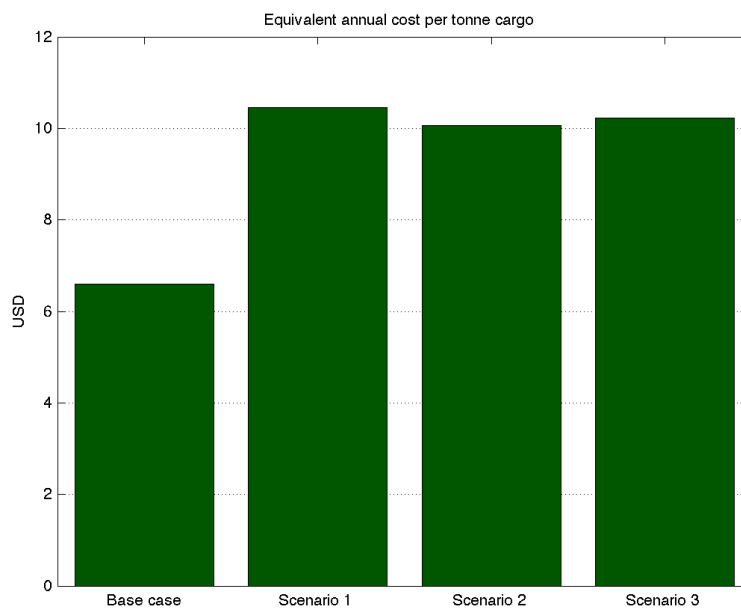


Figure 3.10: EAC per tonne cargo freighted

Chapter 4

Discussion

Based on a case vessel, this study has performed a time series simulations for one year, combining sailing on the NSR and the SCR. An ECA was assumed in the Arctic, which made up 60 % of the total sailing distance on the NSR between the ports of Murmansk and Tianjin. The study considered three alternative scenarios for compliance to ECA emission limits. Both different technologies and fuels for reducing NO_x and SO_x emissions, and combinations of this, was explored. The results of the simulations was outlined in detail in chapter 3.

This section evaluates the results, and compare with previous findings in the literature. Also the framework of the study and the simulation model is discussed.

4.1 Emissions performance

For all scenarios, the results show that a roundtrip voyage on the NSR gives less emissions in total than for the SCR. The scenarios that utilise the NSR for parts of the year therefore have less emissions in a yearly perspective. These scenarios also have a higher number of roundtrips per year, due to the shorter distance of the NSR route. Accordingly, they also have a higher cargo flow per year. Consequently, scenario 1-3 is more environmentally friendly than the base case scenario, as the emissions per tonne cargo transported is less.

Scenario 3 is not a feasible scenario for ECA compliance. The simulations indicate that the chosen emission abatement strategy for scenario 3, an EGR in combination with LNG conversion, does not satisfy IMO Tier III levels for NO_x emissions. The emission reduction efficiency of the EGR is set to 35 %, which is not particularly high. This is based on 2005 numbers. Therefore, further evaluations should consider to investigate more updated numbers for EGR efficiencies.

4.2 Cost performance

Scenario 2 has the highest fuel costs of the scenarios. This is due to the high price of MGO, compared to the other fuels. In addition, the SFC for MGO is higher than for LNG, but lower than HFO. Scenario 1 and 3 have about the same fuel costs. The cost of LNG is more expensive than HFO, but the SFC for LNG is almost half of that of HFO. Therefore, the total costs comes out about the same.

The cost of the scenarios should be evaluated in terms of how much cargo is transported per year for the scenarios. After all, it is the relationship between costs and income that matters to the ship owner.

The base case scenario is the most cost effective per tonne cargo. In order to make a profit for the NSR scenarios, the required freight rate must be increase by a minimum of 3.87 USD/tonne cargo compared to the base case scenario for the investment of the scenarios to be profitable.

Scenario 1 is the overall most cost effective method to reduce emissions per unit of reduced emissions, when comparing the different NSR scenarios. However, comparing the scenarios to the overall reductions in emissions compared to the base case on the SCR, scenario 3 is the overall most cost effective. This is due to the large emission reductions in LNG operation.

4.3 Assessment of the framework for the study

This section will assess the framework of the study that was performed.

4.3.1 Modeling of the route and ice conditions

The choice of ice data has significant importance for the determination of the NSR operation window. For the study, the ice input data was from 2008 and 2009. However, in more recent years the ice extent have decreased to lower levels. If more updated ice data were chosen, the operation window may have been longer. A longer operation window would lead to more voyages on the NSR, and an increased cost effectiveness for the scenarios. Therefore, it is assumed that if the study was performed with more recent ice data, the results would have been more in favour of the NSR scenarios compared to the SCR base case.

4.3.2 Time period of simulations

The simulation time period was for one year only. If a longer time period was used, the results may also have been changed. In a longer time series simulation, forecast trends for future ice extent may also have been included. Also life cycle cost (LCC) analyses could have been performed with a study with a longer time horizon.

4.3.3 Scenario configuration

Scenario 3 is not ECA Tier II compliant by the configuration as defined in the study . This means that scenario 3 is an infeasible choice for the NSR with an Arctic ECA in place. This can be related to that the EGR technology is still not a mature technology. Therefore, alternative NO_x abatement technology should be considered for installation for a scenario operating on DF. Alternatively, the modeling of the scenario and efficiency of the EGR was not accurate enough, and should be considered in terms of how realistic it is.

Furthermore, for scenario 3, the availability of LNG could be an issue. Currently, there are few LNG bunkering facilities. This means that the operational feasibility of the scenario as defined may not be correct. This may change in the future, making scenario 3 a more feasible alternative.

4.3.4 Cost comparison criteria

The fuel costs are a major part of the OPEX. As fuel costs fluctuate according to the oil price, a sensitivity study of the impact of the fuel prices for the scenarios could be performed. Also future forecasts can be evaluated.

The calculation of EAC assume the same lifespan for all equipment installed. This may not be realistic. The lifespan of 20 years is also maybe too high for certain equipment. However, some of the technology are still in development, and it is difficult to estimate the lifespan of the technology with high certainty.

4.4 Evaluation of MATLAB model

The MATLAB model makes some simplifications. This section will evaluate these.

The file `simulate_sailing.m` calculates the emission reductions due to the abatement technologies. Where more than one abatement technology is present, the efficiencies of the technologies are summarised.

If the total efficiency exceeds 100 %, the total emissions is set to zero. This may not be a realistic representation of the reality. In future versions, the combined efficiencies should be investigated further.

For the simulations on legs with ice present, the file `sail_ice.m` is used. The file determines the maximum attainable speed in the current ice conditions, and sets this to the sailing speed on the leg. Thus, the total travel time on the NSR is minimised. However, the total fuel consumption and emissions increase with increased engine load. The model could be modified to a “economy” mode, where slow steaming was implemented. This way, the user could select which mode to use. Slow steaming on the NSR can increase the flexibility of the schedule, and also save money on fuel costs.

The ice conditions along the route at any given time is found with the file `findice.m`. In the calculations, linear ice growth and decline is assumed. This is a simplified approach, and the ice conditions for dates between the measuring points in time should be considered with high uncertainty. This should be investigated further in development of future versions of the model. Other forms of interpolation, such as cubic, can easily be implemented by changing the interpolation algorithm called by MATLAB.

Modeling of ice conditions is difficult. Ice conditions can vary a lot in a short distance. The model considers ice measurements with relatively short intervals on the route, and interpolates the ice conditions linearly. However, this may also not be an accurate representation of the reality.

In general, the cost figures were based on rough estimates. The results should also be treated as such. The increases in OPEX for the abatement technologies are modeled as an percentage of the according CAPEX value. The maintenance cost are often related to operating hours. Therefore, a more complex calculation of maintenance costs, related to operating hours of the equipment, could be implemented.

The modeling of emissions are also based on rough assumptions. The emission profiles of the engine are based on reference values from studies of other engines and general figures. Therefore, the relative difference in the results, rather than the absolute values, are of most interest in the results.

The model has a relatively low computational time (less than 10 seconds on the test computer), so the strength of the model is that a relatively large number of simulations may be carried out in a short time period. This makes parametric studies easier.

4.4.1 Known errors in model

An error was discovered in the file `sail_ice.m`, that performs the performance calculations for legs in ice. The error lead to an overestimation of the speed on the leg, when converting from hours to days in the output. The error is corrected in the files attached to this thesis, but was present in all presentation of results in chapter 3.

4.4.2 Impact of errors on results

The error in the model affected all simulations on the NSR equally. Therefore, the scenarios on the NSR can still be compared, as the relative difference is the same even after the error is corrected.

However, the overestimation of the speed on ice legs lead to an overoptimistic yearly number of trips on the NSR. For the corrected model, only three voyages are made on the NSR in the simulation time period. Therefore, the comparison between the scenarios on the NSR and the base case scenario, only sailing the SCR, will be different in the corrected model. The new difference will be in favour of the base case scenario.

Considering that the base case scenario already came out as the most cost effective alternative, the main findings in the thesis are not considered altered by the discovery of the error in the model.

4.4.3 Simplifications in model

The model does not consider waiting times in the Suez Canal or for icebreaker support. For the aforementioned, the waiting time is usually no more than half a day, depending on arrival time. Icebreaker support

on the NSR, however, may take several days to get. This may obviously affect traveling times greatly.

Further, only main machinery is considered for calculations of emissions, fuel consumption and costs.

Chapter 5

Conclusion

The results in chapter 3 show that utilising the NSR with an Arctic ECA in place will not be cost effective compared to sailing the Southern route. The main reasons for this are:

- Limited operation window on the NSR. The vessel can only make one more roundtrip per year by utilising the NSR. This is not adequate to make up for the added costs. If the number of operation days on the NSR increase, the yearly cargo carrying capacity increase and the cost effectiveness of the NSR will increase.;
- Added CAPEX for the scenarios due from the installation of abatement technology;
- Increase in OPEX due to a large share of ECA operation on the NSR and increased operating costs in these areas.

Of the three approaches to ECA compliance that were studied, the most cost effective method was found to be to combine fuel switch from HFO to MGO in ECAs with exhaust cleaning of NO_x with a catalyst (SCR). However, this alternative was only marginally more cost effective than the other abatement scenarios. The cost data used in the study are approximate, and thus the results may change with more accurate cost data.

5.1 Future work

In future work, the modeling of costs should be given more attention. The increased income from more trips per year should be included in the model.

Also, it would be interesting to consider the cost effectiveness if more ECAs are introduced along the SCR. For instance, if the Mediterranean Sea is defined as a NECA, vessels operating on the SCR must also install abatement technology, and the difference in CAPEX for the NSR scenarios compared to the base case will be severely decreased.

As the ice extent data for more recent years show less ice extent, new simulations should be performed for more recent dates. This will probably give a larger number of operational days on the NSR, increasing the cost effectiveness of utilising the NSR.

Slow steaming on the NSR should also be explored. The SCR is over twice the distance of the NSR, so the average speed on the NSR can be reduced to the half while still performing the same number of yearly roundtrips. This may provide great savings in fuel costs. Slow steaming also provide a more flexible schedule for the ship owners, as the ship can speed up to make up for delays. When sailing in service speed, the increase in cost for increasing the speed by the same amount is significantly greater, as the fuel consumption increase with the cube of the speed.

Further work should also include simulations over longer, future time period. This study considered a one year time period. However, as mentioned, trend forecasting indicate less ice extent in the Arctic in the future. Assuming this will lead to an increase in yearly roundtrips on the NSR, this will also increase the cost effectiveness. For a longer time period, a life cycle cost (LCC) analysis can also be performed. This can give a better picture of the total cost of installing the abatement measures.

In simulations involving a longer future time period, also the future development of emission regulations can be taken into account. Both in terms of global and local fuel sulphur limits but also take into account the development of the required EEDI. The index value is reduced every five years, and to explore how the vessel can be modified to comply with these regulations and how this affects the operation and costs could be interesting.

It would also be interesting to investigate the impact of fuel price on the total cost effectiveness. If simulation for future predictions are done, the development of fuel prices should also be taken into account.

Another interesting aspect that could be considered is the introduction of an emission tax scheme. If this were to be introduced on parts of the SCR, the NSR could prove more cost effective in comparison.

In further work with the model, the operation profile of the vessels should be made more detailed. Aspects such as time in harbour, loading/offloading, manoeuvring, waiting time for Suez Canal and/or icebreaker support on the NSR, should be taken into account.

Also, only emissions and costs related to the main machinery was considered in this study. However, also emissions from auxiliary machinery is regulated in ECA regulations. This should be implemented in further developments of the model.

Alternatively, additional scenarios can also be considered. For instance, if LCC analyses are performed, newbuilds can also be considered against retrofitting new vessels. Newbuilds are often more fuel efficient. Also, vessels with and without ice class can be considered. Additionally, the additional CAPEX from installing abatement technologies on a newbuild is assumed to be lower than for retrofitting. Thus, these scenarios may come out as more cost effective than retrofitting.

Bibliography

- Acciaro, M. (2014). ‘Real option analysis for environmental compliance: LNG and emission control areas’. In: *Transportation Research Part D: Transport and Environment* 28, pp. 41–50 (cit. on pp. 15, 25, 59).
- Æsøy, V. and D. Stenersen (2013). ‘Low Emission LNG Fuelled Ships for Environmental Friendly Operations in Arctic Areas’. In: *Proceedings of the ASME 2013 32nd International Conference on Ocean, Offshore and Arctic Engineering. OMAE2013*. (Nantes, France, 9th–14th June 2013). Vol. 6. American Society of Mechanical Engineers, V006T07A028–V006T07A028. ISBN: 978-0-7918-5540-9. DOI: [10.1115/OMAE2013-11644](https://doi.org/10.1115/OMAE2013-11644) (cit. on p. 56).
- Æsøy, V., S. Ushakov, E. Hennie and J. B. Nielsen (2013). ‘Alternative Marine Fuels and the Effect on Combustion and Emission Characteristics’. In: *CIMAC Congress 2013*. (13th–16th May 2013). Shanghai, China (cit. on pp. 56, 57).
- ‘EU study to assess additional ECAs’ (05/2011). In: *Acid News* 2. Ed. by C. Ågren. URL: <http://www.airclim.org/acidnews/2011/AN2-11/eu-study-assess-additional-ecas> (visited on 06/08/2014) (cit. on p. 16).
- Ågren, C. (06/2014). ‘IMO weakens NOx rules for ships’. In: *Acid News* 2. Ed. by K. Lindqvist. URL: http://www.airclim.org/sites/default/files/acidnews_pdf/AN2-14.pdf (cit. on p. 18).
- Amdahl, J., A. Endal, G. Fuglerud, K. Minsaas, M. Rasmussen, B. Sillerud, B. Sortland and H. Valland (2005). *Kompendium. TMR4100 - Marin Teknikk Intro. TMR4105 - Marin Teknikk 1*. Ed. by G. Fuglerud. Lecture notes. Version 3. NTNU (cit. on pp. 35, 37, 119–121).
- Andreoni, V., A. Miola and A. Perujo (2008). *Cost Effectiveness Analysis of the Emission Abatement in the Shipping Sector Emissions*. Tech. rep. Joint Research Centre, Institute for Environment and Sustainability, European Commission. DOI: [10.2788/77899](https://doi.org/10.2788/77899) (cit. on pp. 23, 26, 28, 31, 54).
- Baltic Marine Environment Protection Commission - Helsinki Commission (2004). *Safety of winter navigation in the Baltic Sea Area*. HELCOM Recommendation 25/7 (cit. on p. 10).
- Bazari, Z. and T. Longva (2011). *Assessment of IMO mandated energy efficiency measures for international shipping. Estimated CO2 emissions reduction from introduction of mandatory technical and operational energy efficiency measures for ships*. Research rep. Lloyd’s Register and DNV (cit. on pp. 21, 22).
- Bimco (18/10/2011). *Bimco EEDI Calculator*. URL: <https://www.bimco.org/Products/EEDI.aspx> (visited on 14/11/2014) (cit. on p. 117).
- Brynolf, S., M. Magnusson, E. Fridell and K. Andersson (2014). ‘Compliance possibilities for the future ECA regulations through the use of abatement technologies or change of fuels’. In: *Transportation Research Part D: Transport and Environment* 28, pp. 6–18 (cit. on p. 26).
- Buhaug, Ø., J. J. Corbett, Ø Endresen, V Eyring, J Faber, S Hanayama, D. S. Lee, D Lee, H Lindstad, A. Z. Markowska, A Mjelde, D Nelissen, J Nilsen, C Pålsson, J. J. Winebrake, W Wu and K Yoshida (2009). *Second IMO GHG Study 2009*. London, UK: International Maritime Organization (cit. on pp. 25, 26).
- Cellini, S. R. and J. E. Kee (2010). ‘Cost-effectiveness and cost-benefit analysis’. In: *Handbook of practical program evaluation*, p. 493 (cit. on p. 60).
- Cooper, D. and T. Gustafsson (2004). *Methodology for calculating emissions from ships: 1. Update of emission factors*. Report series for SMED and SMED&SLU. SMHI Swedish Meteorological and Hydrological Institute (cit. on p. 31).

- Dalsøren, S. B., B. H. Samset, G Myhre, J. J. Corbett, R Minjares, D Lack and J. S. Fuglestedt (2013). ‘Environmental impacts of shipping in 2030 with a particular focus on the Arctic region’. In: *Atmospheric Chemistry and Physics* 13.4, pp. 1941–1955 (cit. on p. 16).
- Det Norske Veritas. ‘DNV ARCON-project. Trans-polar route evaluation’ (cit. on pp. 6, 34).
- DownstreamToday (05/07/2013). *Daewoo to Build Ice-Class Tankers for Yamal LNG*. Interfax News Agency. URL: http://www.downstreamtoday.com/news/article.aspx?a_id=39995&AspxAutoDetectCookieSupport=1 (visited on 13/08/2014) (cit. on p. 13).
- Eilts, P. and H.-J. Borchsenius (2001). ‘Available NOx emission reduction techniques-costs, benefits and field experience’. In: *23rd CIMAC World Congress on Combustion Engine Technology*. (Hamburg, Germany) (cit. on p. 29).
- Entec UK Ltd. (2005a). *Service Contract on Ship Emissions: Assignment, Abatement and Market-based Instruments. Task 2b — NOx Abatement*. Tech. rep. European Commission, Directorate General Environment (cit. on pp. 28, 29, 31, 57).
- (2005b). *Service Contract on Ship Emissions: Assignment, Abatement and Market-based Instruments. Task 2c — SO2 Abatement*. Tech. rep. European Commission, Directorate General Environment (cit. on pp. 24, 25).
- Er, I. D. (2002). ‘Overview of NOx emission controls in marine diesel engines’. In: *Energy Sources* 24.4, pp. 319–327. ISSN: 00908312. DOI: [10.1080/00908310252888691](https://doi.org/10.1080/00908310252888691) (cit. on pp. 29, 32, 54).
- Erceg, S., S. Ehlers, I. H. Ellingsen, D. Slagstad, R. v. B. und Polach and S. O. Erikstad (2013). ‘Ship Performance Assessment for Arctic Transport Routes’. In: *Proceedings of the ASME 2013 32nd International Conference on Ocean, Offshore and Arctic Engineering. OMAE2013*. (Nantes, France, 9th–14th June 2013). Vol. 6. American Society of Mechanical Engineers, V006T07A016–V006T07A016. ISBN: 978-0-7918-5540-9. DOI: [10.1115/OMAE2013-10733](https://doi.org/10.1115/OMAE2013-10733) (cit. on p. 8).
- Erikstad, S. O. and S. Ehlers (2012). ‘Decision Support Framework for Exploiting Northern Sea Route Transport Opportunities’. In: *Ship Technology Research* 59.2, pp. 34–42 (cit. on pp. 10, 11).
- Eyring, V., H. W. Köhler, J. Van Aardenne and A. Lauer (2005). ‘Emissions from international shipping: 1. The last 50 years’. In: *Journal of Geophysical Research: Atmospheres* 110.D17 (cit. on p. 25).
- George, J. (19/09/2013). *Northwest Passage draws adventurers, dreamers, commercial marine traffic in 2013*. Nunatsiaq Online. URL: http://www.nunatsiaqonline.ca/stories/article/65674northwest_passage_draws_adventurers_dreamers_and_commercial_marine_tra/ (visited on 20/10/2014) (cit. on p. 33).
- Germanischer Lloyd (2011). *Costs and benefits of LNG as ship fuel for container vessels. Key results from a GL and MAN joint study* (cit. on p. 52).
- (07/2012). *LNG, Powering the future of shipping*. Hamburg, Germany (cit. on p. 25).
- Gold, E. (2000). ‘Transiting the Northern Sea Routes: Shipping and Marine Insurance Interests’. Proceedings of the Northern Sea Route User Conference. In: *The 21st Century – Turning Point for the Northern Sea Route?* (Oslo, Norway, 18th–20th Nov. 1999). Ed. by C. L. Ragner. The Netherlands: Kluwer Academic Publishers. ISBN: 0-7923-6365-5 (cit. on p. 10).
- Graykowski, J. (14/10/2013). *LNG: Ports as Catalyst?* Petromedia Ltd. URL: <http://www.bunkerworld.com/forum/blogs/83/125391/John-Graykowski/LNG-Ports-as-Catalyst> (visited on 04/08/2014) (cit. on p. 15).
- Halvorsen, E. (22/06/2010). *Paving the way for ECA compliance*. DNV. URL: http://www.dnv.com/press_area/press_releases/2010/pavingthewayforeca.asp (visited on 04/08/2014) (cit. on p. 4).
- Holmes, O. and S. Kalin (05/08/2014). *Egypt plans to dig new Suez Canal costing \$4 billion*. Ed. by L. Noueihed and J. Gaunt. Reuters. URL: <http://www.reuters.com/article/2014/08/05/us-egypt-suezcanal-project-idUSKBN0G500H20140805> (visited on 06/08/2014) (cit. on p. 3).
- International Maritime Organization (2008). *Amendments to the technical code on control of emission of nitrogen oxides from marine diesel engines. Resolution MEPC.177(58)*. (NOx Technical Code 2008) (cit. on p. 18).
- (2009). *Guidelines for voluntary use of the ship Energy Efficiency Operational Indicator (EEOI). MEPC.1/Circ.684* (cit. on pp. 21, 22).

- (2010). *Guidelines for Ships Operating in Polar Waters. Resolution A.1024(26)*. London, UK (cit. on pp. 45, 47).
- (2011). *Inclusion of regulations on energy efficiency for ships in MARPOL Annex VI. Resolution MEPC.203(62)*. MEPC 62/64/Add.1. Annex 19. (Cit. on pp. 19, 20).
- (2012a). *2012 guidelines for the development of a Ship Energy Efficiency Management Plan. Resolution MEPC.213(63)*. MEPC 63/23. Annex 9. (Cit. on p. 20).
- (2012b). *2012 guidelines on the method of calculation of the attained Energy Efficiency Design Index (EEDI) for new ships. Resolution MEPC.212(63)*. MEPC 63/23. Annex 8. (Cit. on pp. 115, 116).
- (2012c). *Guidelines for calculation of reference lines for use with the Energy Efficiency Design Index (EEDI). Resolution MEPC.215(63)*. MEPC 63/23/Add.1. Annex 11. (Cit. on p. 19).
- (2014a). *IMO Begins Work on Air Pollution*. URL: <http://www.imo.org/OurWork/Environment/PollutionPrevention/AirPollution/Pages/IMO-begins-work-on-air-pollution.aspx> (visited on 29/07/2014) (cit. on p. 16).
- (04/04/2014b). *Marine Environment Protection Committee (MEPC), 66th session, 31 March to 4 April 2014*. IMO. URL: <http://www.imo.org/MediaCentre/MeetingSummaries/MEPC/Pages/MEPC66.aspx> (visited on 05/08/2014) (cit. on pp. 18, 19).
- (2014c). *Nitrogen Oxides (NOx) – Regulation 13*. URL: [http://www.imo.org/OurWork/Environment/PollutionPrevention/AirPollution/Pages/Nitrogen-oxides-\(NOx\)-Regulation-13.aspx](http://www.imo.org/OurWork/Environment/PollutionPrevention/AirPollution/Pages/Nitrogen-oxides-(NOx)-Regulation-13.aspx) (visited on 18/08/2014) (cit. on p. 18).
- (2014d). *Prevention of Air Pollution from Ships*. URL: <http://www.imo.org/OurWork/Environment/PollutionPrevention/AirPollution/Pages/Air-Pollution.aspx> (visited on 29/07/2014) (cit. on p. 16).
- (2014e). *Shipping in polar waters. Development of an international code of safety for ships operating in polar waters (Polar Code)*. URL: <http://www.imo.org/MediaCentre/HotTopics/polar/Pages/default.aspx> (visited on 05/08/2014) (cit. on p. 18).
- (2014f). *Special areas under MARPOL*. URL: <http://www.imo.org/OurWork/Environment/PollutionPrevention/SpecialAreasUnderMARPOL/Pages/Default.aspx> (visited on 04/08/2014) (cit. on pp. 2, 16, 18, 45).
- (24/01/2014g). *Sub-Committee on Ship Design and Construction (SDC): 1st session, 20 to 24 January 2014*. IMO. URL: <http://www.imo.org/MediaCentre/MeetingSummaries/DE/Pages/SDC-1-.aspx> (visited on 05/08/2014) (cit. on p. 18).
- (2014h). *Sulphur Oxides (SOx) – Regulation 14*. URL: [http://www.imo.org/OurWork/Environment/PollutionPrevention/AirPollution/Pages/Sulphur-oxides-\(SOx\)-Regulation-14.aspx](http://www.imo.org/OurWork/Environment/PollutionPrevention/AirPollution/Pages/Sulphur-oxides-(SOx)-Regulation-14.aspx) (visited on 18/08/2014) (cit. on p. 17).
- (2014i). *Technical and Operational Measures*. URL: <http://www.imo.org/OurWork/Environment/PollutionPrevention/AirPollution/Pages/Technical-and-Operational-Measures.aspx> (visited on 07/08/2014) (cit. on p. 19).
- Jones, T. W. and J. D. Smith (1982). ‘An historical perspective of net present value and equivalent annual cost’. In: *The Accounting Historians Journal* 9.1, pp. 103–110 (cit. on p. 60).
- Juva, M. and K. Riska (2002). *On the power requirements in the Finnish-Swedish Ice Class Rules*. Research Report 53. Winter Navigation Research Board (cit. on pp. 40, 41, 43, 77, 123, 124).
- Karila, K., T. Kärkkäinen, M. Larmi, S. Niemi, C.-E. Sandström, J. Tamminen and J. Tiainen (2004). *Reduction of particulate emissions in compression ignition engines*. Espoo, Finland: Helsinki University of Technology (cit. on p. 25).
- Kendrick, L. (28/06/2014). *Map Shortcomings Could Hinder Northern Sea Route Growth*. BarentsObserver. URL: <http://barentsobserver.com/en/arctic/2014/06/map-shortcomings-could-hinder-northern-sea-route-growth-28-06> (visited on 13/08/2014) (cit. on pp. 4, 9).
- Lack, D. A. and J. J. Corbett (2012). ‘Black carbon from ships: A review of the effects of ship speed, fuel quality and exhaust gas scrubbing’. In: *Atmospheric Chemistry and Physics* 12.9, pp. 3985–4000. ISSN: 16807316. DOI: [10.5194/acp-12-3985-2012](https://doi.org/10.5194/acp-12-3985-2012) (cit. on p. 22).
- Levander, K. (2009). *System Based Ship Design. SeaKey Naval Architecture*. Lecture Notes (cit. on pp. 11, 34, 59, 113, 114).

- Libra, J. (18/11/2013). *Arctic black carbon, maritime trade, and ECA mitigation potential*. Major Economies and Climate Change Research Group, The University of Texas at Austin. URL: <http://blogs.utexas.edu/mecc/2013/11/18/arctic-black-carbon-maritime-trade-and-eca-mitigation-potential/> (visited on 04/08/2014) (cit. on p. 17).
- Lundy, W. M. (29/10/2013). *Black Carbon, Arctic Climate & the International Maritime Organization*. Presentation. Washington, DC, USA: Clean Air Act Advisory Committee. URL: <http://www.epa.gov/oar/caaac/mstrs/oct2013/lundy.pdf> (visited on 05/08/2014) (cit. on p. 17).
- Madsen, S. and T. C. Olsson (2012). 'Cost-Efficient Emission Control Area Compliancy'. MA thesis. Norwegian University of Science and Technology (cit. on p. 32).
- Maersk Group (2014). *Triple-E vessels*. URL: <http://www.maersktechnology.com/stories/stories/pages/triple-evessels.aspx> (visited on 18/09/2014) (cit. on p. 12).
- MAN B&W (2010). *S60MC-C8-TII Project Guide. Camshaft Controlled Two-stroke Engines*. Version 1 (cit. on p. 52).
- (2012). *ME-GI Dual Fuel MAN B&W Engines. A technical, operational and cost-effective solution for ships fuelled by gas* (cit. on p. 52).
- (06/2014). *Emission Project Guide for Marpol Annex VI Regulations. MAN B&W Two-stroke Marine Engines* (cit. on pp. 25–27, 29–31, 50, 51).
- McCallum, J. (1996). *Safe speed in ice: An analysis of transit speed and ice decision numerals*. Ottawa, Canada: Ship Safety Northern (AMNS), Transport Canada (cit. on p. 22).
- McGrath, M. (26/11/2012). *Gas tanker Ob River attempts first winter Arctic crossing*. BBC News. URL: <http://www.bbc.com/news/science-environment-20454757> (visited on 13/08/2014) (cit. on p. 13).
- Meech, R. (10/2010). *Emission Control Areas (ECAs)*. Regional Workshop on the Ratification and Implementation of MARPOL Annex VI. Presentation. Athens, Greece: IMO (cit. on pp. 2, 4, 16).
- Miola, A., B. Ciuffo, E. Giovine and M. Marra (2010). *Regulating Air Emissions from Ships. The State of the Art on Methodologies, Technologies and Policy Options*. Research rep. Joint Research Centre, Institute for Environment and Sustainability, European Commission. DOI: [10.2788/4171](https://doi.org/10.2788/4171) (cit. on pp. 14, 16, 23).
- National Snow & Ice Data Center (07/10/2014). *2014 melt season in review*. URL: <http://nsidc.org/arcticseaicenews/2014/10/2014-melt-season-in-review/> (visited on 25/11/2014) (cit. on pp. 7, 8, 48).
- Nikopoulou, Z., K. Cullinane and A. Jensen (2013). 'The role of a cap-and-trade market in reducing NOx and SOx emissions: Prospects and benefits for ships within the Northern European ECA'. In: *Proceedings of the Institution of Mechanical Engineers Part M: Journal of Engineering for the Maritime Environment* 227.2, pp. 136–154. ISSN: 14750902. DOI: [10.1177/1475090212459130](https://doi.org/10.1177/1475090212459130) (cit. on pp. 15, 25, 26).
- Nilsen, T. (15/12/2010). *Statoil may expand LNG plant at Hammerfest*. BarentsObserver. URL: <http://barentsobserver.com/en/sections/articles/statoil-may-expand-lng-plant-hammerfest> (visited on 13/08/2014) (cit. on p. 12).
- (06/11/2012). *Hammerfest LNG set sails for Japan via Arctic route*. BarentsObserver. URL: <http://barentsobserver.com/en/arctic/hammerfest-lng-set-sails-japan-arctic-route-06-11> (visited on 13/08/2014) (cit. on p. 12).
- Nordic Bulk Carriers (30/08/2011). *Fact sheet – The Northern Sea Route*. URL: http://www.nordicbulcarriers.com/images/Media/Filer/nsr2011_factsheet.pdf (visited on 16/09/2014) (cit. on p. 33).
- Northern Sea Route Information Office (2014). *Northern Sea Route Information Office*. URL: <http://www.arctic-lio.com> (cit. on pp. 6, 8).
- Norwegian Petroleum Directorate (2013). *Facts 2013 – The Norwegian petroleum sector*. Norwegian Petroleum Directorate and Ministry of Petroleum and Energy (cit. on p. 12).
- Østreng, W., K. M. Eger, B. Fløistad, A. Jørgensen-Dahl, L. Lothe, M. Mejlænder-Larsen and T. Wergeland (2013). *Shipping in Arctic waters. A Comparison of the Northeast, Northwest and Trans Polar Passages*. Springer (cit. on pp. 6, 11, 12).

- Pettersen, T. (26/08/2010). *Northern Sea Route should not be expensive*. BarentsObserver. URL: <http://barentsobserver.com/en/sections/topics/northern-sea-route-should-not-be-expensive> (visited on 13/08/2014) (cit. on p. 11).
- (08/05/2014). *Baltiysky Shipyard to build three new icebreakers by 2020*. BarentsObserver. URL: <http://barentsobserver.com/en/arctic/2014/05/baltiysky-shipyard-build-three-new-icebreakers-2020-08-05> (visited on 13/08/2014) (cit. on p. 5).
- ‘Polar bearings’ (12/07/2014). In: *The Economist*. URL: <http://www.economist.com/news/china/21606898-china-pursues-its-interest-frozen-north-polar-bearings> (visited on 12/08/2014) (cit. on p. 1).
- Proceedings of the ASME 2013 32nd International Conference on Ocean, Offshore and Arctic Engineering* (2013). (Nantes, France, 9th–14th June 2013). Vol. 6. American Society of Mechanical Engineers. ISBN: 978-0-7918-5540-9.
- Ragner, C. L., ed. (2000). *The 21st Century – Turning Point for the Northern Sea Route?* Proceedings of the Northern Sea Route User Conference. (Oslo, Norway, 18th–20th Nov. 1999). The Netherlands: Kluwer Academic Publishers. ISBN: 0-7923-6365-5 (cit. on pp. 4, 5).
- (2008). ‘The Northern Sea Route’. In: *Barents – ett gränsländ i Norden*. Ed. by T. Hallberg. Stockholm, Sweden: Arena Norden, pp. 114–127 (cit. on pp. 4, 9).
- Reimer, N. and Q.-T. Duong (2013). ‘Prediction of Travelling Time and Exhaust Gas Emission of Ships on the Northern Sea Route’. In: *Proceedings of the ASME 2013 32nd International Conference on Ocean, Offshore and Arctic Engineering. OMAE2013*. (Nantes, France, 9th–14th June 2013). Vol. 6. American Society of Mechanical Engineers, V006T07A012–V006T07A012. ISBN: 978-0-7918-5540-9. DOI: [10.1115/OMAE2013-10606](https://doi.org/10.1115/OMAE2013-10606) (cit. on p. 8).
- Riska, K. (2013). ‘Lecture notes, Ship design for ice’ (cit. on pp. 5, 9, 10, 40).
- Riska, K., M. Wilhelmson and K. Englund (1997). *Performance of merchant vessels in ice in the Baltic*. Research rep. 52. Winter Navigation Research Board (cit. on pp. 38, 39, 41).
- SCF Group (21/06/2013). *Russia: Sovcomflot, NOVATEK and VEB to Cooperate in Yamal LNG Project*. World Maritime News. URL: <http://worldmaritimeneeds.com/archives/87104/russia-sovcomflot-novatek-and-veb-to-cooperate-at-yamal-lng-project/> (visited on 13/08/2014) (cit. on p. 13).
- Schuler, M. (20/01/2014). *Somali Pirates’ First Hijacking Attempt of 2014 Ends with Arrests*. Unofficial Networks. URL: <http://gcaptain.com/somalia-pirates-first-hijacking-attempt-of-2014-ends-with-arrests/> (visited on 08/08/2014) (cit. on p. 4).
- Sea-Web (2014). *Sea-web: Ship Detail*. URL: http://www.sea-web.com/authenticated/authenticated_handler.aspx?control=shipovw&qs=9529463&LRNO=9529463 (cit. on p. 33).
- Shinagawa, M. (2000). ‘A Foreign Company’s View of Northern Sea Route Technology and Infrastructure – Perceived Problems and Uncertainties’. Proceedings of the Northern Sea Route User Conference. In: *The 21st Century – Turning Point for the Northern Sea Route?* (Oslo, Norway, 18th–20th Nov. 1999). Ed. by C. L. Ragner. The Netherlands: Kluwer Academic Publishers. ISBN: 0-7923-6365-5 (cit. on p. 5).
- Sørstrand, S. S. (2012). ‘A Decision Support Model for Merchant Vessels Operating on the Arctic Sea’. MA thesis. Norwegian University of Science and Technology (cit. on p. 5).
- Staalesen, A. (21/08/2013a). *First container ship on Northern Sea Route*. BarentsObserver. URL: <http://barentsobserver.com/en/arctic/2013/08/first-container-ship-northern-sea-route-21-08> (visited on 13/08/2014) (cit. on p. 12).
- (07/08/2013b). *“Northern Sea Route comes to life”*. BarentsObserver. URL: <http://barentsobserver.com/en/arctic/2013/08/northern-sea-route-comes-life-07-08> (visited on 13/08/2014) (cit. on p. 6).
- (29/07/2014). *No more nuclear power for Arctic tourists*. BarentsObserver. URL: <http://barentsobserver.com/en/arctic/2014/07/no-more-nuclear-power-arctic-tourists-29-07> (visited on 13/08/2014) (cit. on p. 4).
- Suez Canal Authority (2007). *Suez Canal Rules of Navigation*. URL: <http://www.suezcanal.gov.eg/NR.aspx?node=81> (visited on 12/08/2014) (cit. on p. 3).

- Suez Canal Authority (2010). *Circular No. 2/2010*. URL: <http://www.suezcanal.gov.eg/showNc.aspx?id=56> (visited on 12/08/2014) (cit. on p. 3).
- (2014a). *Suez Canal Toll Calculator*. URL: <http://www.suezcanal.gov.eg/calc.aspx> (visited on 05/12/2014) (cit. on p. 59).
- (2014b). *Traffic System*. URL: <http://www.suezcanal.gov.eg/sc.aspx?show=13> (visited on 14/11/2014) (cit. on p. 45).
- Töns, T. (2014). ‘Ice condition database for the Arctic sea’. In: *33rd International Conference on Ocean, Offshore and Arctic Engineering, American Society of Mechanical Engineers*. (Cit. on p. 47).
- U.S. Environmental Protection Agency (2009). *Regulatory Impact Analysis: Control of Emissions of Air Pollution from Category 3 Marine Diesel Engines*. Tech. rep. (cit. on pp. 15, 25, 31).
- U.S. National Ice Center (2014). *Products on demand*. URL: <http://www.natice.noaa.gov/ps/javascriptproductviewer/> (cit. on p. 47).
- Valland, H. (2008). ‘Primær energiomforming ved forbrenning’. Norwegian. In: *Framdriftsmaskineri. Kompendium i fag TMR4310* (cit. on pp. 14, 15).
- Verny, J. and C. Grigentin (2009). ‘Container shipping on the Northern Sea Route’. In: *International Journal of Production Economics* 122.1, pp. 107–117 (cit. on p. 5).
- Wärtsilä (2005). ‘Marine Technologies for Reduced Emissions’. In: *The 2nd Annual Conference on Green Ship Technology*. (Amsterdam, Netherlands, 13th–15th Apr. 2005) (cit. on pp. 24, 26, 28, 29).
- (2010). *Boosting energy efficiency*. Brochure (cit. on p. 24).
- Watson, D. M. G. (1998). *Practical Ship Design*. Oxford, UK: Elsevier Science Ltd. ISBN: 0-08-042999-8 (cit. on p. 35).
- Woodyard, D. (2009). ‘Exhaust Emissions and Control’. In: *Pounder’s marine diesel engines and gas turbines*. 9th ed. Oxford: Butterworth-Heinemann. Chap. 3. ISBN: 978-0-7506-8984-7 (cit. on p. 55).
- Woud, H. K. and D. Stapersma (2002). *Design of Propulsion and Electric Power Generation Systems*. London, UK: IMarEST (cit. on p. 55).
- Yang, Z. L., D Zhang, O Caglayan, I. D. Jenkinson, S Bonsall, J Wang, M Huang and X. P. Yan (2012). ‘Selection of techniques for reducing shipping NOx and SOx emissions’. In: *Transportation Research Part D: Transport and Environment* 17, pp. 478–486 (cit. on p. 26).

Appendix A

General arrangement of Panamax bulk carrier

These drawings of the general arrangement (GA) of a typical Panamax bulk carrier from Levander (2009) were used to estimate some of the case ship's coefficients.

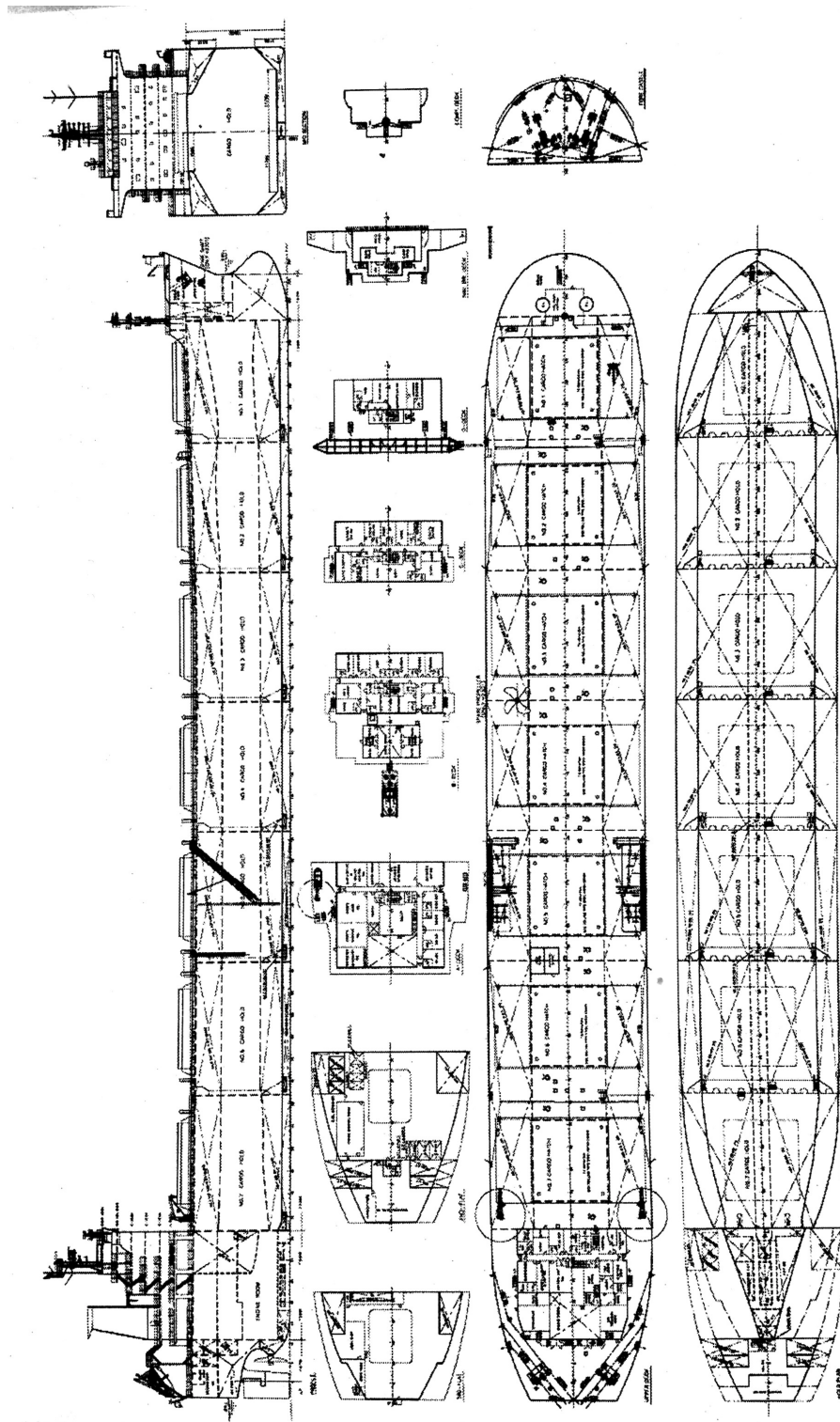


Figure A.1: GA of a typical Panamax bulk carrier. Source: Levander (2009)

Appendix B

Method for calculation of attained EEDI for a specific ship

According to IMO (2012b), the attained EEDI for a ship is calculated by the following formula;

$$\frac{\Theta}{f_i \cdot f_c \cdot Capacity \cdot f_w \cdot V_{ref}}, \quad (\text{B.1})$$

where

$$\begin{aligned} \Theta = & \left(\prod_{j=1}^n f_j \right) \left(\sum_{i=1}^{nME} P_{ME(i)} \cdot C_{FME(i)} \cdot SFC_{ME(i)} \right) \\ & + (P_{AE} \cdot C_{FAE} \cdot SFC_{AE*}) \\ & + \left(\left(\prod_{j=1}^n f_j \cdot \sum_{i=1}^{nPTI} P_{PTI(i)} - \sum_{i=1}^{neff} f_{eff(i)} \cdot P_{AEeff(i)} \right) C_{FAE} \cdot SFC_{AE} \right) \\ & - \left(\sum_{i=1}^{neff} f_{eff(i)} \cdot P_{eff(i)} \cdot C_{FME} \cdot SFC_{ME} ** \right). \end{aligned} \quad (\text{B.2})$$

The coefficients of Equation B.1 and Equation B.2 are explained in Table B.1. For additional details, see IMO (2012b).

The attained EEDI is a function of many aspects of the ship's design. C_F is a non-dimensional conversion factor between fuel consumption and CO₂ emissions, both measured in grams, based on the carbon content of the fuel. V_{ref} is the ship's speed in knots. $Capacity$ is defined differently, depending on ship type: For bulk carriers, tankers, gas tankers, ro-ro cargo ships, general cargo ships, refrigerated cargo carrier and combination carriers, dead weight (DWT) is used as $Capacity$, for passenger ships and ro-ro passenger ships, gross tonnage (GT) is used and for container ships 70 % of DWT is used as $Capacity$. P is the power of the main and auxiliary engines in kW. Subscripts ME and AE refer to the main and auxiliary engine(s), respectively. The summation i is for all engines, with the number of engines nME .

Table B.1: Coefficients in determining the attained EEDI for a specific ship. Source: (IMO, 2012b)

Coefficient	Meaning
C_F	Conversion factor between fuel consumption and CO ₂ emission
V_{ref}	Ship speed
$Capacity$	Function of DWT or GT, depending on ship type
P	Power of main (ME) and auxiliary engines (AE)
SFC	Specific fuel consumption
f_j	Correction factor for ship specific design elements
f_w	Weather factor
f_{eff}	Availability factor of innovative energy efficiency technology
f_i	Capacity factor
f_c	Cubic capacity correction factor

Appendix C

Calculation of attained EEDI calculations for the case vessel

The EEDI calculator produced by Bimco (v1.40) was used to obtain the value (Bimco, 2011). The input values, and the parameters for Equation B.1 is described below.

BIMCO		EEDI Calculator		Your calculator is up to date	
Ship details		Corrections		Download	
Name	Nordic Orion	Displacement		Ice Class	IA
IMO No.:	9529463	Breadth [m]		Lpp [m]	220,00
Type	Bulk carrier	Draught [m]		Crane reach [m]	
Sup type	Bulk carrier	Deadweight [T]		Crane SWL [T]	
Max. Capacity	75 603 DWT (ton)			# of cranes	
LWT _{CSR}					
DWT reference design					
Cubic capacity					
Main Engine(s)		Shaft Motor		Innovative energy efficiency technology	
	MCR [kW]	SFC [g/kWh]	Shaft limit		
no.1.	13 560	170,0			
no.2.					
no.3.					
no.4.					
Fuel type	Heavy Fuel Oil, ISO 8217, RME - RMK				
Auxiliary Engine(s)		Index Condition		Reference speed	
	MCR [kW]	SFC [g/kWh]	Generator η	Knots	
no.1.	610	185,0	0,93	@ Index Condition	
no.2.				14,50	
no.3.					
no.4.					
no.5.					
Fuel type	Diesel/Gas Oil, ISO 8217, DMC - DMX				
Shaft Generator		Delivery date		Mandatory field	
	kW	SG installed	No	Optional field	
no.1.		Calculation option	N/A	Ignored field	
no.2.					
<small>The information and results expressed by the BIMCO EEDI Calculator constitute an implementation of IMO MEPC.1/Circ.681, amended by WP.9 of MEPC 63 in March 2012, by MEPC 65/4/4 on inclusion of Ro-Ro cargo and passenger ships as well as by MEPC 65/4/5 on correction of EEDI for General Cargo Ship, and are subject to change without notice. The information and results expressed by the Calculator have been formed in good faith on the basis of the best information available at the time of implementation from sources believed to be reliable, but no warranty, express or implied, is made as to its accuracy, completeness or correctness. BIMCO accept no liability arising out of or in connection with the results of the Calculator and you are advised that any usage is at your own risk. In particular, the results should not be construed as certified, legal or otherwise.</small>		Version 1.40	Calculation ref:	19808	

Figure C.1: Input to the Bimco EEDI calculator



BIMCO

Parameter List

MCR _{ME}	13560	[kW]
SFC _{ME}	170,0	[g/kWh]
C _{FME}	3,1144	
Shaft limit	13560	[kW]
P _{ME}	10170	[kW]
SFC _{AE}	185,0	[g/kWh]
C _{FAE}	3,2060	
SFC for P _{AE} calculation	185,0	[g/kWh]
C _F for P _{AE} calculation	3,2060	
P _{AE}	589	[kW]
η _{generator}	0,93	
P _{PTO}	0	[kW]
P _{PTI}	0	[kW]
Shaft power from P _{PTI}	0	[kW]
P _{AEeff}	0	[kW]
f _{eff}	1,00	
P _{eff}	0	[kW]
f _{eff}	0,50	
SFC for P _{eff} calculation	170,0	[g/kWh]
C _F for P _{eff} calculation	3,1144	
f _i for ice class	1,1019	
f _i for voluntary enhancements	1,0000	
f _{cranes}	1,0000	
f _i for CSR built ships	1,0000	
f _i for ice class	0,8461	
f _i for shuttle tankers	0,7700	
f _i for General cargo ships	#DIV/0!	
f _i for Ro-Ro Cargo and Passenger ships	1,0000	
L _{pp}	220,00	[m]
f _c for cubic capacity correction	1,0000	
f _c for RoPax	1,0000	
Capacity in EEDI condition	75603	DWT [ton]
Speed in EEDI condition	14,50	[knots]
Attained EEDI	4,060	[g/DWT x nm]
Required EEDI for compliance phase	4,076	[g/DWT x nm]
Compliance phase selected	Phase 1: 1 Jan 2015 – 31 Dec 2019	

Figure C.2: Parameters used by the Bimco EEDI calculator as input to Equation B.1

Appendix D

Diagram to find C_R for slenderness ratio = 5.0

This diagram was used in Gulddammer and Harvald's method in order to determine the coefficient of residual resistance, C_R , for the case ship (see section 2.1.1). The diagram is retrieved from Amdahl et al. (2005).

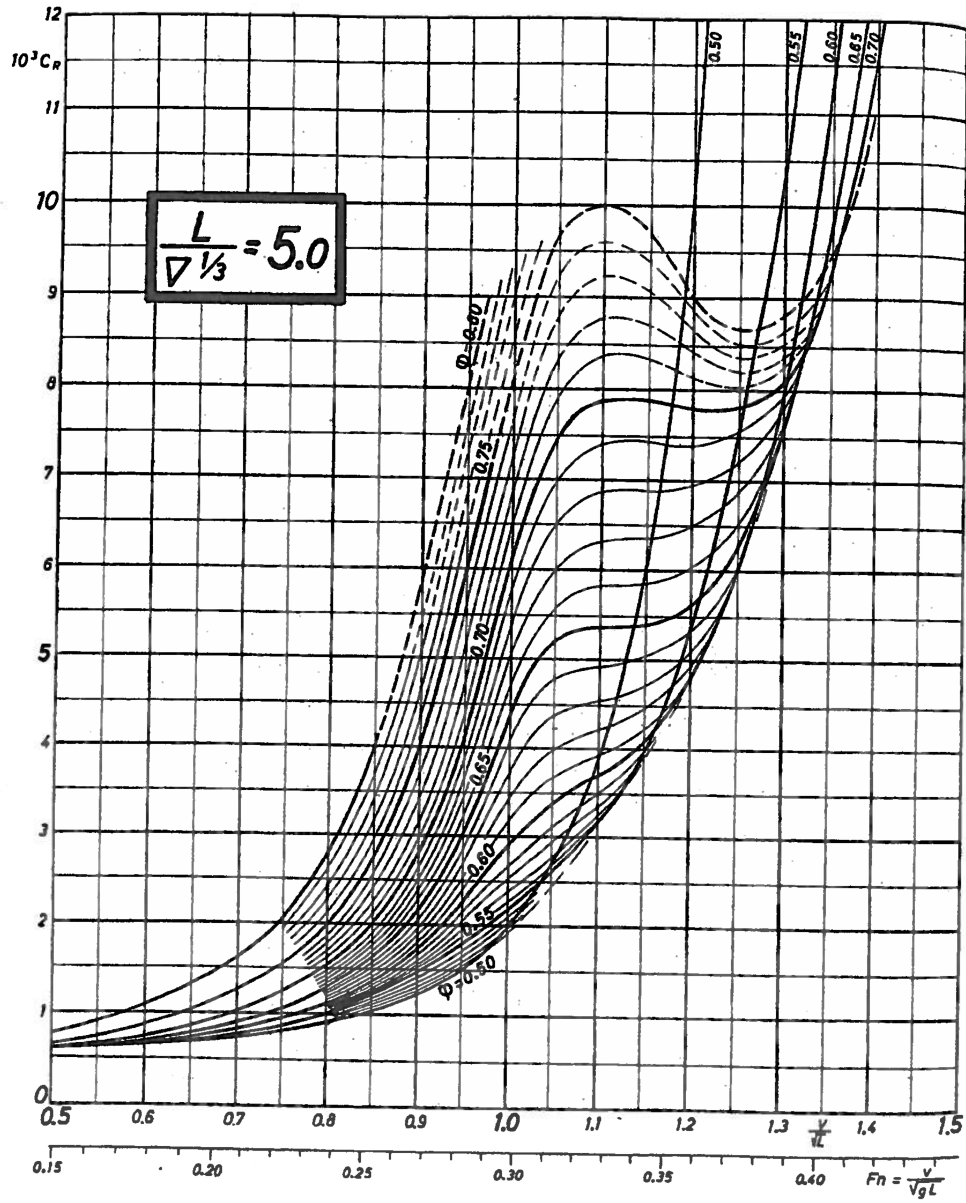


Figure D.1: Diagram for slenderness ratio 5.0. Source: Amdahl et al. (2005)

Appendix E

Diagram to find k for estimating the wet surface S

This diagram was used to estimate the coefficient k in Equation 2.15 to find the wet surface S for the case ship.

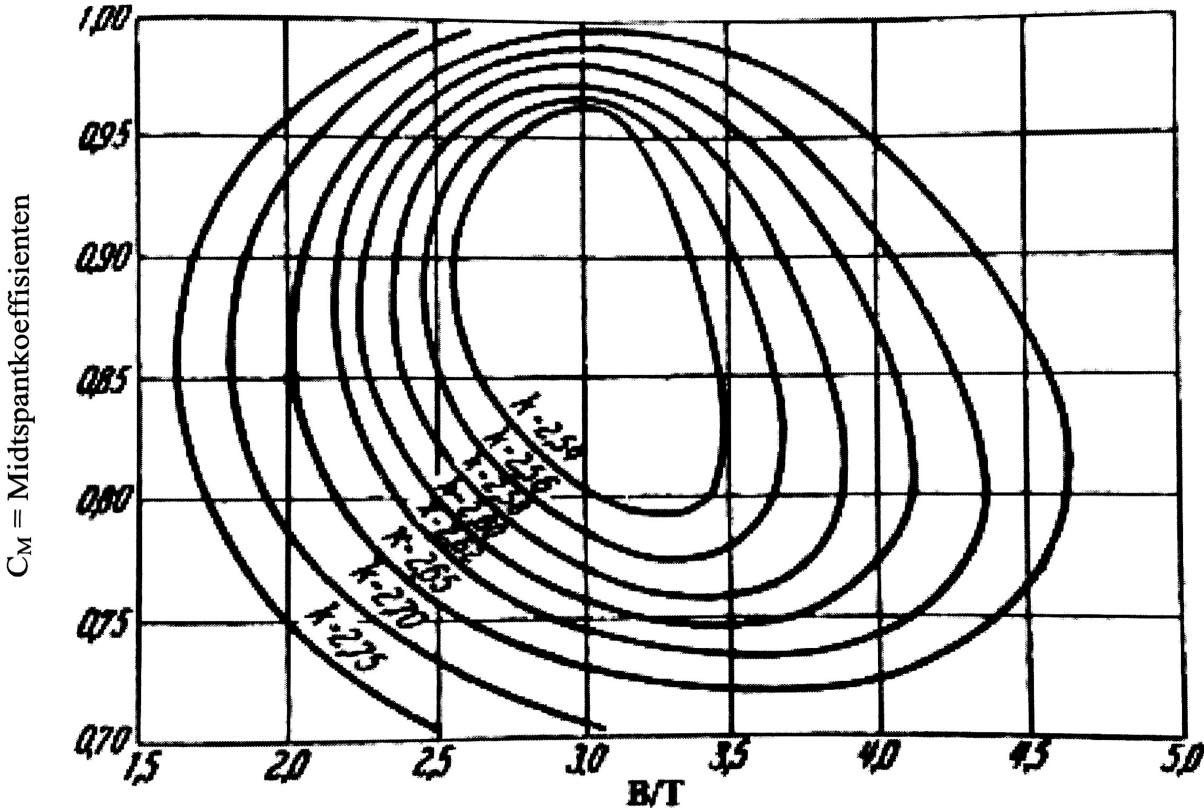


Figure E.1: Diagram for determining the constant k in estimation of the wet surface S . Source: Amdahl et al. (2005)

Appendix F

Method of determining brash ice resistance

This section describes the background for the simplified Equation 2.17 used to determine the brash ice resistance in section 2.1.1. According to Juva and Riska (2002), the brash ice resistance R_{ch} can be calculated as

$$R_{ch} = \frac{1}{2}\mu_B\rho_{\Delta}gH_F^2K_P \left[\frac{1}{2} + \frac{H_M}{2H_F} \right]^2 \left[B + 2H_F \left(\cos \delta - \frac{1}{\tan \psi} \right) \right] (\mu_h \cos \phi + \sin \psi \sin \alpha) \\ + \mu_B\rho_{\Delta}gK_0\mu_hL_{par}H_F^2 + \rho_{\Delta}g \left[\frac{LT}{B^2} \right]^3 H_M A_{wf} \text{Fn}^2 \quad (\text{F.1})$$

where $\mu_B = 1 - p$ and p is porosity ($\mu_B = 0.8 \dots 0.9$), ρ_{Δ} the difference between the densities of water and ice, g the gravity constant, K_P the constant of passive stress, H_M the thickness of the brash ice in the middle of the channel, δ the slope angle of the side wall of the brash ice, μ_H the coefficient of friction between the ice and the hull, ϕ the angle between the waterline and the vertical at $B/2$, K_0 the coefficient of lateral stress at rest, L_{par} the length of the parallel midbody at the waterline, A_{wf} the waterline area of the foreship and Fn the Froude number. H_F describes the thickness of the brash ice layer which is displaced by the bow and is moved to the side against the parallel midbody (see Figure F.2), and is calculated as

$$H_F = H_M + \frac{B}{2} \tan \gamma + (\tan \gamma + \tan \delta) \sqrt{\frac{B [H_M + \frac{B}{4} \tan \gamma]}{\tan \gamma + \tan \delta}} \quad (\text{F.2})$$

For $B > 10$ m and $H_M > 0.4$ m, H_F can be simplified to

$$H_F = 0.26 + (BH_M)^{0.5} \quad (\text{F.3})$$

According to Juva and Riska (2002), the slope angles γ and δ can be assumed as 2° to 22.6° respectively.

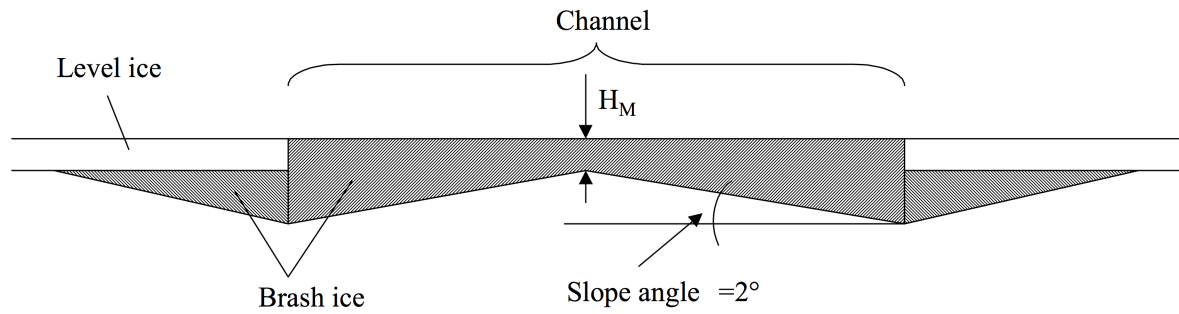


Figure F.1: Definitions for H_M and γ . Source: Juva and Riska (2002)

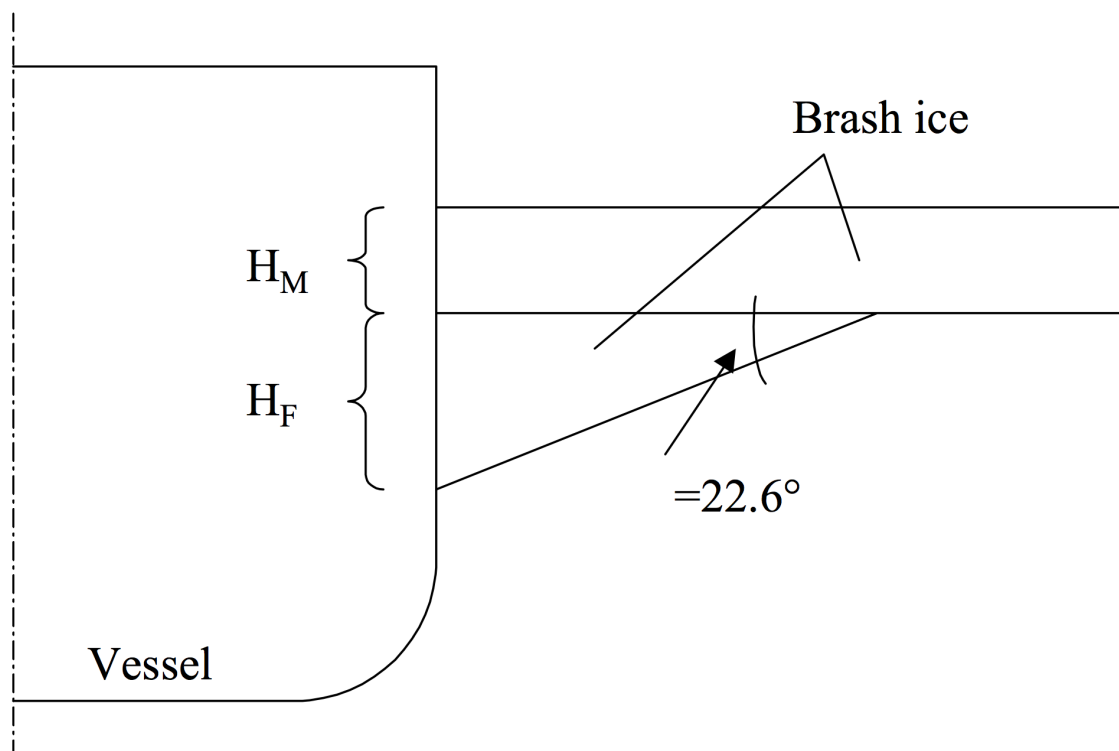


Figure F.2: Definitions for H_M , H_F and δ . Source: Juva and Riska (2002)

Appendix G

MATLAB model

abatement_tech.m

```
1 % ABATEMENT_TECH.m define the properties of the different abatement
2 % technologies
3 clear;
4
5 % Additional fuel consumption (percent) [high scenarios assumed]
6 scrubber.addfc = 3; % 1-3 percent incr
7 EGR.addfc = 3; % 1-3 percent incr
8 SCRe.addfc = 10; % 10 percent incr due to cons of urea
9 LNGconv.addfc = 1; % 1 percent additional fuel consumption for operation of fuel system
10
11 none.addfc = 0;
12
13 % Reduction of emissions (percent)
14 scrubber.SOxred = -75;
15 scrubber.NOxred = -10;
16 scrubber.PMred = -25;
17 EGR.SOxred = 0;
18 EGR.NOxred = -35;
19 EGR.PMred = +10;
20 SCRe.SOxred = 0;
21 SCRe.NOxred = -95;
22 SCRe.PMred = -30;
23 LNGconv.SOxred = 0;
24 LNGconv.NOxred = 0;
25 LNGconv.PMred = 0;
26
27 % For those with no abatement tech
28 none.SOxred = 0;
29 none.NOxred = 0;
30 none.PMred = 0;
31
32 save('abatementtech.mat', '-v7.3');
```

costs.m

```
1 % COSTS.m define the costs used in the simulations
2
3 clear;
4 %% Constants
5 discontrate = 4; % percent
6 lifespan = 20; % years
7 exchratesUSDtoEUR = 0.8; % 1 USD = 0.8 EUR
```

```

8
9 %% Additional capital costs
10 % Abatement tech
11 % Installation costs (USD) [high scenarios assumed]
12 capex.scrubber = 3 * 10^6; % Retrofit (1 main engine +3 aux.engines): 2,5-3 mill.
13 capex.EGR = 2 * 10^6 * exchratesUSDtoEUR; % From MAN (mail Vilmar, via Solvang)
14 capex.SCR = 3 * 10^6; % Approx. 3 mill
15 capex.LNGconv = 20 * 10^6; % Retrofit: 15-20 mill (2000 m3 LNG tank capacity), ...
    installation included
16 capex.none = 0;
17
18 %% Additional operating costs (annual)
19
20 % Abatement tech
21 % Added maintenance costs (USD) [high scenarios assumed]
22 opex.addmaint.scrubber = capex.scrubber * 0.10; % 5-10 percent of capex annually
23 opex.addmaint.EGR = 0; % none
24 opex.addmaint.SCR = capex.SCR * 0.10; % 5-10 percent of capex annually
25 opex.addmaint.LNGconv = 0; % none
26 opex.addmaint.none = 0;
27
28 % Fuel prices (USD/ton)
29 fuelprice.HFO = 450;
30 fuelprice.MGO = 750;
31 fuelprice.LNG = 650;
32
33 % Fees (USD)
34 fee.SuezCanal = 205496; % Average fee (ballast/laden)
35 fee.NSR = 1.1 * fee.SuezCanal;
36
37 % Save to file
38 save('costs.mat', '-v7.3');

```

emissions_calc.m

```

1 function [emissions] = emissions_calc(fuelcons,energy,MCR,fueltype)
2
3 % EMISSIONS_CALC.m calculates the emissions of CO2, NOx, SOx and PM for a
4 % given fuel consumption and energy use for the case ship.
5 %
6 % -----
7 % Input
8 %
9 % fuelcons Fuel consumption on leg kg
10 % energy Energy used on leg kWh
11 % MCR Percentage of MCR used on leg percent
12 % fueltype Type of fuel used on leg (HFO, MGO or
13 % LNG), input as string
14 %
15 % -----
16 % Output
17 %
18 % CO2 Total emissions on leg g
19 % NOx Total emissions on leg g
20 % SOx Total emissions on leg g
21 % PM Total emissions on leg mg
22 % -----
23 % Runa A. Skarb\o | runaaman@stud.ntnu.no | v1.0 03 Dec 2014
24
25 % Load datafile with emission values
26 eng = load('enginedata.mat');
27
28 % Names of variables needed from L2
29 NOxvar = sprintf('p_NOx_%s', fueltype);

```

```

30 PMvar = sprintf('p_PM%s', fueltype);
31
32 % Find NOx and PM specific emissions for given MCR
33 speNOx = polyval(eng.(NOxvar), MCR); % g/kWh
34 spePM = polyval(eng.(PMvar), MCR); % mg/kWh
35
36 % Find sulphur percentage in fuel
37 S_perc = eng.sulphur.(fueltype); % percent
38
39 % Emissions; CO2, SOx, NOx (g) and PM (mg)
40 CO2 = eng.PER.CO2.(fueltype) * fuelcons;
41 SOx = eng.PER.SOx.(fueltype) * S_perc * fuelcons;
42 NOx = speNOx * energy;
43 PM = spePM * energy;
44
45 emissions = [CO2,NOx,SOx,PM];
46
47 end

```

engine_data.m

```

1 % ENGINE_DATA.m fuel and engine properties. Also,
2 % - define input data for the fuel and emissions calculations,
3 % - makes polynomial functions for NOx and PM emissions
4 % - saves data to file 'emissionsdata.mat'
5 % - plots SFC and NOx and PM emissions over the engine load range
6 % (optional)
7 % - saves plots (optional)
8
9 clear;
10 %% Define input data for fuel and engine
11 % Engine loads
12 Loadvec = [25 50 75 100];
13
14 % Specific fuel consumption for the fuels (g fuel/kWh) (read at 30, 50, 85
15 % and 100 % load)
16 SFC.HFO = [9.40 8.73 8.61 8.67]/8.61 * 174; % 174 g/kWh at optimum, from ...
    [#man-bw_2010a]. Ref. numbers from [#aesoyushakov_2013a] in MJ/kWh.
17 SFC.MGO = [8.96 8.66 8.53 8.63]/8.53 * 154.4; % SFC for MGO @ 75 % MCR = 154.4 g/kWh from ...
    [#GL_2011a]. Ref. numbers from [#aesoyushakov_2013a] in MJ/kWh.
18 SFC.LNG = [130.1 127.9 126.5 130.9]; % [#GL_2011a]
19
20 % Percent sulphur in the fuels
21 sulphur.HFO = 2.1 ;
22 sulphur.MGO = 0.05;
23 sulphur.LNG = 0 ;
24
25 % Fuel dependent emissions (CO2 and SOx):
26 % CO2 pollutant emission ratio (g CO2/kg fuel)
27 PER.CO2.HFO = 3200; % [#woud_2002a]
28 PER.CO2.MGO = 3200; % [#woud_2002a]
29 PER.CO2.LNG = 2743; % From stoichiometric calc (see report)
30
31 % SOx pollutant emission ratio (g SOx/kg fuel per % S in fuel)
32 PER.SOx.HFO = 20 * sulphur.HFO; % 20 g SOx/kg fuel per % S in fuel (from [#woud_2002a])
33 PER.SOx.MGO = 20 * sulphur.MGO; % [#woud_2002a]
34 PER.SOx.LNG = 20 * sulphur.LNG; % [#woud_2002a]
35
36 % Combustion dependent emissions (NOx and PM):
37 % NOx reference factors for specific emissions (relative values from
38 % [#aesoyushakov_2013a])
39 relativevalues.NOx.HFO = [14.9 12.5 10.9 9.7]/10.9;
40 relativevalues.NOx.MGO = [15.1 12.5 10.4 8.9]/10.4;
41

```

```

42 % NOx base line specific emission values (g NOx/kWh)
43 refvalues.NOx.HFO = 12; % g/kWh, [#aesoystenersen_2013a]
44 refvalues.NOx.MGO = 11; % g/kWh, [#aesoystenersen_2013a]
45 refvalues.NOx.LNG = 5; % g/kWh (from Vilmar)
46
47 % NOx specific emissions (g NOx/kWh)
48 SPE.NOx.HFO = relativevalues.NOx.HFO * refvalues.NOx.HFO;
49 SPE.NOx.MGO = relativevalues.NOx.MGO * refvalues.NOx.MGO;
50 SPE.NOx.LNG = relativevalues.NOx.MGO * refvalues.NOx.LNG;
51
52 % Specific PM emissions (mg/kWh):
53 SPE.PM.HFO = [233 254 267 299]; % [#aesoyushakov_2013a]
54 SPE.PM.MGO = [ 79  76  83 108]; % [#aesoyushakov_2013a]
55 % Taken at 50 and 100 % load:
56 SPE.PM.LNG = [ 10 5]; % (from Vilmar)
57
58 %% Generate polynomial functions for SFC, NOx and PM
59 p_SFC_HFO = polyfit([30 50 75 100], SFC.HFO,2);
60 p_SFC_MGO = polyfit([30 50 75 100], SFC.MGO,2);
61 p_SFC_LNG = polyfit([30 50 75 100], SFC.LNG,2);
62
63 p_NOx_HFO = polyfit(Loadvec, SPE.NOx.HFO,2);
64 p_NOx_MGO = polyfit(Loadvec, SPE.NOx.MGO,2);
65 p_NOx_LNG = polyfit(Loadvec, SPE.NOx.LNG,2);
66
67 p_PM_HFO = polyfit(Loadvec, SPE.PM.HFO,3); % 3poly
68 p_PM_MGO = polyfit(Loadvec, SPE.PM.MGO,2);
69 p_PM_LNG = polyfit([50 100], SPE.PM.LNG,1); % Linear relationship
70
71 %% Save polynomial functions for SCF, NOx and PM, sulphur percentage and PER for later use
72 save('enginedata.mat','p_SFC*','p_NOx*','p_PM*','sulphur','PER','-v7.3');
73
74 %% Plot SFC, NOx and PM over engine load range, save plots (optional)
75 %{
76 % Evaluate polynomials to prepare for plotting
77 x = linspace(20,100);
78
79 sfc_HFO = polyval(p_SFC_HFO,x);
80 sfc_MGO = polyval(p_SFC_MGO,x);
81 sfc_LNG = polyval(p_SFC_LNG,x);
82
83 NOx_HFO = polyval(p_NOx_HFO,x);
84 NOx_MGO = polyval(p_NOx_MGO,x);
85 NOx_LNG = polyval(p_NOx_LNG,x);
86
87 PM_HFO = polyval(p_PM_HFO,x);
88 PM_MGO = polyval(p_PM_MGO,x);
89 PM_LNG = polyval(p_PM_LNG,x);
90
91 clf
92 %{
93 % Plot SFC
94 SFCchange = figure(1);
95 hold on
96 points = plot( [30 50 75 100], SFC.HFO,'x', ...
97               [30 50 75 100], SFC.MGO,'x', ...
98               [30 50 75 100], SFC.LNG,'x');
99
100 poly = plot( x,sfc_HFO,'-', ...
101             x,sfc_MGO,'-', ...
102             x,sfc_LNG,'-');
103
104 xlabel('Engine load %')
105 ylabel('SFC [g/kWh]')
106 legend(poly,'HFO','MGO','LNG','Location','northeast')
107 title('Specific fuel consumption (SFC) for varying engine load')

```



```

108 saveas(SFCchange, 'SFCchange.png')
109 %}
110
111 %{
112 % Plot NOx
113 NOxchange = figure(2);
114 hold on
115 points = plot(Loadvec, SPE.NOx.HFO, 'x', ...
116             Loadvec, SPE.NOx.MGO, 'x', ...
117             Loadvec, SPE.NOx.LNG, 'x');
118
119 poly = plot(x, NOx_HFO, '-', ...
120           x, NOx_MGO, '-', ...
121           x, NOx_LNG, '-');
122
123 xlabel('Engine load %')
124 ylabel('Specific NOx emissions [g/kWh]')
125 legend(poly, 'HFO', 'MGO', 'LNG')
126 title('Specific NOx emissions for varying engine load')
127 saveas(NOxchange, 'NOxchange.png')
128 %}
129
130 %{
131 % Plot PM
132 PMchange = figure(3);
133 hold on; box on; grid on;
134 points = plot(Loadvec, SPE.PM.HFO, 'x', ...
135             Loadvec, SPE.PM.MGO, 'x', ...
136             [50 100], SPE.PM.LNG, 'x');
137
138 poly = plot(x, PM_HFO, '-', ...
139           x, PM_MGO, '-', ...
140           x, PM_LNG, '-');
141
142 xlabel('Engine load %')
143 ylabel('Specific PM emissions [mg/kWh]')
144 legend(poly, 'HFO', 'MGO', 'LNG')
145 title('Specific emissions of particulate matter (PM)')
146 saveas(PMchange, 'PMchange.png')
147 %}
148 %}

```

findice.m

```

1 function [iceT,iceC] = findice(leg,date)
2
3 % FINDICE.m interpolates to determine the ice conditions for a given date
4 % on a certain leg on the NSR. A linear relationship for ice growth is
5 % assumed.
6 %
7 % -----
8 % Outputs:
9 %
10 % iceT      Ice thickness          cm
11 % iceC      Ice concentration      cm
12 %
13 % -----
14 % Inputs:
15 %
16 % leg       Leg number on the icedata vector
17 % date      Current date in serial date
18 %           number format
19 %
20 % -----

```

```

21 % Runa A. Skarb\o | runaaman@stud.ntnu.no | v1.0, 04 Dec 2014
22
23 icedata = load('icedata.mat');
24
25 datevec = icedata.ice_dates;
26 iceTvec = icedata.ice_t;
27 iceCvec = icedata.ice_c;
28
29 if date < datevec(1) || date > datevec(length(datevec))
30     error('Date outside date range for measurements')
31     return
32 end
33
34 % Find closest date to current date
35 [~,idx1] = min(abs(datevec - date));
36
37 % Find other date to interpolate between
38 if date < datevec(idx1)
39     idx2 = idx1 - 1;
40 else
41     idx2 = idx1 + 1;
42 end
43
44 % Find ice conditions for current date
45 iceT = interp1([datevec(idx1), datevec(idx2)], ...
46     [iceTvec(leg,idx1), iceTvec(leg,idx2)], date);
47 iceC = interp1([datevec(idx1), datevec(idx2)], ...
48     [iceCvec(leg,idx1), iceCvec(leg,idx2)], date);
49
50 end

```

hv_input.m

```

1 % HV_INPUT.m generate the input required for HV.m,
2 % - give the input for the script HV.m,
3 % - saves the calculated values from HV.m to the file 'hv.mat',
4 % - plots curves for net thrust, ice resistance and the hv-curve (optional)
5 % - saves plots as png
6
7 clear;
8 %% Give input for the script HV.m
9 load('variables.mat','V_max','Lbp','Loa','B','T');
10
11 V = V_max;
12
13 Lpar = 164.4; % Parallel midbody length, m
14 phi = 40; % Stem angle, deg
15 alpha = 48;
16
17 PB = 13560; % Engine power, kW
18 Dp = 7.5; % Propeller diameter, m.
19 Ke = 0.78*0.9; % Empirical factor for bollard pull (see Juva and Riska, 2002)
20
21 [h, V, Tnet, Ri] = hv(V, Lbp, B, T, Lpar, phi, alpha, PB, Dp, Ke);
22
23 %% Save hv-curve values
24 save('hv.mat','h','V','Tnet','Ri','-v7.3')
25
26 %% Plot curves for net thrust, ice resistance and hv-curve
27 %{
28 clf;
29 % Plot net thrust vs V
30 thrust = figure(1);
31 hold on

```

```

32 handle1 = plot(V,Tnet);
33 xlabel('Speed, kn')
34 ylabel('Net thrust, kN')
35 title('Thrust available to overcome ice resistance')
36
37 % Plot channel ice resistance vs ice thickness
38 ice = figure(2);
39 hold on
40 handle2 = plot(h,Ri);
41 xlabel('Ice thickness, m')
42 ylabel('Resistance, kN')
43 title('Brash ice resistance')
44 %%}
45
46 % h-v curve plot
47 hv = figure(3);
48 hold on
49 plot(V,h);
50 %plot([5 5],ylim,'k','LineStyle','--'); % Lower speed limit
51 xlabel('Speed, kn')
52 ylabel('Ice thickness, m')
53 title('Attainable speed in brash ice')
54
55
56 %}
57 %% Save plots as png
58 %{
59 saveas(thrust,'Tnet','png');
60 saveas(ice,'iceresistance','png');
61 saveas(hv,'hvcurve','png');
62 %}

```

hv.m

```

1 function [H, V, Tnet, Ri] = hv(V,L,B,T,Lpar,phi,alpha,PB,Dp,K)
2
3 % HV.m calculates the ship performance in brash ice. In addition
4 % to the essential data (h & v) for generating ship performance
5 % in ice (h-v) curves, the algorithm can optionally return the
6 % information on net thrust (Tnet) and brash ice resistance (Ri)
7 % for a desired vessel. Finally, computed h-v plot is readily
8 % available.
9 %
10 % The script is based on a Matlab function made by Sandro Erceg for the
11 % Sustainable Arctic Sea Transport module given at Marine Technology
12 % department, NTNU. It was originally made for calculating ship performance
13 % in level ice, and has been edited to only consider performance in brash
14 % ice.
15 %
16 % The algorithm uses one subfunction:
17 % - ice_resistance.m: to compute ship resistance in brash ice according to
18 % the formulation presented by Juva and Riska (2002).
19 %
20 % -----
21 % Outputs: [h, V, Tnet, Ri] + h-v plot
22 %
23 % H          Ice thickness (vector or scalar)          m
24 % V          Attainble speed (vector or scalar)        kn
25 % Tnet       Net thrust vector                        kN
26 % Ri        Brash ice resistance (Juva and Riska, 2002) kN
27 %
28 % h-v plot  Ice thickness vs. Ship speed (h-v) curve
29 %
30 % -----

```

```

31 % Inputs:
32 %
33 % V      Max ship speed in open water      kn
34 %
35 % L      Ship length                        m
36 % B      Ship breadth                      m
37 % T      Ship draft                       m
38 %
39 % Lpar   Parallel midbody length          m
40 % phi    Stem angle at B/4                deg
41 % alpha  Waterline entrance angle         deg
42 %
43 % PB     Engine power                      kW
44 % Dp     Propeller diameter               m
45 % K      Empirical factor for bollard pull
46 %        (see Chapter 6 of Juva and Riska, 2002:
47 %        On the power requirement in the FSICR;
48 %        Research Report No. 53)
49 %
50 % -----
51 % Runa A. Skarb\o | runaaman@stud.ntnu.no | v 1.3 25 Nov 2014
52
53 etas = 0.99;          % Transmission efficiency coefficient
54 PD   = PB*etas;      % Power delivered to the propeller, kW
55
56 Hmin = 0.4; % m (Ri only valid for h >= 0.4 m (Juva and Riska, 2002))
57 Hmax = 2 ; % m
58 h    = linspace(Hmin, Hmax, 200); % Ice thickness vector, m
59 Vvec = linspace(0, V, 200); % Ship speed vector, kn
60 v    = V * 0.5144; % kn to m/s conversion
61 vvec = Vvec * 0.5144; % kn to m/s conversion
62
63 % Net thrust concept (see Juva and Riska, 2002)
64 Tnet = K * (PD*Dp)^(2/3) * (1 - (1/3)*(vvec/v) - (2/3)*(vvec/v).^2); % values in kN
65 p_Tnet = polyfit(Tnet,Vvec,2);
66
67 % Find resistance in ice for different ice thicknesses
68 Ri    = ice_resistance(h, phi, alpha, L, B, T, Lpar);
69 p_Ri = polyfit(h,Ri,2);
70
71 % Find attainable speed for each ice thickness (Tnet = Ri)
72 for i = 1:length(h)
73     % Find Ri for current ice thickness
74     R = polyval(p_Ri,h(i));
75     % Find speed V from R(h(i)) = T(v(i))
76     V(i) = polyval(p_Tnet,R);
77
78     H(i) = h(i);
79     if V(i) < 0
80         V(i) = nan;
81         H(i) = nan;
82     end
83 end
84
85 V = V(isfinite(V));
86 H = H(isfinite(V));
87 Tnet = Tnet(isfinite(V));
88 Ri = Ri(isfinite(V));
89 end

```

ice_resistance.m

```

1 function [Ri] = ice_resistance(H_M, phi2, alpha, L, B, T, Lpar)
2

```

```

3 % ICE_RESISTANCE.m calculates the ice resistance for the case vessel with
4 % the method of Juva and Riska, 2002.
5 %
6 % -----
7 % Outputs: [Ri]
8 %
9 % Ri          Ice resistance in brash ice          kN
10 %
11 % -----
12 % Inputs:
13 %
14 % H_M          Channel brash ice thickness (can be a    cm
15 %              vector or a scalar)
16 % phi2         Stem angle between the bow and the     deg
17 %              waterline at B/4
18 % alpha        Waterline entrance angle              deg
19 % L            Ship length (between perpendiculars)   m
20 % B            Ship breadth                            m
21 % T            Ship draught                           m
22 % Lpar         Length of the parallel midbody at     m
23 %              midships
24 %
25 % -----
26 % Runa A. Skarb\o | runaaman@stud.ntnu.no | v1.0, 04 Nov 2014
27
28
29
30 H_F = 0.26 + (H_M * B).^0.5;
31
32 psi = atan(tan(phi2)/sin(alpha));
33
34 C_mu = 0.15 * cos(phi2) + sin(psi) * sin(alpha);
35 if C_mu < 0.45
36     C_mu = 0.45;
37 end
38
39 C_psi = 0.047 * psi - 2.115;
40 if C_psi < 0
41     C_psi = 0;
42 end
43
44 % For ice classes lower than 1A Super:
45 C1 = 0;
46 C2 = 0;
47
48 C3 = 845.576; % kg/(m^2 s^2)
49 C4 = 41.74; % kg/(m^2 s^2)
50
51 C5 = 825.6; % kg/s
52
53 LTB = (L*T/B^2)^3;
54 if LTB > 20
55     LBT = 20;
56 elseif LTB < 5
57     LTB = 5;
58 end
59
60 Awf = 0.25 * L * B;
61
62 Ri = (C1 + C2 + C3.*(H_F + H_M).^2.*(B + C_psi + H_F).*C_mu + C4*Lpar*H_F.^2 ...
63     + C5*LTB*Awf/L) *10^-3; % kN
64
65 end

```

maindim.m

```

1 % MAINDIM.m define the properties for the case vessel and calculates the open
2 % water resistance using OW_RESISTANCE.m.
3 %
4 % -----
5 % Runa A. Skarb\o | runaaman@stud.ntnu.no | v1.3, 04 Nov 2014
6
7 clear;
8 %% Define vessel dimensions
9 % Input values are read from files defined from Excel.
10 %{
11 % Vessel input
12 [vfile,msg] = fopen('vessel_input.txt','r');
13 vessel_input = fscanf(vfile,
14 status = fclose(vfile);
15
16 % Route input
17 [rfile,msg] = fopen('route_input.txt','r');
18 route_input = fscanf(rfile,
19 status = fclose(rfile);
20 %}
21
22 % Vessel dimensions must me manually defined below until reading is fixed
23
24 % Dimensions
25 Loa = 225 ; % m
26 Lbp = 220 ; % m
27 Lwl = 221 ; % m
28 B = 32.3; % m
29 T = 14.1; % m
30
31 % Weights
32 dwt = 75603; % tonne
33 wls = 14950; % tonne
34
35 GT = 41142;
36 NT = 25265;
37
38 % Speed
39 V_s = 14.5; % kn (service speed)
40 V_max = 15.4; % kn
41
42 % Propeller diameter
43 D_p = 7.5; % m
44
45 voldispl = 88344; % m^3
46 weightdispl = 90553; % tonne
47
48 % Hull coefficients
49 Cb = 0.878;
50 Cm = 0.98 ;
51 Cp = Cb/Cm;
52
53 % Wet surface
54 wetsurf = 2.73 * sqrt(voldispl * Lwl); % m^2
55
56 %% Calculate open water resistance
57 % This section uses the script ow_resistance.m to calculate the open water
58 % resistance for the case ship. The resistance in ice is found with the
59 % script ice_resistance.m.
60
61 % Open water resistance
62 plot_Rt = 0; % = 1 if output plot of Rt, = 0 otherwise
63 plot_coef = 0; % = 1 if output plot of resistance coefficients, = 0 otherwise
64 [V_vec, Row] = ow_resistance(Lwl,B,T,V_max,wetsurf,plot_Rt,plot_coef);
65 clear plot_Rt plot_coef
66

```

```

67 %% Save variables to file 'variables.mat'
68 % This section saves the variables generated in this script, to avoid
69 % running the script at every startup
70 save('shipdata.mat','-v7.3');
71
72 %{
73 %% Calculate resistance in ice
74 % Coefficients for ice resistance calculations:
75 alpha = 48; % deg
76 phi2 = 40; % deg
77 Lpar = 164.4; % m
78 H_M = linspace(0,200); % Ice thickness vector (up to 2 m)
79 Ri = ice_resistance(H_M,phi2,alpha,Lbp,B,T,Lpar);
80
81 %% Map route with /MAPPINGFOLDER/ROUTEDATA.M
82 % This section use the mapping toolbox to generate the route
83 cd mappingfolder
84 routedata
85 cd ..
86 %}

```

ow_resistance.m

```

1 function [V, Rt] = ow_resistance(Lwl,B,T,V_max,S,plot_Rt,plot_coef)
2
3 % OW_RESISTANCE.m calculate open water resistance with Guldhammer-Harvald's
4 % method. The script is made from the approach as described in Amdahl et
5 % al, 2005.
6 %
7 % -----
8 % Outputs: [Rt] (+ Rt-V plot + Ci-V plot optionally)
9 %
10 % Rt          Open water resistance          kN
11 %
12 % Rt-V plot   Open water resistance vs. ship speed
13 % Ci-V plot   Coefficients of resistance vs. ship speed
14 % -----
15 % Inputs:
16 %
17 % Lwl         Ship length (on water line)      m
18 % B           Ship breadth                    m
19 % T           Ship draught                    m
20 % V_max       Max speed                       kn
21 % S           Wet surface                     m^2
22 %
23 % plot_Rt     Binary, = 1 if Rt-V plot desired,
24 %             = 0 otherwise
25 % plot_coef   Binary, = 1 if Ci-V plot desired,
26 %             = 0 otherwise
27 %
28 % -----
29 % Runa A. Skarb\o | runaaman@stud.ntnu.no | v1.4, 04 Nov 2014
30
31 %% Initiation
32 g           = 9.81; % m^2/s
33 rho_sw     = 1025; % kg/m^3
34
35 % Ship speed
36 V = 0:1:ceil(V_max); % kn
37 v = V * 0.5144; % Conversion from kn to m/s
38
39 % Froude's number
40 Fn = v / sqrt(g * Lwl); % [-]
41

```

```

42 % Reynold's number. Kinematic viscosity for water of 5 deg C:
43 Re = v * Lwl / (1.519*10^-6); % [-]
44
45 %% Calculations
46 % Coefficients matrix
47 C = zeros(6,length(Fn));
48
49 % Frictional resistance coefficient (ITTC'57 line):
50 C(1,:) = 0.075 ./ (log10(Re) - 2).^2;
51
52 % Residual resistance coefficient. Values from diagram on p. F-4 of
53 % [#amdahlendal_2005a] for L/voldispl^(1/3) = 5.0 and C_P = 0.8). The
54 % diagram does not display C_R for Fn < 0.15 (V = 14 kn).
55 C(2,2:14) = 0.6*10^-3;
56 C(2,15:17) = [0.79 1.0 1.14]*10^-3;
57
58 % Corrections
59
60 % Scale effects. Table on p. 197 [#amdahlendal_2005a]. Interpolate
61 % between L = 200 and L = 250:
62 C(3,:) = (0 + (Lwl-200)/(250-200)*(-0.2 - 0))*10^-3;
63
64 % B/T corrections
65 C(4,:) = (0.16 * ((B/T) - 2.5))*10^-3;
66
67 % Hull shape. Assumed "normal" hull shape.
68 C(5,:) = 0;
69
70 % Bulbous bow. Table on p. 199 in [#amdahlendal_2005a] for C_P = 0.8.
71 % Interpolate between Fn = 0.15 and 0.18.
72 for i = 2:length(Fn)
73
74     if Fn(i) < 0.15
75         C(6,i) = 0;
76
77     elseif Fn(i) == 15
78         C(6,i) = 0.1*10^-3;
79
80     else
81         C(6,i) = (0.1 + (Fn(i)-0.15)/(0.18-0.15)*(0-0.1))*10^-3;
82
83     end
84 end
85
86 % Zero for all coefficients at v = 0 kn
87 C(:,1) = 0;
88
89 % Total resistance coefficient:
90 C_T = sum(C);
91
92 % Total resistance:
93 Rt = 0.5 * rho_sw * S .* v.^2 .* C_T *10^-3; % kN
94
95 % Frictional resistance:
96 % Rf = 0.5 * rho_sw * S .* (V .* 0.5144).^2 .* C_F;
97
98 %% Plot
99 if plot_Rt == 1 || plot_coef == 1
100     close all
101 end
102
103 % Total resistance plot
104 if plot_Rt == 1
105     rr = figure;
106     plot(V,Rt);
107     title('Open water resistance for the case ship')

```



```

108     xlabel('Speed [kn]')
109     ylabel('Total resistance [kN]')
110     %saveas(rr,'ow_resistance','png')
111 end
112
113 % Plot of coefficients
114 if plot_coef == 1
115
116     % Positive components:
117     fh(1) = figure;
118     hP    = bar(V,C'.*(C '>0)', 'stacked');
119     ahP   = gca;
120
121     % Negative components:
122     fh(2) = figure;
123     hN    = bar(V,C'.*(C '<0)', 'stacked');
124
125     % Total C_T
126     fh(3) = figure;
127     hC    = plot(V(2:length(V)),C_T(2:length(V)), 'k', 'LineWidth', 2.0);
128
129     % Clean up
130     set([hP,hN,hC], 'parent', ahP);
131     close(fh(2));close(fh(3));
132
133     axis([0 17 -0.3*10^-3 4*10^-3]);
134     xlabel('Speed [kn]')
135     ylabel('C_i [-]')
136     title('Frictional coefficients for determining open water resistance for the case ship')
137     legend('C_F, frictional','C_R, residual','C_{scale}, scale effects', ...
138           'C_{BT}, breadth/draught relationship', 'C_{frame}, frame shape', ...
139           'C_{bulb}, bulbous bow', 'Location', 'north')
140     %saveas(fh(1),'resistance_coef','png')
141 end

```

read_ice.m

```

1 function[] = read_ice()
2
3 % READ_ICE.m reads the ice condition and thickness data from the
4 % Excel-files 'icedata_ct.xlsx' and 'icedata_thicknesses.xlsx' and saves
5 % the data in variables. Also, the coordinates for the ice data and the
6 % dates are stored in separate vectors. The data is saved for later use in
7 % the simulations.
8
9 cd data
10 ice_coord = xlsread('icedata_ct.xlsx',1,'A4:B103'); % N, E, in decimals
11 [n, dates] = xlsread('icedata_ct.xlsx',1,'E3:AF3'); % dates in date format
12 formatIn = 'dd.mm.yyyy';
13 ice_dates = datenum(dates,formatIn);
14
15 % Read ice data (lower limit)
16 datarange = 'E4:AF103';
17 ice_c = xlsread('icedata_ct.xlsx',2,datarange); % given in percent
18 ice_t = xlsread('icedata_thicknesses.xlsx',2,datarange); % given in cm
19 cd ..
20
21 % Save data
22 save('icedata.mat','ice_coord','ice_dates','ice_c','ice_t','-v7.3');
23
24 end

```

routedata.m

```

1 % ROUTEDATA.m imports route data from files. The data is saved as geopoint
2 % vectors. The script requires the Mapping Toolbox. Routes can also be
3 % plotted (optional).
4 %
5 % Requirements:
6 % - Mapping Toolbox
7
8 %% Import route data
9 % Import route data from .gpx files in the 'data' directory
10 cd data
11 % The gpxread function returns an n-by-1 geopoint vector where n is the
12 % number of waypoints or points that define a route or track
13 route.NSR = gpxread('NSR_waypoints.gpx');
14 route.SCR = gpxread('SCR_waypoints.gpx');
15 cd ..
16
17 % Flip and start routes in Murmansk (not Tianjin)
18 route.NSR = flipud(route.NSR);
19 route.SCR = flipud(route.SCR);
20
21 %% Save route data coords as double (to access coordinates without Mapping Toolbox)
22 route.legcoordinates.NSR = [route.NSR.Latitude; route.NSR.Longitude]';
23 route.legcoordinates.SCR = [route.SCR.Latitude; route.SCR.Longitude]';
24
25 %% Replace NSR Arctic coordinates with ice data points
26 icedata = load('icedata.mat');
27 coord.CapeKaninNos = [68.8 43.2];
28
29 % Find ice data points east of CKN
30 i_startice = find(icedata.ice_coord(:,2) > coord.CapeKaninNos(2)); % Find indexes
31 i_startice = i_startice(1); % Index of first point east of CKN
32
33 % Find route data points east of CKN
34 i_startroute = find(route.legcoordinates.NSR(:,2) > coord.CapeKaninNos(2)); % Find indexes
35 i_startroute = i_startroute(1); % Index of first point on route after CKN
36
37 % Find route data points south of ice data
38 coord.stopice = icedata.ice_coord(length(icedata.ice_coord),:); % Coordinates of last ice ...
39 % data point
40 i_stoprout = find(route.legcoordinates.NSR(:,1) < coord.stopice(1)); % Indexes of points ...
41 % on route south of last ice data point
42 i_stoprout = i_stoprout(1)-1; % Index of last point on route before south of ice area
43
44 % All points from i_startroute to (and including) i_stoprout to be
45 % replaced by ice data points
46
47 % Replace route coordinates between these points with ice data coordinates
48 coordsbefore = route.legcoordinates.NSR([1:i_startroute-1],:);
49 coordsmiddle = icedata.ice_coord;
50 coordsafter = route.legcoordinates.NSR([i_stoprout+1:length(route.legcoordinates.NSR)],:);
51
52 route.legcoordinates.NSRnew = [coordsbefore; ...
53 %                               coordsmiddle; ...
54 %                               coordsafter];
55
56 %% Find the geographic properties of the routes
57
58 % Get port coordinates
59 coord.Murmansk = [route.NSR(1).Latitude route.NSR(1).Longitude];
60 coord.Tianjin = [route.NSR(length(route.NSR)).Latitude ...
61 %               route.NSR(length(route.NSR)).Longitude];
62
63 % Find course and distance for each leg
64 [course.NSRnew, dist.NSRnew] = legs(route.legcoordinates.NSRnew);
65 [course.SCR, dist.SCR] = legs(route.SCR.Latitude, route.SCR.Longitude);
66
67
68
69
70
71
72
73
74
75
76
77
78
79
80
81
82
83
84
85
86
87
88
89
90
91
92
93
94
95
96
97
98
99

```

```

64 dist.NSRtot = sum(dist.NSRnew);
65 dist.SCRtot = sum(dist.SCR);
66
67 %% Save route data in file 'routedata.mat'
68 save('routedata.mat','route','coord','dist','i_startice','i_startroute','-append','-v7.3'); ...
    % append, routegen.m also writes to 'routedata.mat'
69
70 %% Plot routes data in map
71 % Comment out to plot:
72 %{
73 % Generate map
74 routes = worldmap([ 0 80], ...
75                 [-15 -165]);
76 title('Generated routes for the case vessel')
77
78 % Display coast lines
79 %load coast
80 %plotm(lat, long,'Color','blue')
81
82 % Display land areas as black
83 geoshow('landareas.shp','FaceColor','black')
84
85 % Display topography
86 % load topo
87 % geoshow(topo, topolegend, 'DisplayType', 'texturemap')
88 % demcmap(topo)
89
90 % Plot routes
91 r1 = geoshow(route.NSR.Latitude, route.NSR.Longitude, 'DisplayType', 'line', ...
92             'Color', 'r', 'LineWidth', 1.5);
93 r2 = geoshow(route.SCR.Latitude, route.SCR.Longitude, 'DisplayType', 'line', ...
94             'Color', 'b', 'LineWidth', 1.5, 'LineStyle', '--');
95 legend([r1 r2], 'Northern Sea Route', 'Suez Canal Route', 'Location', 'best')
96
97 % Plot cities
98 geoshow(coord.Murmansk(1), coord.Murmansk(2), 'DisplayType', 'point', ...
99         'MarkerEdgeColor', 'y', 'MarkerFaceColor', 'auto', 'Marker', 'o')
100 geoshow(coord.Tianjin(1), coord.Tianjin(2), 'DisplayType', 'point', ...
101         'MarkerEdgeColor', 'y', 'MarkerFaceColor', 'auto', 'Marker', 'o')
102
103 % Label cities
104 textm(coord.Murmansk(1)-12, coord.Murmansk(2)-10, 'Murmansk', 'BackgroundColor', 'w')
105 textm(coord.Tianjin(1)+7, coord.Tianjin(2)-15, 'Tianjin', 'BackgroundColor', 'w')
106
107 % Uncomment to save map as .png-file
108 %saveas(routes, 'routes', 'png')
109 %}

```

sail_ice.m

```

1 function [T, fc, emissions, energy] = sail_ice(distance, ice_c, h, fueltype)
2
3 % SAIL_ICE.m calculates time, fuel consumption and emissions for a given
4 % leg in ice on a route. The leg is divided in an open water and an ice
5 % part, as weighted by the ice concentration. The output is found
6 % separately for the open water and the ice part, and then summed in the
7 % end.
8 %
9 % -----
10 % Input
11 %
12 % distance      Sailing distance          nm
13 % ice_c         Ice concentration         percent
14 % h             Ice thickness              cm

```

```

15 % fueltype    Type of fuel used on leg (HFO, MGO or
16 %            LNG), input as string
17 %
18 % -----
19 % Output
20 %
21 % T          Total sailing time on leg          days
22 % fuelcons   Total fuel consumption on leg     tonnes
23 % emissions  Total emissions of CO2, SOx, NOx and tonnes
24 %            PM for the whole leg
25 % energy     Energy consumption for leg        kWh
26 % -----
27 % Runa A. Skarb\o | runaaman@stud.ntnu.no | v1.2 03 Dec 2014
28
29 % Vessel info
30 V_s = 14.5; % kn
31 PB = 13560; % Brake power, kW
32 etas = 0.99; % Transmission efficiency coefficient
33 PD = etas * PB; % Power delivered to the propeller, kW
34
35 % If ice thickness < 40 cm or no ice, open water sailing is assumed
36 if (h < 40) || (ice_c == 0)
37     [T, fc, emissions, energy] = sail_ow(V_s, distance, fueltype);
38     return
39 end
40
41 % Distance sailed in ice and ow
42 dist_ice = (ice_c/100) * distance;
43 dist_ow = (1-(ice_c/100)) * distance;
44
45 %% Open water sailing
46 emissions_ow = zeros(1,4);
47 [T_ow, fc_ow, emissions_ow(:), energy_ow] = sail_ow(V_s, dist_ow, fueltype);
48
49 %% Sailing in ice
50 hvdata = load('hv.mat');
51 shipdata = load('shipdata.mat');
52
53 % Ice sailing on leg
54 V_ice = interp1(hvdata.h, hvdata.V, h/100, 'cubic');
55 if V_ice < 3
56     error(sprintf('Speed in ice below minimum requirement of 3 knots, V = %2.0f for h = ...
57                 %2.0f cm"',V_ice,h));
58 elseif V_ice > V_s
59     error(sprintf('Speed in ice above service speed, V = %2.0f',V_ice));
60     return
61 end
62 T_ice = dist_ice / V_ice; % hrs
63
64 % Resistance
65 R_ice = interp1(hvdata.h, hvdata.Ri, h/100, 'cubic'); % kN
66 R_ow = interp1(shipdata.V_vec, shipdata.Row, V_ice, 'cubic'); % kN
67 R_tot = R_ow + R_ice; % kN
68
69 % Required power
70 PE = R_tot * (V_ice * 0.5144); % Convert V to m/s. Pe [kW]
71 %PE = R_tot * convvel(V_ice, 'kts','m/s'); % kW
72
73 % MCR
74 MCR = PE / PB * 100; % percent
75 if MCR < 0 || MCR > 100
76     error(sprintf('MCR out of range: MCR = %2.0f. Must be between 0 and 100 %%.',MCR));
77     return
78 end
79

```

```

80 % Energy used on ice part of leg
81 energy_ice = PE * T_ice; % kWh
82
83 % Find SFC for fuel type
84 SFCvar = sprintf('p_SFC_%s', fueltype);
85 engdata = load('enginedata.mat');
86 SFC_ice = polyval(engdata.(SFCvar), MCR); % g/kWh
87
88 % Fuel consumption on leg
89 fc_ice = energy_ice * SFC_ice * 10^-3; % kg fuel
90
91 % Emissions from ice part of leg
92 emissions_ice(:, :) = emissions_calc(fc_ice, energy_ice, MCR, fueltype); % [g g g mg] [CO2 ...
    SOx NOx PM]
93
94 %% Total (incl conversions)
95 T = T_ow + T_ice / 24; % days
96 fc = fc_ow + fc_ice * 10^-3; % tonnes
97 emissions_ice(4) = emissions_ice(4) * 10^-3; % tonnes PM
98 emissions = emissions_ow + emissions_ice * 10^-6; % tonnes
99
100 energy = energy_ice + energy_ow; % kWh
101
102 end

```

sail_ow.m

```

1 function [T, fuelcons, emissions, energy] = sail_ow(V, distance, fueltype)
2
3 % SAIL_OW.m calculates time, fuel consumption and emissions for a given
4 % open water leg on a route. The speed is fixed for the whole leg.
5 %
6 % -----
7 % Input
8 %
9 % V          Sailing speed (constant on leg)          kn
10 % distance   Sailing distance                          nm
11 % fueltype   Type of fuel used on leg (HFO, MGO or
12 %           LNG), input as string
13 %
14 % -----
15 % Output
16 %
17 % T          Total sailing time on leg                  days
18 % fuelcons   Total fuel consumption on leg              tonnes
19 % emissions  Total emissions of CO2, SOx, NOx and
20 %           PM for the whole leg                       tonnes
21 % energy     Energy consumption for leg                 kWh
22 %
23 % -----
24 % Runa A. Skarb\o | runaaman@stud.ntnu.no | v1.1 28 Nov 2014
25
26 PB = 13560; % Brake power, kW
27 etas = 0.99; % Transmission efficiency coefficient
28 PD = etas * PB; % Power delivered to the propeller, kW
29
30 % Sailing time on leg
31 T = distance / V; % hrs
32
33 ship = load('shipdata.mat');
34
35 % Resistance at given speed interpolated from total resistance curve
36 R = interp1(ship.V_vec, ship.Row, V); % kN
37

```

```

38 % Necessary power to attain given speed
39 PE = R * (V * 0.5144); % Convert V to m/s. Pe [kW]
40 %PE = R * convvel(V, 'kts','m/s'); %kW
41
42 % Total energy used on leg
43 energy = PE * T; % kWh
44
45 % Engine load
46 MCR = PE/PB * 100; % percent
47 if MCR < 0 || MCR > 100
48     error(sprintf('MCR out of range: MCR = %2.0f. Must be between 0 and 100 %%.',MCR));
49     return
50 end
51
52 % Find SCR for fuel type
53 SFCvar = sprintf('p_SFC_%s', fueltype);
54 eng = load('enginedata.mat');
55 SFC = polyval(eng.(SFCvar), MCR); % g/kWh
56
57 % Fuel consumption on leg
58 fuelcons = energy * SFC * 10^-3; % kg fuel
59
60 % Emissions on leg
61 emissions(:, :) = emissions_calc(fuelcons, energy, MCR, fueltype); % [g g g mg] [CO2 SOx NOx PM]
62
63 % Conversion
64 T = T / 24; % days
65 fuelcons = fuelcons * 10^-3; % tonnes
66 emissions = emissions * 10^-6; % tonnes
67 emissions(4) = emissions(4) * 10^-3; % tonnes PM
68
69 end

```

sailNSR.m

```

1 % SAILNSR.m is a part of the SIMULATE_SAILING.m-script. It simulates the
2 % sailing on the NSR route.
3
4 numtrips = numtrips + 1;
5
6 voyagefc = struct;
7 voyagefc.(burnfuel) = zeros(1,2);
8 voyagefc.(burnECAFuel) = zeros(1,2);
9 voyageem = zeros(2,4);
10 cumdist = 0;
11
12 route = 'NSRnew';
13 forindex = (1:length(routedata.dist.(route)));
14
15 % Check for which direction the vessel sails. If sails from
16 % Tianjin to M, the for loop shall count backwards:
17 port = char(posvec(pos));
18 switch port
19     case 'Tianjin'
20         forindex = flipud(forindex);
21 end
22
23 starttime = time;
24
25 for j = forindex % for all legs
26     fueltype = burnfuel;
27     distance = routedata.dist.NSRnew(j);
28
29     % Determine ice conditions on leg

```

```

30 if j >= routeicestartidx && j <= (routeicestartidx + numicelegs) % vessel is on an ice leg
31   iceidx = j - routeicestartidx + icestartidx;
32   [iceT,iceC] = findice(iceidx,time);
33   if iceT > h_maxpossible
34     error(sprintf('Ice too thick to sail (h = %2.0f cm at leg %2.0f (N%2.2f ...
35         E%2.2f), on the %s)',iceT,j,route(j,1),route(j,2),datestr(time,1)));
36     return
37   end
38 else % vessel is outside ice area
39   iceT = 0;
40   iceC = 0;
41 end
42 % Determine use of ECA technology
43 if (~ismember(j, routedata.ECA.NSRI) && ismember(j+1, routedata.ECA.NSRI)) || ... % ...
44     vessel not in ECA, but enters on next leg (must switch on this leg) OR
45     (ismember(j, routedata.ECA.NSRI) && ismember(j+1, routedata.ECA.NSRI)) || ... % ...
46     vessel is in ECA and next leg is also in ECA (use ECA tech) OR
47     (ismember(j, routedata.ECA.NSRI) && ~ismember(j+1, routedata.ECA.NSRI)) % ...
48     vessel is in ECA and next leg is not in ECA (switch when outside ECA)
49   fueltype = burnECAfuel;
50   SOxtech = scenarios.(scenarioname).SOxtech;
51   NOxtech = scenarios.(scenarioname).NOxtech;
52 else % vessel is outside ECA
53   SOxtech = 'none';
54   NOxtech = 'none';
55 end
56 % Simulate sailing on leg
57 [t_leg, fc_before, emissions_before, energy] = sail_ice(distance, iceC, iceT, fueltype);
58 % Change in fc due to abatement technologies (if no
59 % technology, then change is defined as 0 % in input
60 % file)
61 fc_after = fc_before * (1+0.01 * (atechdata.(NOxtech).addfc + ...
62     atechdata.(SOxtech).addfc));
63 % Reduction of emissions due to abatement technologies
64 % CO2
65 emissions_after(1) = emissions_before(1);
66 % SOx
67 emissions_after(2) = emissions_before(2) * (1+0.01 * ...
68     (atechdata.(SOxtech).SOxred) + atechdata.(NOxtech).SOxred);
69 %NOx
70 emissions_after(3) = emissions_before(3) * (1+0.01 * ...
71     (atechdata.(SOxtech).NOxred + atechdata.(NOxtech).NOxred));
72 %PM
73 emissions_after(4) = emissions_before(4) * (1+0.01 * ...
74     (atechdata.(SOxtech).PMred + atechdata.(NOxtech).PMred));
75 % In case of negative emissions
76 for i = 2:length(emissions_after)
77   if emissions_after(i) < 0
78     emissions_after(i) = 0;
79   end
80 end
81 % Save sailing info for leg
82 simulationresults.(scenarioname).tourdata(numtrips).legdata(j).time ...
83     = t_leg;
84 simulationresults.(scenarioname).tourdata(numtrips).legdata(j).fuelconsumption.(fueltype) ...
85     = [fc_before, fc_after];
86 simulationresults.(scenarioname).tourdata(numtrips).legdata(j).emissions ...

```

```

        = [emissions_before; emissions_after];
90  simulationresults.(scenarioname).tourdata(numtrips).legdata(j).energy ...
        = energy;
91  simulationresults.(scenarioname).tourdata(numtrips).legdata(j).iceT ...
        = iceT;
92  simulationresults.(scenarioname).tourdata(numtrips).legdata(j).iceC ...
        = iceC;
93
94  % Save cumulative info for voyage
95  voyageem = voyageem + ...
        simulationresults.(scenarioname).tourdata(numtrips).legdata(j).emissions;
96  voyagefc.(fueltype) = voyagefc.(fueltype) + ...
        simulationresults.(scenarioname).tourdata(numtrips).legdata(j).fuelconsumption.(fueltype);
97  cumdist = cumdist + distance;
98
99  % Cumulative time for simulations
100 time = time + t_leg;
101 end
102
103 % Save sailing info for voyage
104 simulationresults.(scenarioname).tourdata(numtrips).route = route;
105 simulationresults.(scenarioname).tourdata(numtrips).starttime = starttime;
106 simulationresults.(scenarioname).tourdata(numtrips).endtime = time;
107 simulationresults.(scenarioname).tourdata(numtrips).duration = time - starttime;
108 simulationresults.(scenarioname).tourdata(numtrips).startpos = char(posvec(pos));
109 simulationresults.(scenarioname).tourdata(numtrips).emissions = voyageem;
110
111 % If fuel in ECA is same as outside ECA
112 if strcmp(burnfuel,burnECAFuel)
113     % Data for voyage
114     simulationresults.(scenarioname).tourdata(numtrips).fuelconsumption.(burnfuel) = ...
        voyagefc.(burnfuel);
115     % Cumulative data for scenario
116     scenariofc.(burnfuel) = scenariofc.(burnfuel) + voyagefc.(burnfuel);
117 else
118     % Data for voyage
119     simulationresults.(scenarioname).tourdata(numtrips).fuelconsumption.(burnfuel) = ...
        voyagefc.(burnfuel);
120     simulationresults.(scenarioname).tourdata(numtrips).fuelconsumption.(burnECAFuel) = ...
        voyagefc.(burnECAFuel);
121
122     % Cumulative data for scenario
123     scenariofc.(burnfuel) = scenariofc.(burnfuel) + voyagefc.(burnfuel);
124     scenariofc.(burnECAFuel) = scenariofc.(burnECAFuel) + voyagefc.(burnECAFuel);
125 end
126
127 % Other cumulative data for scenario
128 scenarioem = scenarioem + voyageem;
129
130 % Change position and keep inventory
131 switch pos
132     case 1
133         tripsMT = tripsMT + 1;
134         pos = 2;
135     otherwise
136         tripsTM = tripsTM + 1;
137         pos = 1;
138 end

```

sailSCR.m

```

1 % SAILSCR.m is a part of the SIMULATE_SAILING.m-script. It simulates the
2 % sailing on the SCR route.
3 %%{

```



```

4
5 numtrips = numtrips + 1;
6
7 voyagefc = struct;
8 voyagefc.(burnfuel) = zeros(1,2);
9 voyagefc.(burnECAfuel) = zeros(1,2);
10 voyageem = zeros(2,4);
11 cumdist = 0;
12
13 route = 'SCR';
14 forindex = (1:length(routedata.dist.(route)));
15
16 % Check for which direction the vessel sails. If sails from
17 % Tianjin to M, the for loop shall count backwards:
18 port = char(posvec(pos));
19 switch port
20     case 'Tianjin'
21         forindex = flipud(forindex);
22     end
23
24 starttime = time;
25
26 for k = forindex
27     fueltype = burnfuel;
28     distance = routedata.dist.SCR(k);
29
30     % Determine use of ECA technology (NOTE! ONLY SECA ON SCR)
31     if (~ismember(k, routedata.ECA.SCRi) && ismember(k+1, routedata.ECA.SCRi)) || ... % ...
32         vessel not in ECA, but enters on next leg (must switch on this leg) OR
33         (ismember(k, routedata.ECA.SCRi) && ismember(k+1, routedata.ECA.SCRi)) || ... % ...
34         vessel is in ECA and next leg is also in ECA (use ECA tech) OR
35         (ismember(k, routedata.ECA.SCRi) && ~ismember(k+1, routedata.ECA.SCRi)) % ...
36         vessel is in ECA and next leg is not in ECA (switch when outside ECA)
37         fueltype = burnECAfuel;
38         SOxtech = scenarios.(scenarioname).SOxtech;
39     else % vessel is outside ECA
40         SOxtech = 'none';
41     end
42
43     % Determine speed limits on leg
44     if routedata.speedlim.(route)(k) > 0
45         V_leg = routedata.speedlim.(route)(k);
46     else
47         V_leg = shipdata.V_s;
48     end
49
50     % Simulate sailing on leg
51     [t_leg, fc_before, emissions_before, energy] = sail_ow(V_leg, distance, fueltype);
52
53     % Change in fc due to abatement technologies (if no
54     % technology, then change is defined as 0 % in input
55     % file)
56     fc_after = fc_before * (1+0.01 * atechdata.(SOxtech).addfc);
57
58     % Reduction of emissions due to abatement technologies
59     % CO2
60     emissions_after(1) = emissions_before(1);
61
62     % SOx
63     emissions_after(2) = emissions_before(2) * (1+0.01 * atechdata.(SOxtech).SOxred);
64
65     %NOx
66     emissions_after(3) = emissions_before(3) * (1+0.01 * atechdata.(SOxtech).NOxred);
67
68     %PM

```

```

67     emissions_after(4) = emissions_before(4) * (1+0.01 * atechdata.(SOxtech).PMred);
68
69     % In case of negative emissions
70     for i = 2:length(emissions_after)
71         if emissions_after(i) < 0
72             emissions_after(i) = 0;
73         end
74     end
75
76     % Save sailing info for leg
77     simulationresults.(scenarioname).tourdata(numtrips).legdata(k).time ...
78         = t_leg;
79     simulationresults.(scenarioname).tourdata(numtrips).legdata(k).fuelconsumption.(fueltype) ...
80         = [fc_before, fc_after];
81     simulationresults.(scenarioname).tourdata(numtrips).legdata(k).emissions ...
82         = [emissions_before; emissions_after];
83     simulationresults.(scenarioname).tourdata(numtrips).legdata(k).energy ...
84         = energy;
85
86     % Save cumulative info for voyage
87     voyageem = voyageem + ...
88         simulationresults.(scenarioname).tourdata(numtrips).legdata(k).emissions;
89     voyagefc.(fueltype) = voyagefc.(fueltype) + ...
90         simulationresults.(scenarioname).tourdata(numtrips).legdata(k).fuelconsumption.(fueltype);
91     cumdist = cumdist + distance;
92
93     % Cumulative time for simulations
94     time = time + t_leg;
95 end
96
97 % Save sailing info for voyage
98 simulationresults.(scenarioname).tourdata(numtrips).route = route;
99 simulationresults.(scenarioname).tourdata(numtrips).starttime = ...
100     starttime;
101 simulationresults.(scenarioname).tourdata(numtrips).endtime = time;
102 simulationresults.(scenarioname).tourdata(numtrips).duration = time ...
103     - starttime;
104 simulationresults.(scenarioname).tourdata(numtrips).startpos = ...
105     char(posvec(pos));
106 simulationresults.(scenarioname).tourdata(numtrips).emissions = voyageem;
107
108 % If fuel in ECA is same as outside ECA
109 if strcmp(burnfuel,burnECAfuel)
110     % Data for voyage
111     simulationresults.(scenarioname).tourdata(numtrips).fuelconsumption.(burnfuel) = ...
112         voyagefc.(burnfuel);
113     % Cumulative data for scenario
114     scenariofc.(burnfuel) = scenariofc.(burnfuel) + voyagefc.(burnfuel);
115 else
116     % Data for voyage
117     simulationresults.(scenarioname).tourdata(numtrips).fuelconsumption.(burnfuel) = ...
118         voyagefc.(burnfuel);
119     simulationresults.(scenarioname).tourdata(numtrips).fuelconsumption.(burnECAfuel) = ...
120         voyagefc.(burnECAfuel);
121
122     % Cumulative data for scenario
123     scenariofc.(burnfuel) = scenariofc.(burnfuel) + voyagefc.(burnfuel);
124     scenariofc.(burnECAfuel) = scenariofc.(burnECAfuel) + voyagefc.(burnECAfuel);
125 end
126
127 % Other cumulative data for scenario
128 scenarioem = scenarioem + voyageem;
129
130 % Change position and keep inventory
131 switch pos
132     case 1

```

```

121         tripsMT = tripsMT + 1;
122         pos = 2;
123     otherwise
124         tripsTM = tripsTM + 1;
125         pos = 1;
126 end
127 %}

```

scenarios.m

```

1 % SCENARIOS.m define the input variables for the different emission
2 % abatement scenarios for the simulations.
3 clear;
4
5 % Define which fuels and technologies are used in ECAs for the different
6 % scenarios
7 basecase.fuel = 'HFO';
8 basecase.ECAfuel = 'MGO';
9 basecase.SOxtech = 'none'; % fuel switch
10 basecase.NOxtech = 'none';
11
12 scenone.fuel = 'HFO';
13 scenone.ECAfuel = 'HFO';
14 scenone.SOxtech = 'scrubber';
15 scenone.NOxtech = 'SCRe'; % SCRe = selective catalytic reduction
16
17 scentwo.fuel = 'HFO';
18 scentwo.ECAfuel = 'MGO';
19 scentwo.SOxtech = 'none'; % fuel switch
20 scentwo.NOxtech = 'SCRe';
21
22 scenthree.fuel = 'HFO';
23 scenthree.ECAfuel = 'LNG';
24 scenthree.SOxtech = 'LNGconv'; % fuel switch
25 scenthree.NOxtech = 'EGR';
26
27 % Save to file
28 save('scenarios.mat', '-v7.3');

```

simulate_sailing.m

```

1 % SIMULATE_SAILING.m simulates the sailing for the whole time period. It
2 % considers ECA areas, choice of route and sailing in ice.
3 %
4 % -----
5 % Runa A. Skarb\o | runaaman@stud.ntnu.no | v 1.9 11 Dec 2014
6
7 clear; clc;
8 %% Load relevant files
9 icedata = load('icedata.mat');
10 hvdata = load('hv.mat');
11 shipdata = load('shipdata.mat');
12 routedata = load('routedata.mat');
13 scenarios = load('scenarios.mat');
14 costsdata = load('costs.mat');
15 atechdata = load('abatementtech.mat');
16
17 %% Initial and boundary conditions
18 % Time period (in serial date number format (number of days))
19 startsimtime = icedata.ice_dates(1);
20 %{
21 endsimtime = icedata.ice_dates(length(icedata.ice_dates));

```

```

22 duration = endsimtime - startsimtime;
23 %}
24 % Change duration to one year (not measurements)
25 duration = 365; % days
26 endsimtime = startsimtime + duration;
27
28 % Find max ice thickness that the vessel can do 3 kn
29 min_speed = 3; % kn
30 h_maxpossible = interp1(hvdata.V, hvdata.h, min_speed, 'cubic') * 100; % cm
31
32 % Determine when the vessel can sail NSR
33 maxiceT = max(icedata.ice_t); % Max ice thickness along route for each date
34 cansailNSR = (maxiceT <= h_maxpossible); % Find for which measured dates vessel can sail
35
36 % Interpolate to find when must stop sailing NSR (when maxiceT > maxiceTpossible)
37 startcount = 0;
38 stopcount = 0;
39 for j = 1:length(cansailNSR)-1
40     if ~cansailNSR(j) && cansailNSR(j+1) % If ice thickness declines
41         startcount = startcount + 1;
42         startsaildate(startcount) = ceil(interp1(maxiceT(j:j+1), ...
43             icedata.ice_dates(j:j+1), ...
44             h_maxpossible, ...
45             'linear'));
46     elseif cansailNSR(j) && ~cansailNSR(j+1) % If ice thickness grows
47         stopcount = stopcount + 1;
48         stopsaildate(stopcount) = floor(interp1(maxiceT(j:j+1), ...
49             icedata.ice_dates(j:j+1), ...
50             h_maxpossible, ...
51             'linear'));
52     end
53 end
54
55 % Find legs on NSR with ice
56 icestartidx = routedata.i_startice; % index of ice vector where ice starts
57 numicelegs = length(icedata.ice_coord) - icestartidx; % number of legs with ice
58 routeicestartidx = routedata.i_startroute; % index of NSR route vector (new) where ice starts
59
60 % Define scenario for simulation
61 possiblescenarios = cellstr({'basecase', 'scenone', 'scentwo', 'scenthree'});
62
63 % Position vector for ship
64 posvec = cellstr({'Murmansk', 'Tianjin'});
65
66 % Annualisation factor
67 r = costsdata.discontrate * 0.01;
68 FAP = (r * (1 + r)^costsdata.lifespan) / ((1 + r)^(costsdata.lifespan - 1));
69
70
71 %% Sailing simulations
72
73 % Create empty structure array to save results
74 simulationresults = struct;
75
76 for scenarionumber = 1:length(possiblescenarios) % For each scenario
77
78     % Initiation
79     tic;
80     tripsMT = 0;
81     tripsTM = 0;
82     numtrips = 0;
83
84     % Start position Murmansk for each scenario
85     pos = 1;
86
87     % Current scenario specifications

```

```

88     scenarioname = char(possiblescenarios(scenarionumber));
89     burnfuel = scenarios.(scenarioname).fuel;
90     burnECAfuel = scenarios.(scenarioname).ECAfuel;
91
92     % Set time counter to start of time period
93     time = startsimtime;
94
95     % Create variables for saving scenario data
96     scenariofc = struct;
97     scenariofc.(burnfuel) = zeros(1,2);
98     scenariofc.(burnECAfuel) = zeros(1,2);
99     scenarioem = zeros(2,4);
100
101     if ~strcmp(scenarioname,'basecase') % All scenarios except base case
102
103         while time < stopsaildate % sail NSR in the allowed operation window
104             sailNSR;
105         end
106
107         % Save total number of trips on NSR
108         simulationresults.(scenarioname).totals.trips.NSR = numtrips;
109
110         % When time > stopsaildate, the vessel sails only on the SCR
111         % for the rest of the time period. The results from sailing the SCR
112         % is constant. Therefore, only one simulation is performed.
113         sailSCR;
114
115     else % for base case scenario only
116         sailSCR;
117
118         simulationresults.(scenarioname).totals.trips.NSR = 0;
119
120     end
121
122     % Find number of times the scenario sails the SCR
123     remainingtime = endsimtime - time; % time remaining in simulation time period
124     sailtimeSCR = simulationresults.(scenarioname).tourdata(numtrips).duration;
125     remainingtrips = remainingtime / sailtimeSCR;
126
127     % Save totals for each voyage in the scenario
128     simulationresults.(scenarioname).totals.trips.SCR = 1 + remainingtrips;
129     simulationresults.(scenarioname).totals.trips.total = ...
130         simulationresults.(scenarioname).totals.trips.SCR + ...
131         simulationresults.(scenarioname).totals.trips.NSR;
132     switch scenarionumber
133     case 1
134         simulationresults.(scenarioname).totals.emissions = voyageem * ...
135             simulationresults.(scenarioname).totals.trips.SCR;
136     otherwise
137         simulationresults.(scenarioname).totals.emissions = scenarioem + voyageem * ...
138             remainingtrips;
139     end
140
141     % If ECA fuel = normal fuel
142     if strcmp(burnfuel,burnECAfuel)
143         simulationresults.(scenarioname).totals.fuelconsumption.(burnfuel) = ...
144             scenariofc.(burnfuel);
145
146         simulationresults.(scenarioname).totals.costs.fuel.(burnfuel) = ...
147             costsdata.fuelprice.(burnfuel) * scenariofc.(burnfuel);
148
149         simulationresults.(scenarioname).totals.costs.fuel.totalfuelcost = ...
150             simulationresults.(scenarioname).totals.costs.fuel.(burnfuel);
151     else
152         simulationresults.(scenarioname).totals.fuelconsumption.(burnfuel) = ...
153             scenariofc.(burnfuel);

```

```

146     simulationresults.(scenarioname).totals.fuelconsumption.(burnECAfuel) = ...
        scenariofc.(burnECAfuel);
147
148     simulationresults.(scenarioname).totals.costs.fuel.(burnfuel) = ...
        costsdata.fuelprice.(burnfuel) * scenariofc.(burnfuel);
149     simulationresults.(scenarioname).totals.costs.fuel.(burnECAfuel) = ...
        costsdata.fuelprice.(burnECAfuel) * scenariofc.(burnECAfuel);
150
151     simulationresults.(scenarioname).totals.costs.fuel.totalfuelcost = ...
        simulationresults.(scenarioname).totals.costs.fuel.(burnfuel) + ...
        simulationresults.(scenarioname).totals.costs.fuel.(burnECAfuel);
152 end
153
154 % Find costs
155 simulationresults.(scenarioname).totals.costs.capex = ...
        costsdata.capex.(scenarios.(scenarioname).SOxtech) + ...
        costsdata.capex.(scenarios.(scenarioname).NOxtech);
156 simulationresults.(scenarioname).totals.costs.fees = (costsdata.fee.SuezCanal * ...
        simulationresults.(scenarioname).totals.trips.SCR) + (costsdata.fee.NSR * ...
        simulationresults.(scenarioname).totals.trips.NSR);
157 simulationresults.(scenarioname).totals.costs.opex = ...
        costsdata.opex.addmaint.(scenarios.(scenarioname).SOxtech) + ...
        costsdata.opex.addmaint.(scenarios.(scenarioname).NOxtech) + ...
        simulationresults.(scenarioname).totals.costs.fees + ...
        simulationresults.(scenarioname).totals.costs.fuel.totalfuelcost(2);
158 if strcmp(scenarios.(scenarioname).NOxtech,'SCRe')
159     % Add 10 % of fuel cost to OPEX as cost of urea
160     simulationresults.(scenarioname).totals.costs.opex = ...
        simulationresults.(scenarioname).totals.costs.opex + 0.1 * ...
        simulationresults.(scenarioname).totals.costs.fuel.totalfuelcost(1);
161 end
162 simulationresults.(scenarioname).totals.costs.note = 'Note: OPEX contains fees and ...
        total fuel costs for scenario';
163
164 % Equivalent annual costs
165 simulationresults.(scenarioname).totals.costs.EAC = ...
        simulationresults.(scenarioname).totals.costs.capex * FAP + ...
        simulationresults.(scenarioname).totals.costs.opex;
166
167 % NPV
168 cashflow(1) = simulationresults.(scenarioname).totals.costs.capex;
169 cashflow(2:costsdata.lifespan) = simulationresults.(scenarioname).totals.costs.opex;
170 rate = r;
171 NPV = 0;
172 for year = 1:costsdata.lifespan
173     NPV = NPV + cashflow(year)/(1+rate)^(year-1);
174 end
175 simulationresults.(scenarioname).totals.costs.NPV = NPV;
176
177 % Cost effectiveness per emission
178 reducedemissions = simulationresults.(scenarioname).totals.emissions(1,:) - ...
        simulationresults.(scenarioname).totals.emissions(2,:);
179 simulationresults.(scenarioname).totals.costs.CER = ...
        simulationresults.(scenarioname).totals.costs.EAC ./ reducedemissions;
180 end
181
182 simulationresults.simulationtime = toc;
183 simulationresults.date = datestr(now);
184
185 %% Save results
186 simdate = datestr(now,30);
187 % What has changed:
188 revision = ('In sail_ice.m, changed dist_ice (was reversed)');
189 filename = sprintf('results_%s.mat',simdate);
190
191 save(filename,'-struct','simulationresults','-v7.3')

```

```
192 save(filename, 'possiblescenarios', 'revision', '-v7.3', '-append')
```